ABSTRACT

Title of Document:	DEVELOPMENT AND BIOPHYSICAL CHARACTERIZATION OF HK POLYMER FOR SIRNA DELIVERY TO TUMOR IN A MOUSE MODEL.
	Szu-Ting Chou, Doctor of Philosophy, 2014
Directed By:	Professor A. James Mixson Department of Pathology, School of Medicine

Delivery has been the major obstacle for nucleic acid therapeutics, including the RNA interference (RNAi) approach. Mixson's lab has been focused on the development of a non-viral peptide-based delivery system, HK (histidine-lysine) polymers, which have shown promise as carriers of plasmids and small interference RNA (siRNA) in several cell lines and in tumor-bearing models. In a previous study, a four-branched peptide, denoted H3K(+H)4b, with the predominant repeating -HHHK- sequence in the branch, has been shown to be the most effective and least toxic carrier *in vitro* and *in vivo*.

Building on these results, I utilized different approaches including several structure and stability molecular characterization methods to study polyplex and to develop more effective carriers for improved therapy with siRNAs targeting malignancies. To

understand the role of histidine in the stability of the H3K(+H)4b/siRNA polyplex, the physicochemical properties were investigated. With the use of isothermal titration calorimetry and heteronuclear single quantum coherence NMR, histidines were shown to form hydrogen bonds with siRNA, which enhanced the stability and biological activity of the polyplexes. In addition, to enhance resistance to nucleases and to target the tumors selectively, H3K(+H)4b was chemically modified with different patterns of polyethylene glycol (PEG) and cyclic RGD (Arg-Gly-Asp, cRGD) peptide conjugates. The luciferase marker gene expressed stably by tumor xenografts in mouse models was targeted in order to evaluate the efficacy of HK carriers of siRNA that differed in location and number of cRGD-PEG attachments. The most effective carrier was $(RGD\text{-}PEG)^4H3K(+H)$ (RP-HK), which has a cRGD-PEG on each of its four terminal branches. Consistent with its prolonged stability, as observed by pharmacokinetic studies, the RP-HK polyplex down-regulated luciferase activity in tumor xenografts by nearly 70% compared with the untreated group. Subsequently, the RP-HK polyplex was used to target the Raf-1 oncogene, an important mediator of tumor cell growth and angiogenesis. As in the luciferase studies, the polyplex reduced Raf-1 mRNA by more than 75%, and more importantly, the treatment inhibited the tumor growth by 60% in a mouse model. We anticipate that further design and engineering of HK carriers will improve the predictability and therapeutic activity of siRNA polyplexes in cancer treatment.

DEVELOPMENT AND BIOPHYSICAL CHARACTERIZATION OF HK POLYMER FOR SIRNA DELIVERY TO TUMOR IN A MOUSE MODEL

By

Szu-Ting Chou

Dissertation submitted to the Faculty of the Graduate School of the
University of Maryland, College Park, in partial fulfillment
of the requirements for the degree of
Doctor of Philosophy
2014

Advisory Committee:
Professor A. James Mixson, Chair
Professor Sheryl Ehrman
Associate Professor Jason D. Kahn
Assistant Professor Jeffery B. Klauda
Professor Srinivasa S. Raghavan
Assistant Professor Joonil Seog

Dedication

This dissertation is dedicated to my parents, Wei-Hsin Chou and Yueh-Ling Lai.

Acknowledgements

I would like first to express my greatest gratitude to my mentor, Dr. A. James Mixson, for his patience, guidance, and encouragement during my graduate career at the University of Maryland. He has inspired me to use my talents to the best capacity, which greatly benefited me as a developing researcher. I would also like to thank my co-advisor, Dr. Joonil Seog, for his advice and persistent help and guidance from the perspective of a bioengineer.

My laboratory colleagues, past and present, Dr. Qixin Leng, Dr. Dilara Begum, and Dr. Lei Yu deserve particular thanks. I especially want to thank Qixin for his support and mentorship in my study. The "HK peptide" group at College Park, which includes Dr. Kahn, Dr. Mixson, Dr. Seog, Adam Karcz, Dr. Lucas Tricoli, Amy Lee, and Jason Hustedt, provided invaluable insight into the molecular interactions between HK peptide and siRNA. I also owe many thanks to Dr. Laura McKnight and Dr. Paul Wilder for assistance with ITC, as well as Dr. Kellie Hom, Dr. Daoning Zhang, and Dr. Michael Shapiro for their guidance with NMR. Scientists at Aparna, Dr. Martin Woodle and Dr. Scaria Puthupparampil, have been supportive of my research.

Finally, I would like to thank my parents Wei-Hsin Chou and Yueh-Ling Lai, my sister, Shih-Han Chou, my girlfriend, Melanie Chen, my family and friends from Taiwan, California, Maryland, and Virginia for their endless support and unfailing love for my endeavors.

Table of Contents

List of Tables

List of Figures

List of Abbreviations

AK	Generic term for alanine-lysine peptides
AUC_{2h}	Area under the curve from 0 to 2 h
DAB	3,3'-Diaminobenzidine
CL	Clearance
CPP	Cell penetrating peptide
cRGD	Cyclic peptide containing arginine-glycine-aspartic acid motif
DLS	Dynamic light scattering
DMEM	Dulbecco's modified eagle medium
DNA	Deoxyribose Nucleic Acid
DOPC	1,2-Dioleoyl-sn-glycero-3-phosphatidylcholine
DOTAP	1,2-Dioleoyl-3-trimethylammonium-propane
EGFR	Epidermal growth factor receptor
EPR	Enhanced permeability and retention
FBS	Fetal bovine serum
HK	Generic term for histidine-lysine peptides
H2K4b	Unmodified four-branched peptides, predominant repeating groups -HHK-
H3K(+H)4b	Unmodified four-branched peptides, predominant repeating groups -HHHK-
HER2	Human epidermal growth factor receptor 2
HSQC	Heteronuclear single quantum coherence
IHC	Immunohistochemistry
ITC	Isothermal titration calorimetry
K4b	Four-branched polylysine
LHRH	Luteinizing hormone releasing hormone
LNA	Locked Nucleic Acid
LPD	Liposome-polycation-DNA
modified HK	$(RGD\text{-}PEG)^4H3K(+H)4b$
MRT	Mean residence time
N/P ratio	Protonatable nitrogen to phosphate ratio
NIR	Near-infrared
NK	Generic term for asparagine-lysine peptides
NMR	Nuclear magnetic resonance
PAMAM	Poly(amidoamine)
PEG-HK	$(PEG)^4$-H3K(+H)4b/H2K4b
PEG	Polyethyleneglycol
PEI	Polyethyleneimine
PEO-PCL	Poly(ethylene oxide)-block-poly(ε-carpolactone)
PDMAEMA	Poly[2-(dimethylamino)ethyl methacrylate]
PLL	Poly-L-lysine
PSMA	Prostate-specific membrane antigen
RISC	RNA-induced silencing complex
RLU	Relative light unit
RP-HK	$(RGD\text{-}PEG)^4H3K(+H)4b/H2K4b$

SELEX	Systematic evolution of ligands by exponential enrichment
shRNA	Short hairpin RNA
siLuc	siRNA that targets luciferase
siRaf-1	siRNA that targets Raf-1
siRNA	Small interfering RNA
SNALP	Stable nucleic acid lipid particle
SWNT	Single walled carbon nanotube
$t_{1/2\beta}$	Terminal half-life
TAT	Transactivator of transcription
TBE	Tris/borate/EDTA
VEGF	Vascular endothelial growth factor

Chapter 1: Introduction

1.1 Motivation

Although siRNA has emerged as an alternative therapeutic for cancer, a significant obstacle has been the lack of an efficient and low-toxic carrier for systemic delivery. To deliver siRNA, Mixson's lab has focused on the development of biodegradable polymers, including linear and branched histidine-lysine (HK) peptides. These peptides synthesized by solid phase methods, have the advantage that their sequences are well-defined and manipulatable for functional and biophysical studies. To improve efficacy and establish an evidence-based approach for carrier development, it is essential to characterize the biophysical properties of peptides differing in sequence and/or number of branches. In addition to passive tumor targeting, carriers have evolved to "functionalized" vehicles with greater stability and specificity toward their targets.

The formation of small and compact nanoparticles is critical for siRNA-mediated gene silencing *in vitro* and *in vivo*. Previously, Mixson's lab has reported that variations in the amino acid sequence and buffering milieu affect the interaction between the HK peptide and siRNA to form polyplexes (Leng and Mixson 2005; Leng, Scaria et al. 2005; Leng, Scaria et al. 2006). The biophysical properties, such as binding interaction and structural rearrangement, can be correlated with one

another and more importantly with *in vivo* inhibition efficiency to define general characteristics of an effective and/or ineffective carrier.

Although HK peptides are capable of packaging negatively charged siRNA, poor pharmacokinetic properties of polyplexes have always been obstacles. A common strategy to protect the siRNA sterically from degradation is the conjugation of polyethylene glycol (PEG) to the polyplex. PEG enhances the stability by adding a brush-like layer, coating the outside of the polyplex (Caliceti and Veronese 2003). Moreover, PEG also increases the hydrophilicity of the polyplex by creating a hydration film which significantly decreases their clearance by the reticuloendothelial system. In addition, a ligand is often conjugated with the carrier to increase the specificity toward the cell of interest and to reduce the off-targeting effects. Because $\alpha_v\beta_3$ and $\alpha_v\beta_5$ integrins are expressed by MDA-MB-435 cells and their angiogenic vessels, their cognate ligand cyclic RGD (cRGD) peptide may enhance receptor-mediated internalization of the polyplex (Arap, Pasqualini et al. 1998).

This study characterized critical physicochemical features of HK peptides that enhance endocytosis of the polyplex. Furthermore, by adding cRGD-PEG conjugates to the HK peptide, more effective carriers were developed.

1.2 RNA Interference and siRNA

Eukaryotic cells have evolved sophisticated pathways to control gene expression, including RNA interference (RNAi). RNAi is a biological mechanism in which the translation of mRNA is interrupted by specific regulatory RNA. In general, this mechanism is initiated by Dicer-induced cleavage of double stranded premature micro RNA (pre miRNA) into micro RNA (miRNA) or small interfering RNA (siRNA). In the cytoplasm (Fig. 1.1), loading of the catalytic protein RNA-induced silencing complex (RISC) with miRNA or siRNA unwinds the duplex and the antisense strand can then target a specific mRNA, leading to degradation. RNAi, which has been utilized to down-regulate aberrant disease-causing genes and to study genes important for signal transduction pathways, has emerged as a promising research and therapeutic strategy (Fire, Xu et al. 1998).

RNAi has been used as a therapeutic by two approaches: chemically synthesized siRNA or vector-based short hairpin RNA (shRNA). Whereas siRNA is usually delivered by non-viral methods, shRNA expression plasmids can be delivered by both viral and non-viral approaches. Compared to siRNA, vectors expressing shRNA have to overcome additional barriers such as import of plasmids into the nucleus and multiple enzymatic processing before the incorporation of shRNA by RISC. Moreover, overexpression of shRNA may saturate endogenous miRNA machinery, leading to toxicity (Grimm, Streetz et al. 2006; Snove and Rossi 2006).

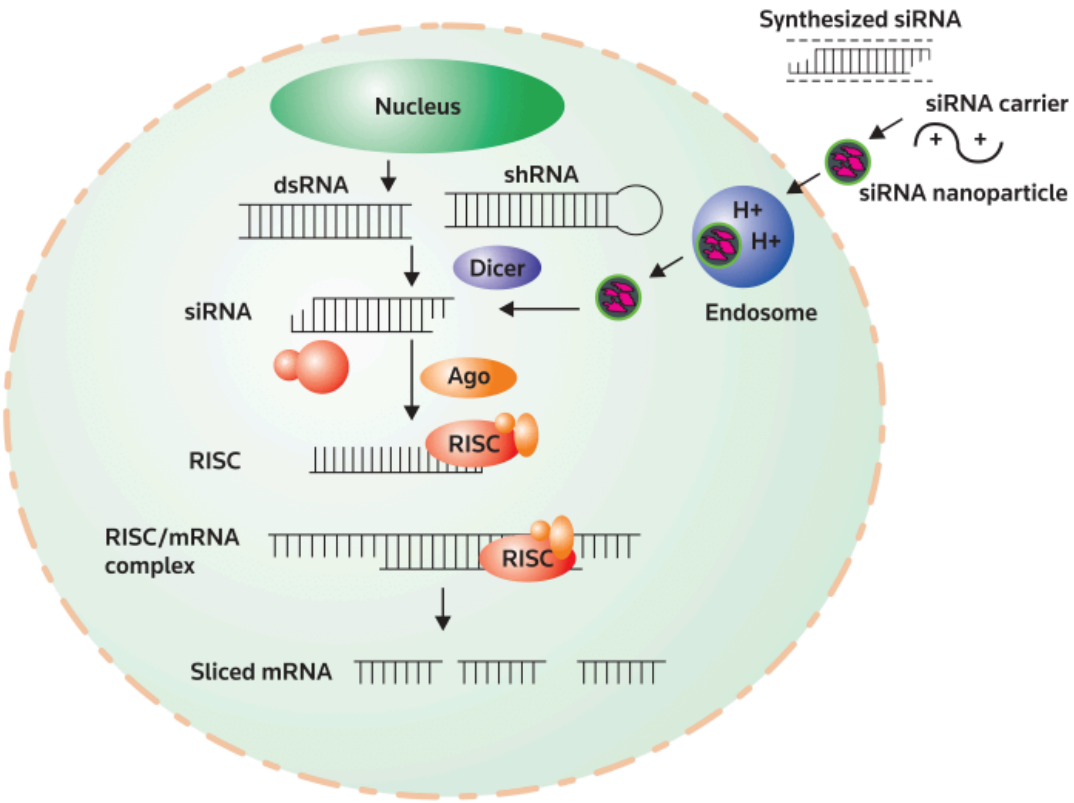

Fig. 1.1. Mechanism of siRNA-mediated mRNA degradation (Leng, Woodle et al. 2009)

Despite significant advances and investment devoted to cancer research, many cancers have a high mortality rate and many molecular aspects of the disease are still poorly understood. Recent advances in the Human Genome Project have provided comprehensive insight into genetic diseases and the function of specific genes. The molecular origins and intracellular signal transduction pathways of cancers can be characterized by examination of tumor specimens from the individual patient, giving rise to the advent of personalized medicine. With features of safe and specific gene regulation, RNAi-based medicine can potentially target any oncogene, enabling its application to personalized medicine.

1.2.1 Small interfering RNA (siRNA)

siRNAs are double stranded RNA duplexes that usually range in size between 19 and 29 base pairs (bp). After the active siRNA of 19-23 bp is incorporated into RNA-induced silencing complex (RISC), an endonuclease of RISC, Argonaute 2, together with the antisense strand of the RNA recognizes and cleaves the target mRNA in a catalytic manner (Grimm, Streetz et al. 2006; Snove and Rossi 2006).

siRNAs larger than 23 bp must be enzymatically processed by the endonuclease Dicer to a size of 23 bp or less prior to their incorporation into the RISC complex. One of the more troublesome aspects initially with introduction of RNAi into mammalian cells was non-specific silencing through cytokine induction by duplexes of 30 bp or larger; this obstacle was overcome to a large extent with the discovery that smaller RNAi duplexes between 19 and 30 bp caused specific silencing without marked cytokine induction. Nevertheless, the smaller siRNAs can still induce cytokines depending on the sequence of the siRNA and its carrier. For example, cationic liposomes in combination with siRNA are particularly potent carriers of siRNA. Induction of cytokines as a result of these siRNA polyplexes is usually dependent on activation of Toll-like receptor 7 or 8.

1.3 Systemic Delivery of siRNA

Despite the promise of siRNA as a therapeutic agent, there are three significant problems that need to be solved before siRNA can be used systemically to treat malignant diseases effectively: 1) prevent or retard degradation of siRNA by nucleases in the bloodstream; 2) specific delivery to the diseased target to prevent side effects in non-targeted tissues; and 3) transport of highly negatively charged siRNA across cellular membranes into the cytosol of the target tissue. To overcome these obstacles, it is essential to stabilize siRNA and facilitate its localization and cellular uptake into the malignant tissue. Two major strategies (chemical modification and physical delivery) for "naked" siRNA delivery will be introduced in the following paragraphs.

1.3.1 Chemical modification of siRNA

Naked siRNA is vulnerable in exposure to nuclease while being administered systemically. To improve the pharmacokinetic (PK) properties and minimize the possibility of an immunostimulatory response due to siRNA (Behlke 2008), a variety of chemical modifications have been made on the 2'-OH group of the ribose. The most common modifications, including 2'-O-methyl, 2'-fluoro, and 2'-hydrogen (Fig. 1.2), have been studied to compare the gene silencing activity, serum stability, and immunostimulatory effect versus unmodified siRNA (Chiu and Rana 2003). The 2'-O-methyl and 2'-fluoro were shown to enhance the serum and thermal stability of

siRNA without interference with silencing activity (Morrissey, Lockridge et al. 2005; Robbins, Judge et al. 2008; Chou, Leng et al. 2011). In addition, 2'-O-methyl-modified siRNA also significantly reduced cytokine induction by antagonizing TLR7/8 receptors (Morrissey, Blanchard et al. 2005; Morrissey, Lockridge et al. 2005; Robbins, Judge et al. 2007; Robbins, Judge et al. 2008). Other modifications such as locked nucleic acids (LNAs) (Elmen, Thonberg et al. 2005) and phosphorothioate linkages (Fig. 1.2) at the 3' end have also resulted in resistance to exonucleases or caused off-target effects (Jackson, Burchard et al. 2006). Even though chemical modifications have been applied to move siRNA therapeutics toward the clinic, most current approaches cannot be universally applied to any gene of interest. Furthermore, bulkier modifications on the sugar moiety may be correlated with decreased siRNA activity.

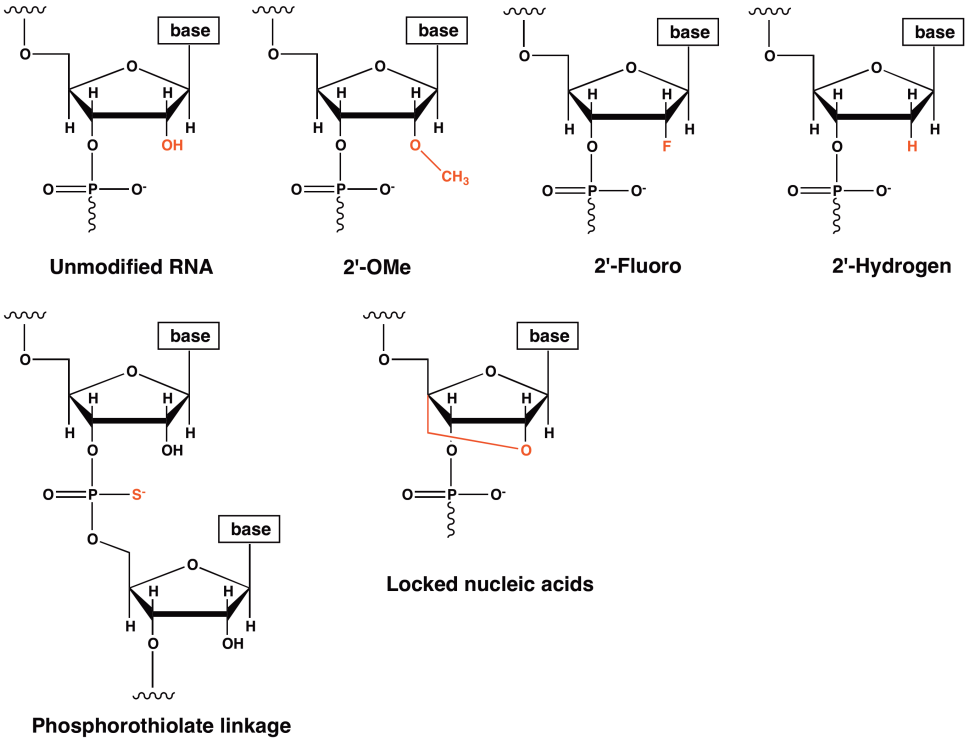

Fig. 1.2. Chemical modifications of siRNA

1.3.2 Physical delivery

The physical methods for siRNA delivery are relatively convenient and may avoid nonspecific immune stimulation. In general, this strategy induces pores in cell membranes for influx of naked siRNA or complexes intracellularly. Electroporation has been a useful tool for DNA or siRNA transfection *in vitro*. For *in vivo* use, electroporation is limited for local delivery to tissues such as brain (Jackson, Burchard et al. 2006) or retina (Matsuda and Cepko 2004). By rapidly injecting a large volume of physiological fluid containing naked nucleic acids, the hydrodynamic delivery approach increases vascular pressure to cells in highly vascularized organs, such as lungs, liver, or kidneys. There have been multiple successful and safe applications for hydrodynamic gene delivery to rodents (Liu, Song et al. 1999; Zhang, Budker et al. 1999) or animals as large as pigs (Yoshino, Hashizume et al. 2006; Kamimura, Zhang et al. 2010) and non-human primates (Zhang, Budker et al. 2001). Nonetheless, it is unlikely that this method can be well-tolerated by humans except for localized delivery.

1.4 Non-viral Carriers

In addition to chemical modification and physical delivery of siRNA, non-viral cationic carriers that form self-assembled nanoplexes with negatively charged siRNA are commonly used.

1.4.1 Liposomes

Cationic liposomes are one of the earliest carriers used for gene delivery and have been commercialized as efficient *in vitro* cell transfection agents such as Lipofectamine 2000, DMRIE-C, Oligofectamine (Invitrogen), DOTAP (Roche Applied Science), X-tremeGene (Roche), siRPORT NeoFx (Ambion), RNAifect (Qiagen), and GeneSilencer (Genlantis). Moreover, they have been used successfully to deliver siRNA in animal models (Chien, Wang et al. 2005; Morrissey, Lockridge et al. 2005; Geisbert, Hensley et al. 2006; Zimmermann, Lee et al. 2006; Aigner 2008; Peer, Park et al. 2008). Although cationic lipids are relatively affordable and quickly formulated, immunogenicity and lack of biocompatibility have become the most significant hurdles for the application of cationic lipoplexes *in vivo*.

To reduce cytokine induction by systemically administered lipoplex, Huang's group has incorporated highly basic protamine to minimize direct ionic interaction between siRNA and 1,2-dioleoyl-3-trimethylammonium propane (DOTAP, Fig. 1.3) (Li, Chono et al. 2008). By further modifying the liposome-protamine-DNA (LPD) with PEG and anisamide ligand, luciferase expression in a lung cancer metastasis model was inhibited by 80% by treatment with LPD and luciferase siRNA complex. Interestingly, while protamine or DOTAP in complex with siRNA individual each induces significant cytokine response, LPD/siRNA shows reduced immunogenicity. Another PEGylated cationic liposome preparation, stable nucleic acid lipid particle (SNALP), has been used to reduce viral infections (HBV siRNA) (Morrissey, Lockridge et al. 2005) and serum cholesterol (APOB siRNA) (Zimmermann, Lee et

al. 2006) in mice or in non-human primates significantly. Several phase I clinical trials have been initiated with the use of SNALP-based products (Alsina, Tabernero et al. 2012; Strumberg, Schultheis et al. 2012).

Since toxicity of cationic liposomes has been correlated to their charge density, several groups have developed neutral liposomes with 1,2-dioleoyl-sn-glycero-3-phosphatidylcholine (DOPC, Fig. 1.3). Neutral liposomes are prepared by mixing DOPC with siRNA in organic solvent, and the mixture is frozen, lyophilized, and re-hydrated for injection. DOPC-siRNA lipoplexes have been used to reduce the tumor growth effectively by targeting EPHA2 (ovarian), thrombin receptor (melanoma), interleukin-8 (ovarian), and focal adhesion kinase (ovarian) oncogenes (Landen, Chavez-Reyes et al. 2005; Halder, Kamat et al. 2006; Landen, Merritt et al. 2006; Merritt, Lin et al. 2008; Villares, Zigler et al. 2008). The second generation of neutral liposomes is coated with hyaluronic acid to prolong the half-life of lipoplexes in the circulation. Moreover, Peer and colleague also conjugated hyaluronic acid-stabilized DOPC with β7 antibody to target activated leukocytes and suppress inflammation specifically (Peer, Park et al. 2008).

1.4.2 Cationic polymers

Synthetic cationic polymers (Fig. 1.3), such as polyethyleneimine (PEI) or polyamidoamine (PAMAM) that has branched structure and amine groups with efficient binding to siRNA, have been extensively investigated for *in vitro* cell transfection as well as systemic delivery of siRNA. Poor pharmacokinetics and

cytotoxicity have been the major obstacles limiting the application of these branched polymers. The strategies to reduce toxicity and non-specific cell internalization of PEI polyplexes is similar to those for cationic liposomes. Modification with polyethylene glycol (PEG) or hyaluronic acid (Jiang, Park et al. 2008; Li, Chen et al. 2008) likely shields the polyplexes to circumvent their interaction with the reticuloendothelial system and blood components. Even though a study showed no extended half-life with PEGylated PEI (Merkel, Librizzi et al. 2009), Kataoka's group has utilized spinning disk confocal microscopy to demonstrate that PEGylation of PEI prevents aggregation of polyplexes in the circulation (Nomoto, Matsumoto et al. 2011). Moreover, to increase the tumor specificity, investigators have conjugated various ligands, including cRGD peptide ($\alpha_v\beta_3$) (Schiffelers, Ansari et al. 2004; Waite and Roth 2009), folate (folate receptor) (Kim, Mok et al. 2006), or Luteinizing Hormone-Releasing Hormone (LHRH receptor) (Minko, Patil et al. 2010). Modified polyplexes are frequently preferred because of their greater specificity and efficacy of tumor inhibition.

1.4.3 Other synthetic carriers

Micelles formed by block copolymers such as poly(ethylene oxide)-block-poly(ε-carpolactone) (PEO-PCL) or poly[2-(dimethylamino)ethyl methacrylate]-block-poly(ε-caprolactone)-block-poly[2-(dimethylamino)ethyl methacrylate] (PDMAEMA–PCL–PDMAEMA) have been explored to deliver siRNA, as well as siRNA-Paclitaxel co-delivery to tumor xenografts (Zhu, Jung et al. 2010; Sun, Du et al. 2011). Furthermore, several groups have directly conjugated gold nanoparticles

with siRNA through disulfide bonds (Rosi, Giljohann et al. 2006; Giljohann, Seferos et al. 2009; Lee, Green et al. 2009). Although these materials have not been applied for systemic delivery of siRNA, topically-administered gold-siRNA conjugates have been shown to be effective for knockdown of EGFR in epidermal cells *in vivo* (Zheng, Giljohann et al. 2012). Single walled carbon nanotube (SWNT) has shown the ability to penetrate mammalian cells without significant cytotoxicity (Pantarotto, Briand et al. 2004). Phospholipids and PEG functionalized SWNT/siRNA polyplex has been intratumorally injected in a mouse model, resulting in tumor inhibition of 70% (Zhang, Yang et al. 2006). Although carbon nanotubes are highly organized and chemically and mechanically stable, their biodegradability remains a challenge.

1.4.4 Natural cationic polymers

There are several vehicles derived from natural products for siRNA delivery currently being studied in preclinical and clinical trials, including cyclodextrin (Fig. 1.3) (Heidel, Yu et al. 2007), protamine (Song, Zhu et al. 2005), atelocollagen (Mu, Nagahara et al. 2009), and chitosans (Rudzinski and Aminabhavi 2010). Although natural cationic polymers are generally biodegradable, these polymers also show relatively lower gene silencing activity compared with PEI. As a result, approaches have been explored to increase siRNA delivery by enhancing the surface recognition of target cells by these polyplexes. Various ligands and antibodies have become important components during development of these natural polymers for siRNA delivery. Transferrin-conjugated cyclodextrin from the Davis' group is the only

polymer-based carrier that has been approved for clinical trials (Davis, Zuckerman et al. 2010).

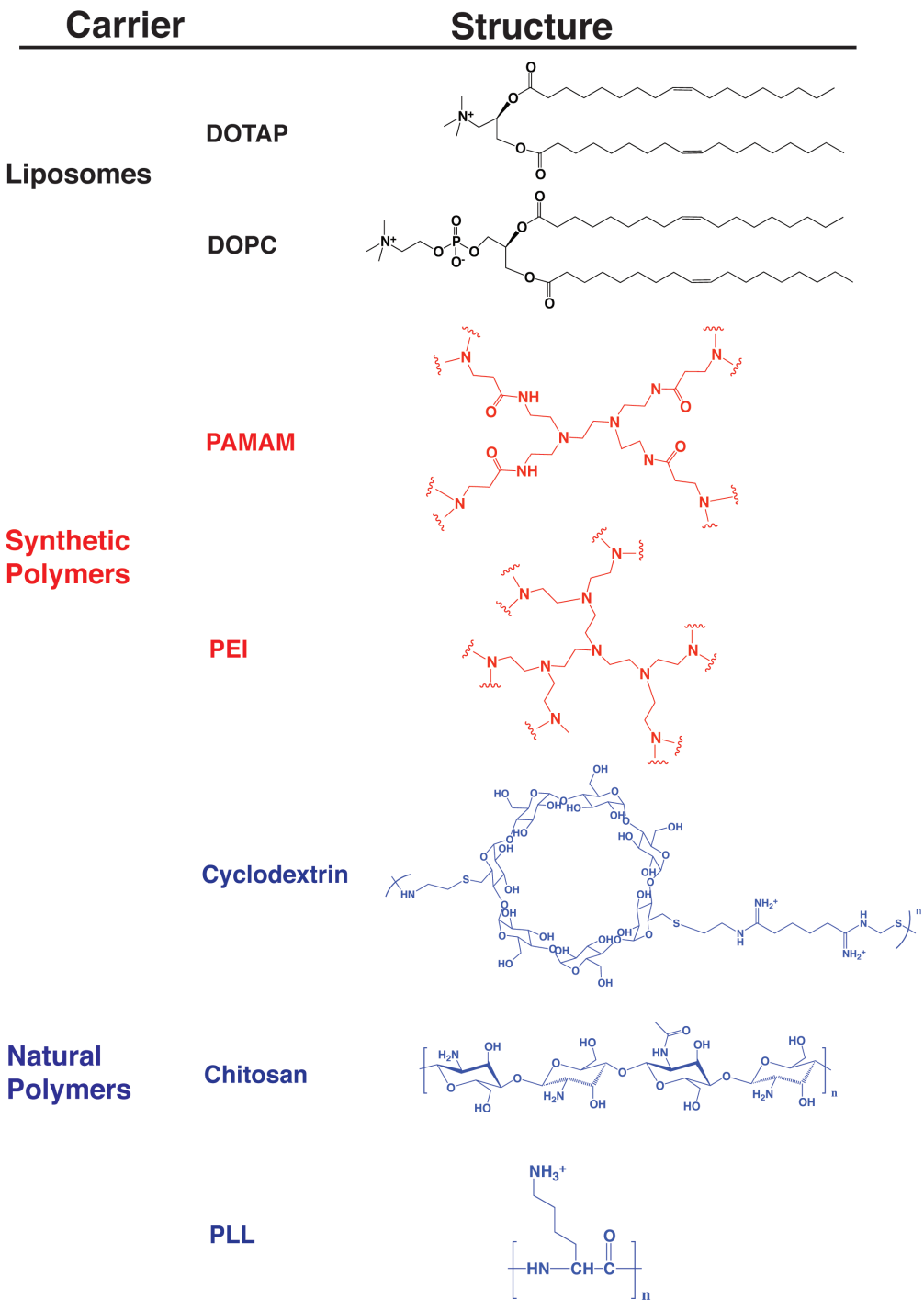

Fig. 1.3. Chemical structures of selected siRNA carriers.

1.4.5 Peptides

Peptides composed of charged residues such as lysines, arginines, and histidines, have been extensively explored for gene delivery. Linear poly-L-lysine (PLL, Fig. 1.3) was one of the earliest polypeptides used for transfection of plasmid, showing effective gene transfer in the liver (Perales, Ferkol et al. 1994). In many cases, however, linear PLL is not an effective carrier for siRNA or DNA due to the instability of the polyplex and its limited ability to escape the endosome. Dendritic PLL was then developed for effective siRNA delivery (Watanabe, Harada-Shiba et al. 2009). The unmodified PLL-based carriers are attractive, although there has been no successful case *in vivo* other than the transfection of hepatocytes.

Kataoka's group has modified the PLL with cRGD-PEG at the N-terminus and with 2-iminothiolane on the amines of side chains of lysines (Christie, Matsumoto et al. 2012). After this thiol-containing polymer forms polyplexes with siRNA, the stability and structure of micelles can be enhanced through disulfide cross-linking. These stabilized micelles incorporating VEGF siRNA showed 50% reduction in VEGF mRNA expression and 80% inhibition of tumor growth. There was no significant difference in body weight when siRNA-treated mice were compared to untreated.

Cell penetrating peptide (CPP), containing arginines, was derived from a transcription factor of HIV, the transactivator of transcription (TAT) protein (Frankel and Pabo 1988). Arginine residues form hydrogen bonds with cell-surface proteoglycans to

induce macropinocytosis (Lundberg, Wikstrom et al. 2003; Nakase, Niwa et al. 2004). Another possible mechanism of internalization not unique to polyarginine polyplexes is the interaction between positively charged peptide and anionic phospholipid of the cell surface to cross the cell membrane (Esbjorner, Lincoln et al. 2007; El-Sayed, Khalil et al. 2008; Ziegler and Seelig 2008). A number of CPP-siRNA conjugates have demonstrated antitumor efficacy by inhibiting oncogenes in animal models (Chiu, Ali et al. 2004; Davidson, Harel et al. 2004; Jiang, Olson et al. 2004). To downregulate target genes effectively *in vivo*, polyarginine can form stable complexes with siRNA using the peptide alone (R15, a 15-mer polyarginine) (Kim, Kim et al. 2010), by conjugating the peptide (R9, a 9-mer polyarginine) to cholesterol (Kim, Christensen et al. 2006) or rabies virus glycoprotein (RVG) (Kumar, Wu et al. 2007).

1.4.6 siRNA conjugates

In contrast to the cationic polymers or liposomes that form complexes by condensing negatively charged nucleic acids, another approach to delivery of siRNA is to conjugate stabilizing and/or tissue-targeting materials, such as cholesterol, PEG, or aptamers to siRNA. Conjugation of cholesterol (Wolfrum, Shi et al. 2007) or α-tocopherol (Nishina, Unno et al. 2008) to siRNA significantly extends serum half-life from 6 to 45 min, compared with unconjugated siRNA. These lipophile-conjugated siRNA are particularly effective for uptake into hepatocytes. Kim and colleagues have developed an LHRH-PEG-siRNA conjugate that self-assembles into micelles with a core-forming PEI (Kim, Jeong et al. 2008). Although this targeted micelle has

not been tested in animal models, it shows marked VEGF silencing at least in A2780 cells.

Aptamers are structured DNA or RNA molecules that can be engineered through SELEX (systematic evolution of ligands by exponential enrichment) to target various receptors, such as prostate-specific membrane antigen (PSMA) (Dassie, Liu et al. 2009) and human epidermal growth factor receptor 2 (Her2) (Thiel, Hernandez et al. 2012). Furthermore, aptamers have been conjugated to PEG-PEI to co-deliver doxorubicin and Bcl-xl siRNA (Kim, Jung et al. 2010). Aptamer siRNA conjugates have emerged as a promising delivery vehicle for siRNA with increased stability against nucleases, specific binding, and low immunogenicity. The library of aptamers remains expandable to target other receptors highly expressed by cancer cells

1.5 Histidine-lysine Rich (HK) Peptides

Mixson's lab has focused on developing an effective *in vitro* and *in vivo* vehicle for small interfering RNA (siRNA). To accomplish this, we have synthesized and screened a number of histidine-lysine rich (HK) peptides to test their ability to carry siRNA. In this context, the lysines are essential for binding siRNA, and the histidines are important for buffering and may aid in the release of siRNA and disruption of endosomes (Chen, Zhang et al. 2001). In contrast to PEI, in which the ethyleneimine serves as both a buffering and nucleic acid binding group, the HK polymer was

originally designed to have its buffering and nucleic acid binding properties on different groups (histidine and lysine). This enables the ratio of the histidines to lysines to be varied to tailor this carrier for different forms of nucleic acids (siRNA vs. plasmids) and for different cells.

In a previous study, several HK polymers were synthesized and examined to compare their ability to deliver siRNA targeting β-galactosidase (β-gal) expressed in SVR-bag4 cells (Chen, Zhang et al. 2001; Leng and Mixson 2005). An eight-branched polymer H3K8b with predominant repeating group -HHHK- was a more effective carrier than H3K(+H)4b and H2K4b. In a subsequent study, we examined various HK polymers as carriers of a Raf-1 siRNA. Raf-1 is an important signal transduction molecule that has an significant role in the growth of many different malignant cells (including MDA-MB-435 cells) and on promotion of tumor angiogenesis. One 4-branched polymer, H3K(+H)4b, whose predominant repeating pattern is -HHHK-, was determined to be an effective carrier of siRNA: the H3K(+H)4b/siRNA polyplexes targeting the Raf-1 oncogene inhibited tumor cell growth both *in vitro* and *in vivo*. Interestingly, H2K4b, which has a higher percentage of lysine, was the most effective carrier to deliver plasmids, but it was not an effective carrier of siRNA. The results show that the efficacy of different HK polymers as carriers of plasmids or siRNA varies and is dependent on the sequence pattern and branching of the polymers.

Although the eight-branched HK polymer with siRNA was slightly more effective than the four-branched HK carrier in silencing its target, we selected the H3K(+H)4b for further siRNA studies *in vivo* based partly on its relative ease of synthesis. In order to prevent aggregation and to target the tumor with the polyplex selectively, we proposed to modify the HK polymers with polyethylene glycol (PEG) and a cyclic RGD (Arg-Gly-Asp) peptide. While PEG increases the hydrophilicity of molecule, cyclic RGD peptide is expected to target the integrin, $\alpha_v\beta_3$ (Wong, Mueller et al. 1998).

As described in this dissertation, H3K(+H)4b as a carrier of siRNA has several advantages over other HK carriers. Although the eight-branched H3K8b was found to be an equally effective carrier of siRNA (as H3K(+H)4b), the eight-branched carrier was difficult to PEGylate at specific locations, perhaps due to steric hindrance. The eight-branched H3K8b polymer has proved relatively resistant to addition of cysteines to its terminal branches, which is a necessary step before the addition of cRGD-PEG. In contrast, the four-branched HK polymer, H3K(+H)4b, can easily be modified with cRGD-PEG at specific locations by adding N-terminal cysteines to each of the branches or by adding a C-terminal cysteine to its core. When cysteines are added to each of the four branches of H3K(+H)4b, there are 4 cRGD-PEG per polymer, but when a cysteine is added off the 3-lysine core, there is only one cRGD-PEG per molecule. The ability to add cysteines at specific locations enables careful control as to where the cRGD-PEG molecules will be inserted within the H3K(+H)4b polymer.

1.6 siRNA-mediated cancer therapeutics in clinical trials

Although several previously mentioned siRNA lipoplexes or polyplexes have shown translatable preclinical activity against cancers, there have been only five cancer clinical trials using nanoparticle-formulated siRNA therapy. These include transferrin-modified cyclodextrin (CALAA-01), stable nucleic acid lipid particle (SNALP; ALN-VSP02 and TKM080301), multi-lipid liposomes (Atu027), and neutral liposome (siRNA-EphA2-DOPC) (http://www.clinicaltrials.gov).

The transferrin-modified cyclodextrin is the only polymer-based siRNA drug approved for clinical trials. While targeting the luciferase expression of tumor xenografts, it reduces 80% of luciferase activity with single dose of the polyplex (Bartlett and Davis 2006; Bartlett, Su et al. 2007). In phase I clinical trials, the melanoma patients received CALAA-01 have shown reduced expression in mRNA of M2 subunit of ribonucleotide reductase (RRM2) compared with pre-treated tumor tissues. Relatively poor pharmacokinetic properties has been a potential factor limiting the therapeutic activity of CALAA-01. Although HK/siRNA and cyclodextrin/siRNA polyplexes have a similar serum half-life, the HK polyplex is cleared by the kidneys significantly later than the cyclodextrin polyplex (2 h vs. 20 min) suggesting a different mechanism of metabolism (Zuckerman, Choi et al. 2012; Chou, Leng et al. 2013).

As described previously, SNALP formulated siRNA nanoparticles have effectively down-regulated various disease-causing genes *in vivo*. As for cancers, it has been

used to target kinesin spindle protein (KSP), polo-like kinase 1 (PLK1), and VEGF in malignant hepatoma (Judge, Robbins et al. 2009). While SNALP has a circulation half-life greater than 18 h (Morrissey, Lockridge et al. 2005), the majority of the lipoplexes is internalized by the liver and spleen. It is suspected that these lipoplexes may not be degraded but accumulate in tissues, leading to liver and spleen toxicity, especially with prolonged dosing. In addition, the application for treatment of solid tumors may be limited if SNALP has the preference for liver or spleen uptake. Sood's group at MD Anderson Cancer Center has shown that siRNA-EphA2-DOPC in combination with paclitaxel results in synergistic anti-tumor efficacy (Landen, Chavez-Reyes et al. 2005). Importantly, the dosage of these cationic liposomes used in the preclinical study is 150 μg/kg which is ten times lower than SNALP or other cationic liposomes. A low-dose treatment that maintains activity is likely to enhance the translatability of DOPC in clinical trials. Moreover, the production of DOPC/siRNA lipoplexes involves lyophilization, which is easier to transport, store, and maintain stability of the lipoplexes. In general, the cost of synthesis of liposomes is 5 to 10 times cheaper than synthetic polymers or peptides in the laboratory scale which is an advantage of liposomal platforms.

Currently, none of these five siRNA therapeutics targeting cancers has advanced to phase II clinical trials. It is too early to determine which of these delivery systems will be effective and receive FDA approval. In addition to the antitumor efficacy (e.g. tumor volume changes, density/opacity changes, and differential distribution patterns) and synergistic effect with co-treatment of chemotherapeutics, the future

siRNA therapeutics have to improve their bioavailability, specificity, and affordability to tackle formidable challenges presented by the complexity of cancers.

1.7 Biophysical Characterization of Carrier/siRNA Complexes

As many carriers have been explored for their ability to deliver siRNA, correlations among the physicochemical properties and the efficacy of siRNA complexes have emerged. These correlations will become indispensable for future improvements in carriers as the field transition from trial and error to principle-based development. For example, multiple studies have shown that passive accumulation in the tumor through the enhanced permeability and retention (EPR) effect is maximal with a nanoparticle size less than 150 nm (Noguchi, Wu et al. 1998; Ishimoto, Takei et al. 2008; Melnikova, Villares et al. 2008; Villares, Zigler et al. 2008). Moreover, the endocytosis pathway also depends on particle size (Medina-Kauwe, Xie et al. 2005). Critical features determined by structure, inter/intra-molecular forces, and complex self-assembly mechanism will likely aid the development of more effective carriers. In addition, the characteristics of suspension media, including temperature, pH, ionic strength, and adulterates such as endotoxins also play a role in the translation of siRNA therapy toward the clinic. In the following paragraphs three techniques, zeta potential, isothermal titration calorimetry (ITC) and nuclear magnetic resonance (NMR), used to determine the biophysical properties of siRNA complexes, will be introduced.

1.7.1 Zeta potential

The zeta potential is related to the surface charge on the nanoparticle and is greatly influenced by the ionic strength of the solution. More specifically, charged particles attract counterions as well as ions that form an electrical double layer near the surface of particles (Fig. 1.4). The inner plane of the double layer (stern layer) consists tightly bound couterions whereas the ions and counterions diffuse freely between the outer layer (slipping plane) and the bulk fluid as a balance of electrostatic force and thermal motion. The zeta potential of a nanoparticle is the electrical charge difference between the slipping plane and the solution.

Zeta potential is measured by the electrophoretic mobility of the nanoparticle determined with light scattering. The electrostatic repulsion or attraction between the particles depends on the magnitude of zeta potential. For electrostatically stabilized dispersions, the value of the zeta potential is generally greater than 20 mV. Therefore, it is an appropriate index for stability, and it can be used to optimize the formulation of biomolecular complexes.

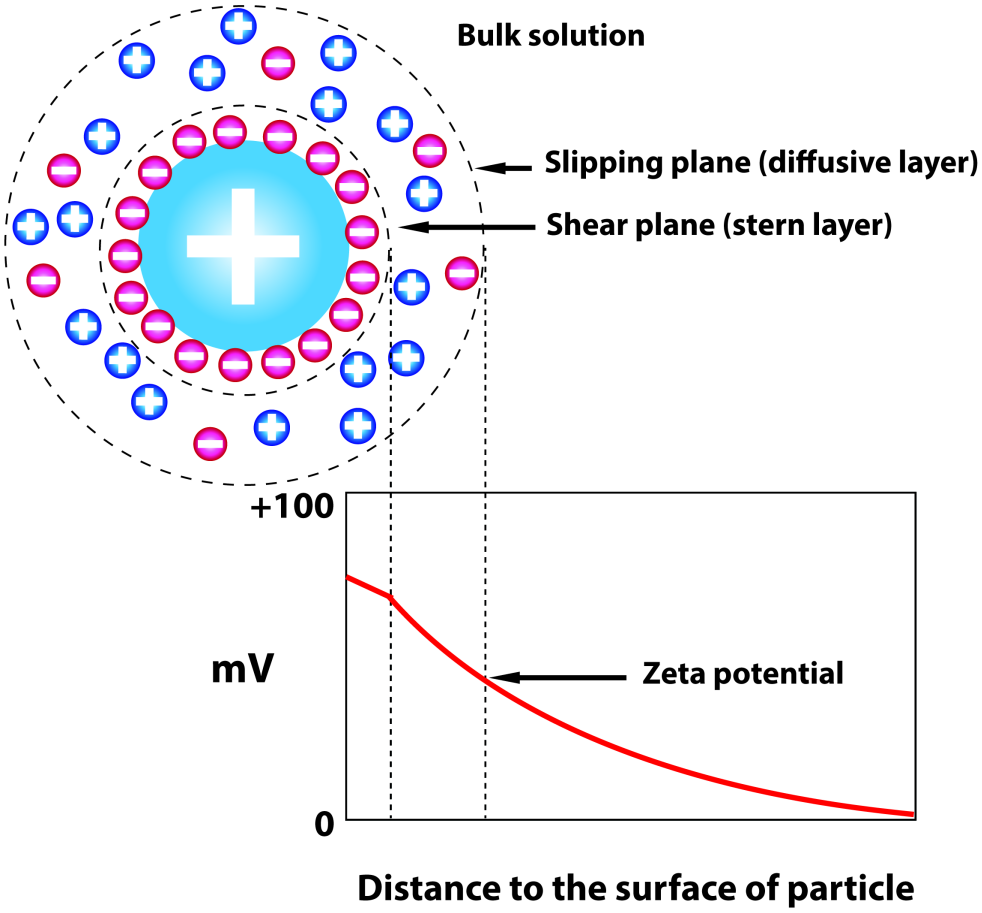

Fig. 1.4. Zeta potential and electric double layer

Because cell membranes consist of negatively charged molecules such as glycoaminoglycans, cationic polyplexes or lipoplexes are likely to be internalized in the cell through electrostatic interactions (Mislick and Baldeschwieler 1996). However, there are several studies showing effective transfection efficacy *in vitro* and *in vivo* with negatively charged complexes, including siRNA coated gold nanoparticles and anionic liposomes (Rosi, Giljohann et al. 2006; Mozafari, Reed et al. 2007; Seferos, Prigodich et al. 2009). Moreover, Whitehead and colleagues have developed lipid analogs and found that there is no statistical correlation between zeta

potential and *in vivo* gene silencing (Whitehead, Matthews et al. 2012) based on a study collected more than 300 data points. While there is a clear correlation between zeta potential and transfection *in vitro*, this correlation is less clear *in vivo*. Scavenger receptors are known to play an important role in the uptake of anionic particles in livers (Furumoto, Nagayama et al. 2004). The cancer cells may also express similar receptors that interact with negatively charged particles. In addition, the high concentration of serum *in vivo* likely masks the intrinsic zeta potential and influence transfection properties of the complex. Therefore, zeta potential should be characterized for each type of carrier to correlate with other properties of polyplexes, such as binding and release profiles, to determine the optimal formulation.

1.7.2 Isothermal titration calorimetry (ITC)

The binding interaction between polycations and siRNA has been extensively studied by gel electrophoresis, fluorescent dye exclusion assay, and isothermal titration calorimetry (ITC). Gel electrophoresis is the most common approach to determine the amount of siRNA neutralized or condensed by cations. Although gel electrophoresis analysis is relatively quick and convenient, it is difficult to quantify binding affinity between carriers and nucleic acids. Molineux *et al.* were the first group to monitor dynamic binding interaction based upon the change of fluorescence properties (Molineux, Pauli et al. 1975; Lohman and Overman 1985). By plotting the fluorescence intensity versus concentration of DNA, the binding free energy and the stoichiometry of binding can be quantified. The binding affinity determined by fluorescence quenching data may be an artifact, however, due to the conformational

change of DNA or non-specific binding between carriers and fluorochromes. In contrast, ITC directly measures the heat exchange, the enthalpy, accompanying any chemical reaction and physical change, allowing the determination of Gibbs free energy, entropy, and stoichiometry. Therefore, ITC has emerged as an appropriate method to analyze interactions between biomolecules.

Binding interaction is the building block of self-assembled polyplexes. ITC can be used to dictate critical features correlated with cell internalization, endosomal escape, and gene silencing efficacy. Lohman's group has studied binding between numerous peptides and nucleic acids by utilizing ITC at a range of salt concentrations. They have shown that, for linear peptides of similar length, binding affinity is totally dependent on charge density (Mascotti and Lohman 1992). In contrast, exothermicity is independent of charge density but dependent on sequence when comparing the nucleic acid binding of oligolysines to oligoarginines (Mascotti and Lohman 1997). The data suggest that arginines form hydrogen bonds with siRNA to enhance the stability. Interestingly, the transfection ability of cell-penetrating peptides, which contain arginine residues, may correlate at least in part with hydrogen bond formation. Prevette and colleagues further analyzed the thermodynamics of carbohydrates and DNA binding to derive the contribution of ionic and non-ionic interaction to the binding free energy (Prevette, Kodger et al. 2007). Although direct evidence is lacking, non-ionic interaction stabilizing the polyplex has been suggested to have a critical role in the biological activity of siRNA complexes.

In addition to intermolecular forces, the complexation of carriers and DNA or siRNA, which occurs after the initial binding, has also been monitored by ITC. Bloomfield *et al*. have observed a multi-stage binding (double endothermic peaks) in the study of cobalt hexamine and plasmids (Matulis, Rouzina et al. 2000). The first stage is a result of ligand-DNA monomer binding and the second transition is attributed to charge neutralization-induced reorganization and condensation. Although a more reliable model of complex self-assembly depends on complementary computational simulations and other biophysical characterization, several groups investigating polycation/nucleic acid binding have observed similar energetic transitions (Jensen, Mortensen et al. 2010; Utsuno and Uludag 2010; Zheng, Pavan et al. 2012). This mechanism of nucleic acid packaging can be correlated to the stability of complexes *in vitro* and *in vivo*. Notably, although the mechanism of complexation is an important factor for cell internalization and endosomal escape, considerably more information on carriers will be required to utilize thermodynamic profiles for development.

1.7.3 Nuclear magnetic resonance (NMR)

While binding interaction can be investigated by ITC macroscopically, binding epitopes on biomolecules and the structural rearrangement induced by binding are often characterized by nuclear magnetic resonance (NMR). The changes in NMR parameters, including chemical shift, coupling constant, and relaxation, provide the basis for analyzing binding events. For example, the ^{1}H nuclei of bound macromolecules show increased transversal relaxation due to slow rotational

tumbling. Therefore, peak-broadening is indicative of complex formation and can be analyzed to quantify binding affinity.

Although the acquisition of the 1D ^{1}H-NMR spectra of biomolecules with or without binding partners has been used to characterize binding, the proton signals alone typically cannot afford high-resolution structural and dynamic properties. Isotope-labeling (^{15}N and/or ^{13}C) of biomolecules is needed to study heteronuclear couplings (^{1}H-^{15}N or ^{1}H-^{13}C). ^{15}N labeling is extensively applied in proteins since heteronuclear ^{1}H-^{15}N correlations can be observed from the backbone amide of each amino acid, except proline. In particular cases such as with histidine, ^{1}H-^{15}N signals in the side-chain can also be detected.

1.7.4 Heteronuclear single quantum coherence (HSQC)

Although the histidines in HK peptides have been hypothesized to mediate non-ionic bonds with nucleic acids to enhance the stability of polyplex, direct evidence has been lacking. Because histidine is so important in physiologically relevant events such as enzymatic reactions or ion channel transport, ^{15}N NMR spectroscopy methods have been designed specifically to study hydrogen bonding by the imidazole side chain. The sensitivity of the ^{1}H-^{15}N cross-peaks of the histidine side chain to hydrogen bonding has been used to study hydrogen bonding in serine protease (Bachovchin 1986; Farr-Jones, Wong et al. 1993), triosephosphate isomerase (Lodi and Knowles 1991), and a membrane component of the phosphotransferase system (Van Dijk, Scheek et al. 1992).

The two nitrogens (Nδ1 and Nε2) and two carbon-attached hydrogens (Hε1 and Hδ2) result in four correlated ^{1}H-^{15}N cross-peaks in the heteronuclear spectrum. To analyze and interpret the ^{1}H-^{15}N couplings, it is essential to know the ^{15}N chemical shifts of various ionic forms of the imidazole ring (Fig. 1.5): deprotonated (type β) nitrogen at 249.5 ppm; protonated (type-α) nitrogen at 167.5 ppm; and charged and protonated (type α+) nitrogen at 176.5 ppm (Bachovchin 1986; Van Dijk, Scheek et al. 1992; Pelton, Torchia et al. 1993). The three-bond $^{3}J_{N\delta 1H\delta 2}$ coupling usually gives rise to relatively weaker intensity (Fig. 1.5), thus, allowing the assignment of each cross-peak.

Type-α and type-β nitrogen chemical shifts are observed when there is no equilibrium between the two tautomers (Fig. 1.5 A and B), usually seen in folded proteins that have histidine buried in a hydrophobic pocket. If the histidine residue is accessible to solvent, both tautomers will be present and the favorable tautomeric form is pH-dependent. Studies have shown that the tautomeric equilibrium of histidines can be quantified based on the difference between the Nδ1 and Nε2 chemical shifts (Bachovchin 1986; Van Dijk, Scheek et al. 1992). For example, if the Nδ1 and Nε2 chemical shifts are found at 222 and 174 ppm, respectively, then 80% of this histidine exists in the Nε2-H tautomeric form. The pKa of a histidine can be determined by curve-fitting of ^{1}H and ^{15}N chemical shifts over a range of pH with non-linear least squares analysis and use of the Henderson-Hasselbalch equation (Markley 1975).

For titratable histidines, a model has established that hydrogen bonding will produce perturbation of ^{15}N chemical shifts in the direction similar to protonation/deprotonation (Schuster and Roberts 1979). Up to 10 ppm downfield or upfield changes of chemical shift can be observed for a hydrogen bond donor or acceptor, respectively.

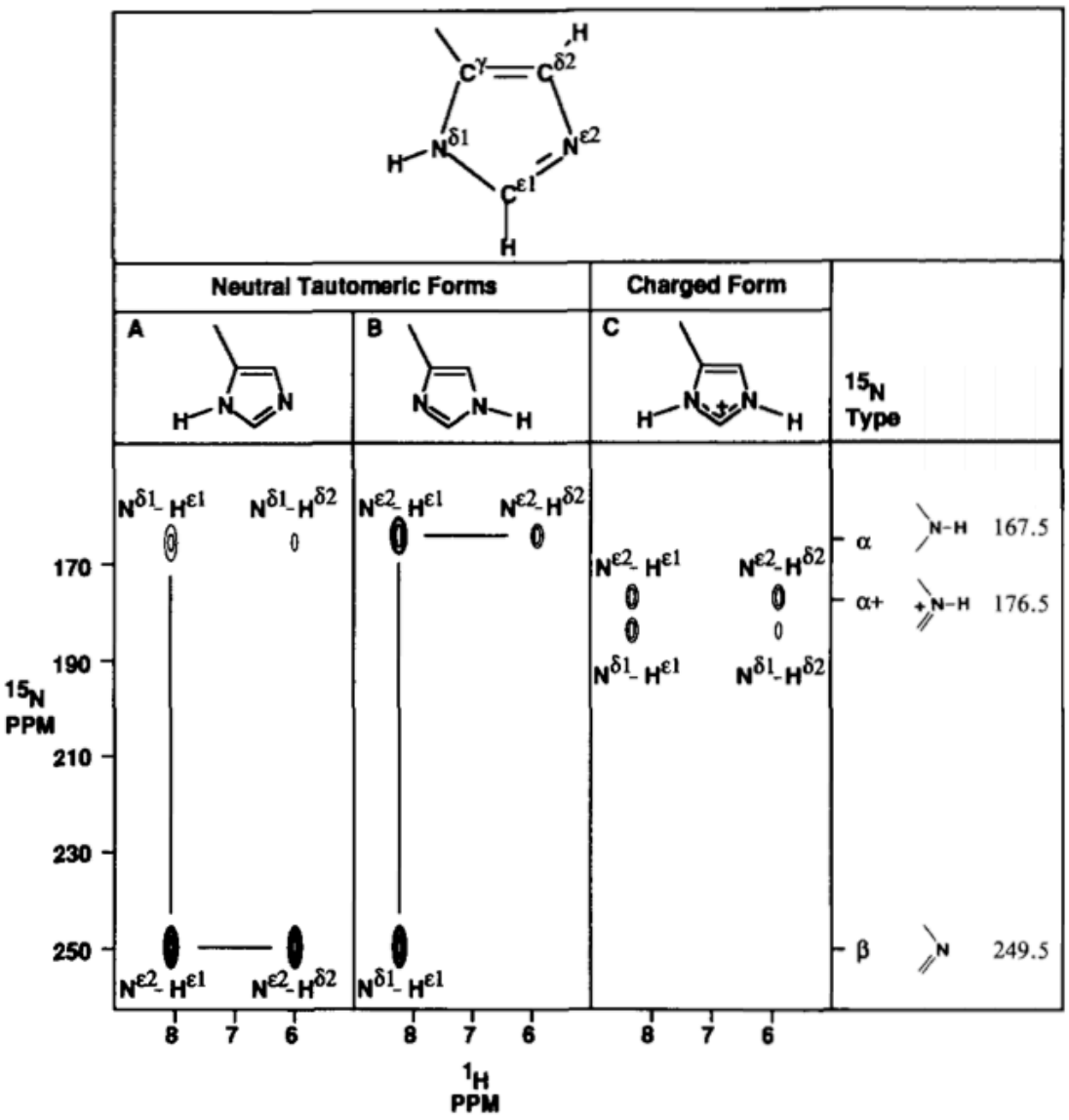

Fig. 1.5. Schematic diagram of tautomeric and protonated forms of histidine, their expected chemical shifts, and characteristics of ^{15}N chemical shifts.

The figure was modified based on the following reference: (Pelton, Torchia et al. 1993)

Chapter 2: Mediation of Silencing Activity and Stability of the HK/siRNA Polyplex by Hydrogen Bonds between Histidine Residues and siRNA

2.1 Abstract

Branched peptides containing histidines and lysines (HK) have been shown to be effective carriers for DNA and siRNA. We anticipate that elucidation of the binding mechanism of HK with siRNA will provide greater insight into the self-assembly and delivery of the HK/siRNA polyplex. Non-covalent bonds between histidine residues and nucleic acid may enhance the stability of siRNA polyplexes. We first compared the polyplex biophysical properties of a branched HK with those of branched asparagine-lysine peptide (NK). Consistent with siRNA silencing experiments, gel electrophoresis demonstrated that the HK/siRNA polyplex maintained its integrity with prolonged incubation in serum, whereas siRNA in complex with NK was degraded in a time-dependent manner. Isothermal titration calorimetry of various peptides binding to siRNA at pH 7.3 showed that the initial binding of branched polylysine, interacted with siRNA was endothermic, whereas branched HK exhibited an exothermic reaction at initial binding. The exothermic interaction indicates formation of non-ionic bonds between histidines and siRNA; purely electrostatic interaction is entropy-driven and endothermic. To investigate the type of non-ionic

bond, we studied the protonation state of imidazole rings of a selectively ^{15}N labeled branched HK by heteronuclear single quantum coherence NMR. The cross-peaks of Nδ1-H tautomers of imidazole shifted downfield (in the direction of deprotonation) by 0.5 to 1.0 ppm with addition of siRNA, providing direct evidence that histidines formed hydrogen bonds with siRNA at physiological pH. These results establish that histidine-rich peptides form hydrogen bonds with siRNA, thereby enhancing the stability and biological activity of the polyplex *in vitro* and *in vivo*.

2.2 Introduction

Strategies involving siRNA provide the potential to manipulate gene expression and facilitate control of diseases. One of the major hurdles in using siRNA or microRNA as therapeutic agents has been the lack of an efficient, stable, and safe delivery vehicle. One means to prevent the degradation of nucleic acids by nucleases in the serum is to condense the nucleic acids with polycations. By binding to the phosphate backbone of nucleic acids through electrostatic interactions, polycationic carriers neutralize their charges and forms polyplexes. Compact forms of polyplexes significantly reduce the exposure of nucleic acids to serum, augment their half-life, and enable their greater penetration within the target tissue. Consequently, polycation carriers such as liposomes, synthetic polymers, and cyclodextrins have shown considerable promise in delivering siRNA or DNA plasmids. Although several promising non-viral polycation agents for gene delivery have been developed and tested in animal models and human investigational trials (Brower 2010; Davis,

Zuckerman et al. 2010; Strumberg, Schultheis et al. 2012), no siRNA carrier has been approved by the FDA for systemic delivery.

To optimize delivery of siRNA by non-viral carriers, it is essential to understand the binding mechanisms and the biophysical properties of the carrier/siRNA complex. Correlating the factors that influence the compactness and stability of polyplexes with biological activity may help development of more effective carriers of siRNA. Fluorescent molecules such as ethidium bromide, acridine orange, and Hoechst dye have been used to study the binding affinity of polycations and siRNA or DNA plasmids, but binding exclusion assays with these dyes only examine binding affinity indirectly (Basu, Schwietert et al. 1990). Furthermore, free fluorescent molecules may interact with carriers and result in artifacts. Isothermal titration calorimetry (ITC) has become an important technique for studying thermodynamics of protein-protein or protein-nucleic acid binding. Quantitative analysis of thermodynamic parameters provides greater insight into the binding mechanism of carrier and nucleic acids (Utsuno and Uludag 2010; Zheng, Pavan et al. 2012). In addition to ITC, nuclear magnetic resonance (NMR) spectroscopy can directly detect molecular interactions in biological solutions (Zuiderweg 2002), thereby providing a powerful and versatile technique for assessing peptide siRNA binding at the atomic level. For example, ^{15}N chemical shifts of the imidazole ring have been studied to elucidate hydrogen bonding interactions in serine protease (Bachovchin 1986; Farr-Jones, Wong et al. 1993), triosephosphate isomerase (Lodi and Knowles 1991), and a membrane component of the phosphotransferase system (Van Dijk, Scheek et al. 1992).

Mixson's lab is particularly interested in histidine-lysine (HK) peptide carriers (Fig. 2.1) of siRNAs, which can effectively inhibited Raf-1 oncogene in tumor xenografts and reduce tumor growth by 60% (Leng and Mixson 2005; Leng, Scaria et al. 2005). Initially, in several laboratories including Mixson's it was thought that formation of the HK polyplexes depended primarily on the electrostatic interaction of positively charged lysines with negatively charged phosphates and that the role of histidine was to buffer endosomes and aid release of nucleic acids (Midoux and Monsigny 1999; Chen, Zhang et al. 2001; Putnam, Gentry et al. 2001; Hatefi, Megeed et al. 2006; Kichler, Mason et al. 2006; Thiel, Hernandez et al. 2012). In contrast to poly-L-lysine (PLL) polyplexes, HK peptide in complex with plasmids is resistant to enzymatic degradation and provided high transfection efficiency (Zhang, Ambulos et al. 2004). As a result, we hypothesized that histidines may play an important role in increased stability of polyplexes through non-ionic interactions, in addition to its role in buffering of endosomes.

To explore types of non-covalent interactions other than Coulombic forces, a number of studies have examined binding behaviors between polymers and DNA (and/or RNA) in solutions with a range of salt concentrations by using ITC (Lohman, deHaseth et al. 1980; Mascotti and Lohman 1997; Prevette, Kodger et al. 2007). On the basis of the counterion condensation theory (Manning 1969; Manning 1978), experiments at a range of salt concentration allow the contributions of non-electrostatic interactions to the binding free energy to be determined. For example,

Lohman's group has shown that a salt-dependent equilibrium constant is thermodynamically comparable for peptides containing lysine or arginine with the same net charge. Nonetheless, compared with oligolysines, oligoarginines have more favorable enthalpic contributions to binding free energy, suggesting hydrogen bond formation between arginines and nucleic acids (Mascotti and Lohman 1997). Prevette and colleagues modeled their ITC data and calculated that the contribution to the free energy from non-electrostatic interaction of carbohydrates and DNA binding accounts for more than 60% of total free energy (Prevette, Kodger et al. 2007). Moreover, in a conformational study using circular dichroism, poly-L-histidine was shown to form complexes with DNA at elevated sodium chloride concentrations (2 M) (Burckhardt, Zimmer et al. 1976), suggesting that non-ionic interactions may have a role in the complex formation. More recently, investigators have used molecular dynamics to probe hydrogen bond formation and potential hydrogen bond donors/acceptors of carriers and DNA (Karatasos, Posocco et al. 2012; Kim, Afonin et al. 2013). Although hydrogen bond formation between polymers and nucleic acids has been suggested by both salt-dependent thermodynamics and molecular modeling, direct evidence is lacking.

The aim of this study was to investigate the role of histidine component of HK peptides in binding to siRNA. We proposed that stable formation of the HK/siRNA polyplex, its resistance to serum, and its enhanced biological activity are the results of a combination of electrostatic and hydrogen-bond interactions. The thermodynamic profiles of peptide siRNA binding were studied by isothermal titration calorimetry. To explore the presence

of histidine-mediated hydrogen bonds, protonation of imidazoles was characterized using heteronuclear single quantum coherence (HSQC) NMR. It is anticipated that consideration of those characteristics will radically reorient current procedures for evaluation of siRNA carriers.

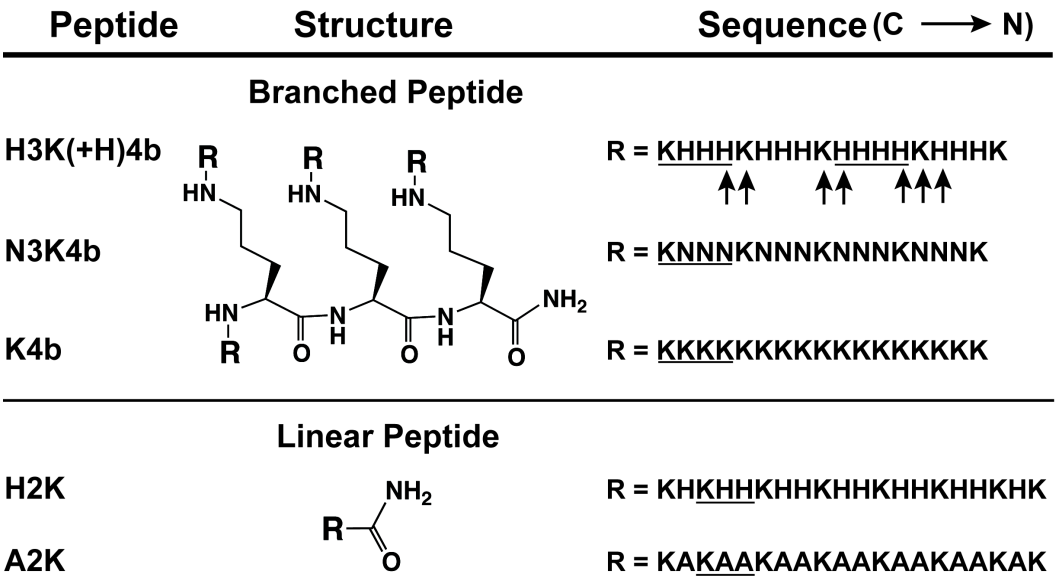

Fig. 2.1. Schematic structures and sequences of branched and linear peptides.

Branched peptides are composed of a three-lysine core, with four branches attached at the four amino groups (N-terminal) of the core. The 20-mer linear H2K peptides have a sequence similar to a branch of H2K4b. The predominant repeating groups are underlined. Labeled histidines (U-15N3) and lysines (U-13C6 and U-15N2) are represented by arrows.

2.3 Materials and Methods

2.3.1 Cell line

Human malignant MDA-MB-435 cells were cultivated in Dulbecco's minimal essential medium (DMEM) supplemented with 10% fetal bovine serum (FBS) and 20 mM glutamine. Stable MDA-MB-435 cells expressing firefly luciferase were obtained by electroporation with a linearized pCpG-Luc plasmid and selection of a high expressing clone in the presence of genetecin (G418). The pCpG-Luc vector was constructed by ligating the luciferase gene (digested from pMOD-Luc plasmid, InvivoGen, San Diego, CA) into the multiple cloning sites of pCpG-mcs (InvivoGen) as previously described (Leng, Scaria et al. 2006).

2.3.2 siRNA

The following siRNA sequences targeting luciferase were used: sense, 5'-CUG-CAC-AAG-GCC-AUG-AAG-A-dTdT-3'; antisense, 5'-UCU-UCA-UGG-CCU-UGU-GCA-G-dTdT-3' (Thermo Scientific, Dharmacon Division, Lafayette, CO). For duplex annealing, each siRNA was maintained in siRNA buffer (Dharmacon) at room temperature for 30 min.

2.3.3 Synthesis and sequences of HK peptides

The four-branched H3(+H)4b, N3K4b, and K4b peptides with predominant repeating groups -HHHK-, -NNNK- and -KKKK-, respectively, as well as the linear H2K (-HHK-) and A2K (-AAK-) peptides (Fig. 2.1) were synthesized on a Rainin Voyager synthesizer (PTI, Tucson, AZ) by the biopolymer core facility at the University of Maryland Baltimore, as previously described (Leng and Mixson 2005).

2.3.4 Peptide/siRNA polyplex preparation

The peptides H3K(+H)4b, and N3K4b were mixed with equal volumes (37.5 μl) of siRNA (10 μg, 20 μM) and maintained at room temperature for 30 min. The resulting polyplexes were tested for stability in serum and/or silencing activity. The peptide/siRNA molar ratios (3/1 for H3K(+H)4b and 6/1 for N3K4b) were chosen based on the amounts needed for complete electrophoretic retardation of the polyplexes in the absence of serum (Chou, Leng et al. 2011).

2.3.5 Stability of peptide/siRNA polyplexes in serum

The stability of peptide/siRNA polyplexes was determined with gel electrophoresis. After the peptide/siRNA polyplexes formed at room temperature for 30 minutes, the resulting polyplexes (7.5 μl) were mixed with FBS (7.5 μl) and incubated at 37°C for 0, 1, 4, 6, and 24 h. Each sample, containing 1 μg of siRNA (total volume 15 μl) was then analyzed by gel electrophoresis (3% agarose) 100V, 30 min. Naked siRNA (lane

1), freshly formed polyplexes in the absence of serum (lane 2), and 50% FBS (lane 7) were also prepared as controls (Fig. 2.2).

2.3.6 Gene silencing by peptide/siRNA polyplexes incubated with serum

Luciferase-expressing MDA-MB-435 cells were plated in 24-well plates (0.5 ml of DMEM, 10% serum) 24 h before transfection at a density of 3×10^4 cells per well. The cells were then treated with H3K(+H)4b/siRNA or N3K4b/siRNA polyplexes (1 μg siRNA/well) targeting luciferase that had been previously incubated in 50% FBS for 0, 4, or 24 h. Control (untreated) cells received 15 μl of DMEM/FBS (50%). Forty-eight hours after the addition of polyplexes, the cells were incubated with 200 μl of lysis buffer (Promega, Madison, WI) followed by centrifugation at 13,000 g for 5 min. After luciferase substrate (Promega) was added to the cell lysates, luciferase activity was measured by a Turner TD 20/20 luminometer (Promega).

2.3.7 Isothermal titration calorimetry

Peptides, and siRNA were dissolved in phosphate buffer (10 mM, pH 7.3). H3K(+H)4b was dissolved in 10 mM 2-(*N*-morpholino)ethanesulfonic acid (MES) buffer pH 5.0 and 6.0 for pH dependence experiments. The thermodynamic profile of nucleic acid binding with HK peptides was obtained at 37°C with use of VP-ITC (MicroCal Inc., Northampton, MA). The sample cell was filled with siRNA (1 μM, 1.45 ml), and the syringe contained peptide solution (25 μM, 5 μl per injection). Each injection (5 μl, a total of 56 injections) was carried out for 10 sec at 360 sec intervals,

except the titration at pH 5 (2.5 μl/injection, 180 sec intervals, and a total of 117 injections). Heat of dilution was determined by titration of peptides into a buffer without siRNA. Molar enthalpy and final figures were generated by Origin 5.0 (OriginLab Corporation, Northampton, MA).

2.3.8 NMR spectroscopy

Heteronuclear Single Quantum Coherence (HSQC) NMR spectra were recorded at 23°C on a 600 MHz Bruker Avance III spectrometer (Bruker BioSpin, Billerica, MA) equipped with a cryoprobe TXI probe, and analyzed using NMRpipe (Delaglio, Grzesiek et al. 1995) and Sparky (UCSF). The H3K(+H)4b peptide was selectively labeled with ^{15}N or ^{13}C as follows. In each terminal branch sequence KHHHKHHHKHHHKHHHK, the underlined histidines were uniformly labeled with U-15N3, and lysines were double labeled with U-13C6 and U-15N2 (Cambridge Isotopes, Cambridge, MA). Sample buffer was either 10 mM phosphate buffer (pH 7.3; with or without 100 mM NaCl) or 10 mM MES buffer, pH 5.0, containing 5% D_2O. For analysis of ^{15}N relaxation data in the presence of siRNA, H3(+H)K4b:siRNA ratios of 10:1, 4:1, and 2:1 were selected. To determine the pKa of each histidine signal, HSQC spectra were obtained with 0.1 mM labeled H3K(+H)4b at pH values of 3.9, 4.4, 4.7, 5.1, 5.5, 5.9, 6.2, 6.5, 6.8, 7.2, and 7.9 in 10 mM phosphate-citrate buffer. This experiment specifically examined the amide protons on the imidazole ring. A pH curve was developed with the proton and nitrogen chemical shifts at different pH values. The pKa values of histidines were calculated by non-linear least

squares analysis with the use of Henderson-Hasselbalch equation (Markley 1975) in Matlab.

2.4 Results

2.4.1 Stability of peptide/siRNA polyplexes in serum

We first studied the stability of peptide/siRNA polyplexes in serum (50%) by gel electrophoresis. Polyplexes are retarded in the well, and upon disruption of the polyplex, the siRNA can be released or degraded. A four-branched HK, H3K(+H)4b (Fig. 2.1) was compared with a four-branched asparagine-lysine-rich peptide (N3K4b); degradation of naked siRNA in the presence of serum was used as a control. The peptide/siRNA molar ratios (H3K(+H)4b, 3/1; N3K4b, 6/1) used in this study were selected because they provided complete retardation of siRNA (saturated binding). The self-assembled polyplexes were incubated in FBS (50%) for 0, 1, 4, 6, and 24 h at 37°C, and then analyzed by gel electrophoresis. To determine the band intensities and integrity of the polyplexes, the gels were pre-stained with ethidium bromide. As seen in Fig. 2.2, H3K(+H)4b/siRNA polyplexes maintained their integrity for up to 24 h in the medium containing serum. In contrast, the siRNA of N3K4b polyplexes was degraded in a time-dependent manner, with kinetics of degradation comparable to that of naked siRNA alone in serum. This indicates that asparagine-lysine (NK) polyplexes were much more sensitive to serum exposure than were HK polyplexes.

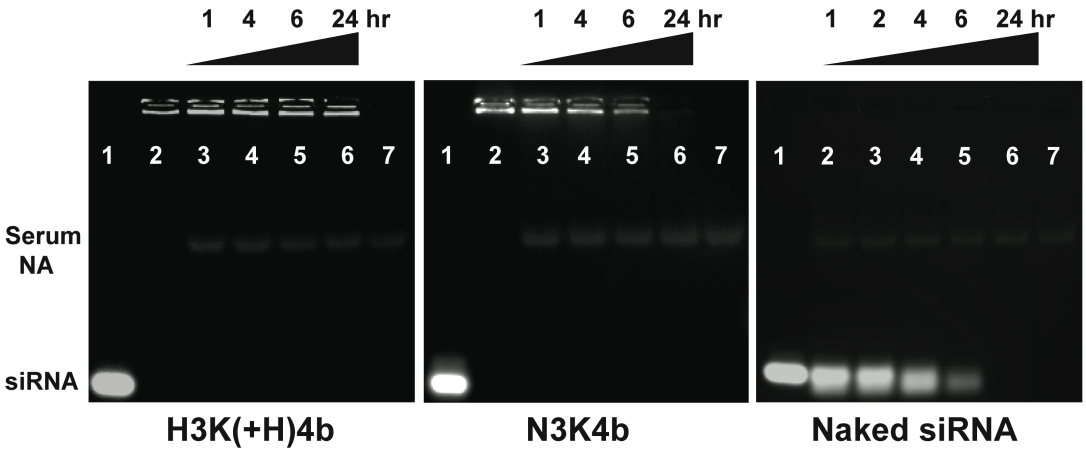

Fig. 2.2. HK polyplexes showed resistance to dissociation and degradation by serum.

siRNA in complex with H3K(+H)4b or N3K4b was incubated with 50% FBS at 37°C for the indicated times. Lanes are as follows: naked siRNA (1), polyplexes without serum (2), polyplexes with 1 h of serum incubation (3), 4 h (4), 6 h (5), 24 h (6), and 50% FBS without siRNA (7). For naked siRNA in the absence of peptide carriers, lanes 2 to 6 were the siRNA maintained in serum for 1, 2, 4, 6, and 24 h, respectively. Serum NA, serum nucleic acids (a faint band is visible in each lane on the original exposure).

2.4.2 Luciferase silencing of serum incubated polyplexes

We hypothesized that the stability of complexes would significantly affect the ability of peptide/siRNA polyplexes to silence target genes. Polyplexes pre-incubated in serum for 4 or 24 h were examined for their ability to silence luciferase expressed by MDA-MB-435 cells. In the absence of serum, H3K(+H)4b and N3K4b in complex with Luc siRNA inhibited luciferase expression by 90% and 50%, respectively (Fig. 2.3). The silencing activity of H3K(+H)4b/siRNA polyplexes was maintained even after 24 h of serum exposure, whereas silencing activity of serum incubated N3K4b polyplexes was markedly reduced, by 20% and 60% in 4 h and 24 h, respectively.

Thus, biological activity of the polyplexes appears to correlate with their stability in serum, and HK polyplex is much more stable and effective than NK polyplex.

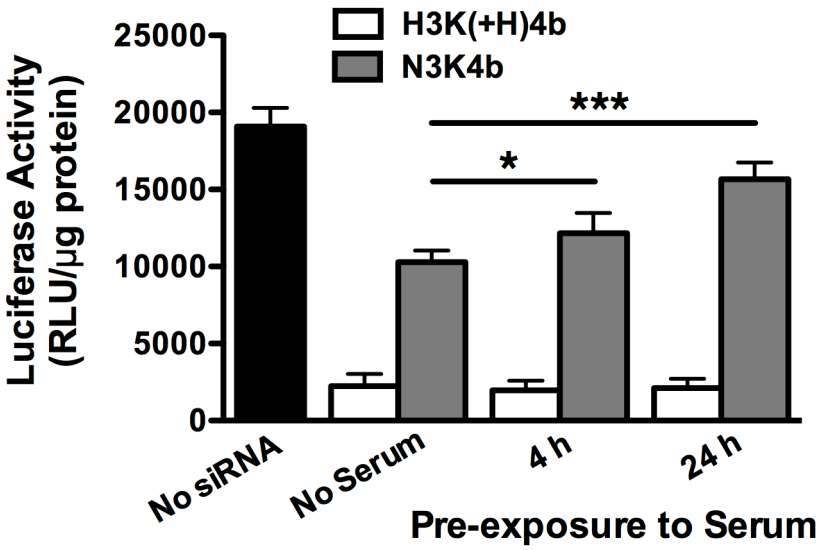

Fig. 2.3. H3K(+H)4b polyplexes incubated with serum maintained high transfection efficiency.

Prior to the transfection of MDA-MB-435 cells that stably express luciferase, H3K(+H)4b/siRNA and N3K4b/siRNA polyplexes were maintained at 37°C with serum (50%) for 0, 4, or 24 h. While silencing of luciferase expression with H3K(+H)4b polyplexes was not affected by serum, silencing with N3K4b polyplexes was markedly reduced by incubation with serum. The data represent the mean ± SD of luciferase of six determinations for each treatment. *, $P < 0.05$; ***, $P < 0.001$.

2.4.3 Thermodynamics of siRNA binding to branched peptides

To study the different binding behaviors that presumably underlie the differences in stability of polyplex against nucleases in serum, we investigated peptide-siRNA binding using isothermal titration calorimetry (ITC). The addition of H3K(+H)4b to siRNA (Fig. 2.4) resulted in three peaks in the integrated enthalpy binding profile. The initial interaction showed an exothermic reaction, with $\Delta H \sim$ -80 kcal/mol of injectant. At this

stage, with siRNA in large excess, the interaction likely represents bimolecular binding of HK and siRNA with minimal formation of polyplexes. The absence of siRNA polyplexes as detected by dynamic light scattering (DLS) at ratios corresponding to this initial phase further validates this hypothesis. This initial enthalpy-driven binding of HK peptides to siRNA suggests the importance of non-ionic interactions, such as hydrogen bonding, stacking, or van der Waals interaction (Ross and Subramanian 1981).

The initial phase was followed by two more transitions at HK peptide:siRNA molar ratios of 1.5 and 2.5: the second phase showed ΔH ~ -20 kcal/mol and the third was endothermic. The transition from exothermic to endothermic binding was likely due to particle aggregation induced or permitted by charge neutralization of the siRNA phosphate backbone with HK peptides (Matulis, Rouzina et al. 2000). The release of water and counterions upon aggregation apparently provides an entropic driving force for the interaction that compensate for its unfavorable endothermic enthalpy from electrostatic interaction (*e.g.*, K4b with siRNA) (Mascotti and Lohman 1992; Matulis, Rouzina et al. 2000). The aggregation was demonstrated by detection of polyplexes by DLS at peptide/siRNA molar ratios of 0.75 and 2.0, giving average particle size of 247 and 1419 nm, respectively. In contrast to binding of HK with siRNA, the initial binding of the branched K4b with siRNA showed an endothermic reaction (ΔH +35 kcal/mole of injectant), indicative of purely entropy-driven electrostatic binding in accord with prior studies (Matulis, Rouzina et al. 2000).

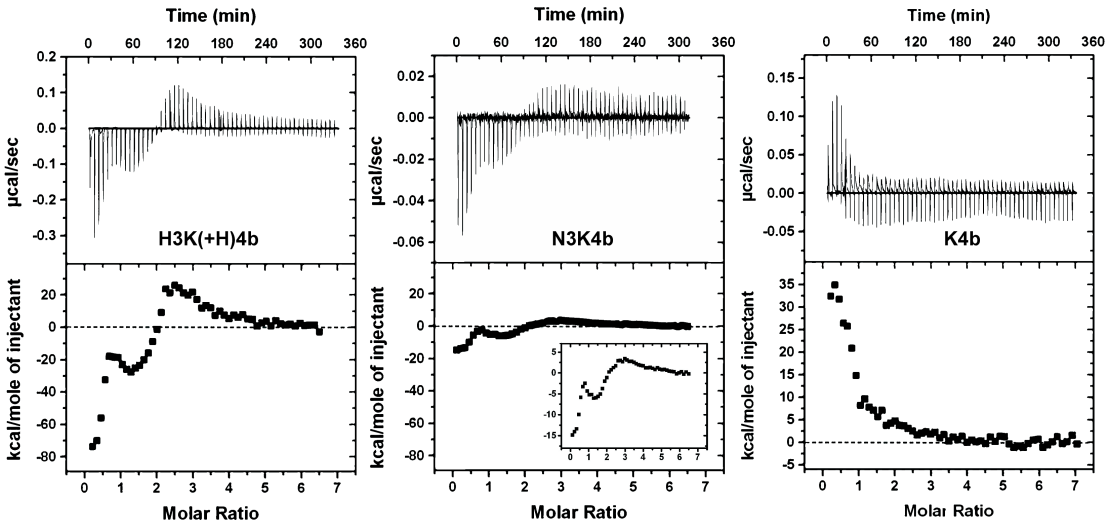

Fig. 2.4. Isothermal titration calorimetry of peptide siRNA interaction.

Representative isothermal titration calorimetry (ITC) raw data and integrated heat release for H3K(+H)4b, N3K4b and K4b peptides (0.12 molar ratio/injection) in 10 mM phosphate buffer, pH 7.0. Comparing H3K(+H)4b and N3K4b with K4b, histidine- and asparagine-containing peptides show exothermic binding at peptide siRNA molar ratios from 0 to 2.5, while K4b binding to siRNA is an endothermic reaction.

Interestingly, asparagine-containing N3K4b siRNA interaction showed an enthalpy profile similar to that of H3K(+H)4b but at a reduced scale. Since the imidazole groups of histidines and amide groups of the asparagines can both function as hydrogen bond donors and acceptors, the formation of hydrogen bonds may play a major role in the exothermic binding at a peptide siRNA molar ratio of 0.1 to 1.0. The exothermicity for H3K(+H)4b binding with siRNA was 5 times greater than that for N3K4b. This suggests that, H3K(+H)4b may have greater capacity to form hydrogen bonds with siRNA at physiological pH than N3K4b, thereby decreasing the sensitivity of the HK polyplex to serum (see Discussion below).

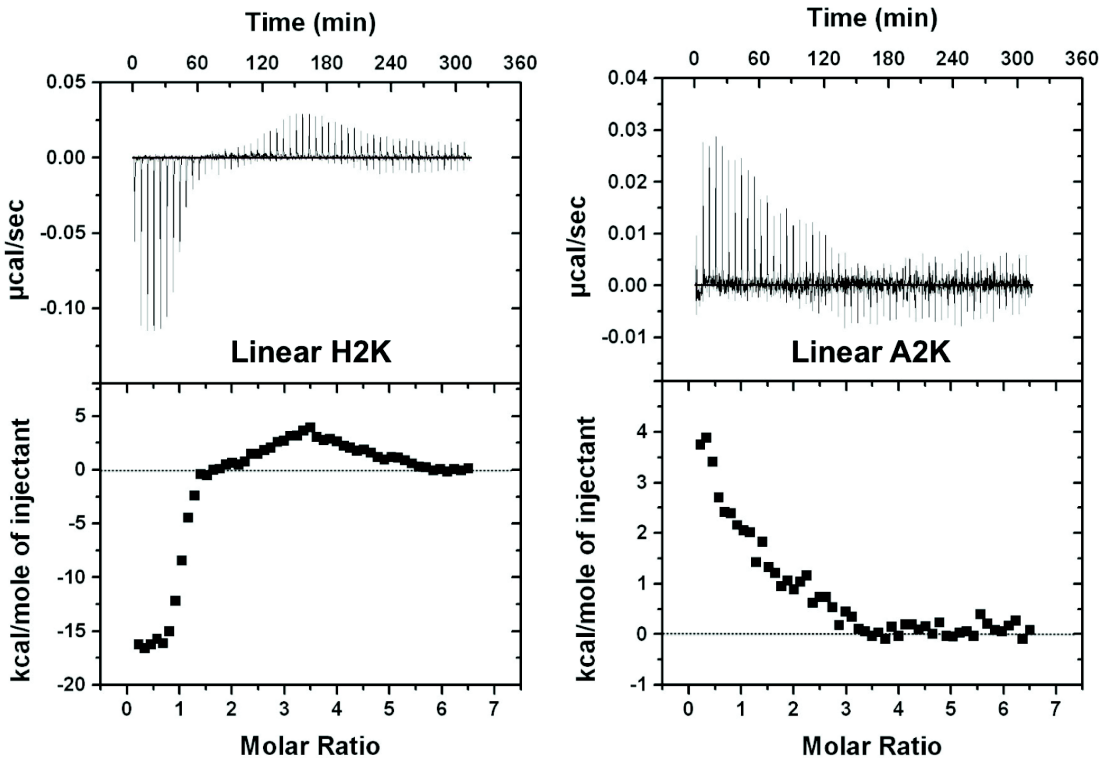

Fig. 2.5. Linear peptides exhibit ITC profiles similar to the branched peptides.

ITC profiles for linear peptides H2K and A2K (25 μM, 0.12 molar ratio/injection) titrated into siRNA (1 μM) were studied. Similar to branched peptides, histidine-containing H2K show exothermic binding at molar ratio 0 to 1.5. In contrast, when histidines were replaced with alanines, A2K behaved similarly to K4b: only an endothermic reaction is observed.

2.4.4 Independence of peptide structure to exothermicity

The effect of HK structures on thermodynamic profiles were then investigated. We synthesized two linear peptides (20-mer): histidine-lysine-rich H2K and A2K, in which histidines were replaced with alanines. ITC profiles of linear and branched HKs with siRNA were assessed to distinguish sequence-related results from the two types of polyplexes. Similar to H3K(+H)4b, linear H2K showed a negative enthalpy change at low molar ratios, followed by a transition to an endothermic region (Fig. 2.5). The exothermicity of binding of H2K to siRNA was approximately one-fourth

that of H3K(+H)4b, which contained four times more histidine. In contrast, when the histidines were replaced with alanines, A2K showed endothermic binding with siRNA similar to that of K4b. Thus, the effects of linear HK peptides parallel those of branched peptides, showing that the balance of ionic and non-ionic interaction is determined by local sequence, not branching patterns.

2.4.5 pH dependence of binding

At a pH lower than the pKa of imidazole groups, protonation of histidine residues increases. ITC profiles obtained at pH 5 or 6 show a much smaller molar ratio of peptide:siRNA at saturation, indicating that the charge density per HK peptide was greatly increased at lower pH (Fig. 2.6). Notably, with decreasing pH, the exothermic reaction was enhanced (pH 6.0, -90; pH 5.0, -120 kcal/mol) while the endothermic reaction was diminished. Protonation of histidines potentially increases the number of hydrogen bond donors and thus increases the likelihood of hydrogen bond formation. Nevertheless, the fully charged HK peptides may also avoid aggregation due to excess positive charges with electrostatic repulsion, which attenuated the rearrangement of small complexes formed in the first phase of binding (Fig. 2.7). Specifically, the thermodynamic profile of fully protonated H3K(+H)4b was in marked contrast with that of K4b (Fig. 2.4), indicating that the HK polyplexes formed at low pH were stabilized by non-electrostatic interactions, even though their charge density is comparable to that of K4b.

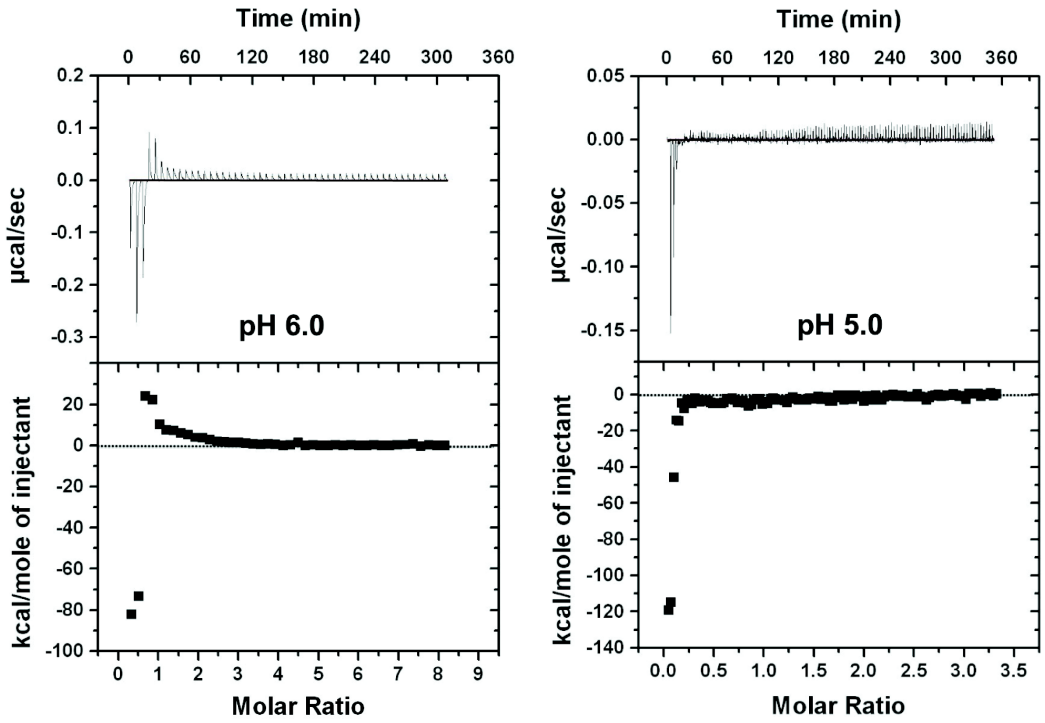

Fig. 2.6. pH dependence of measured enthalpy of H3K(+H)4b siRNA binding.

Representative ITC data for H3K(+H)4b addition to siRNA in 10 mM MES buffer, pH 6.0 and 5.0, are shown. With decreased pH and increased positive charge density of H3K(+H)4b, the amplitude of exothermic reaction was enhanced, while endothermic reaction was diminished.

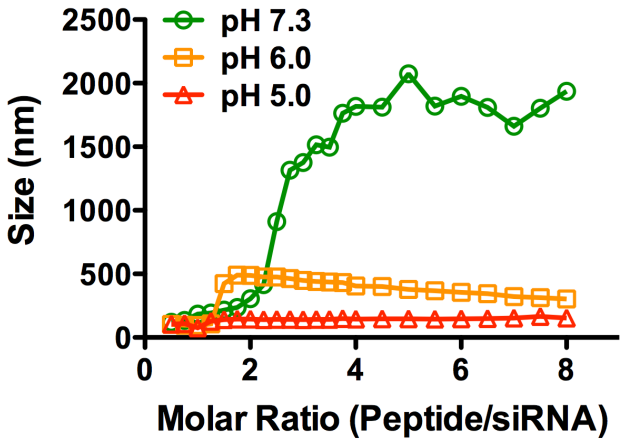

Fig. 2.7. Particle size measurement of H3K(+H)4b/siRNA titration

The particle size of polyplexes while titrating the H3K(+H)4b to siRNA was measured by DLS.

2.4.6 NMR spectroscopy of free peptides and peptide/siRNA polyplexes

To determine the type of non-ionic interaction that results in an enthalpy-driven binding of HK peptide with siRNA, we studied the protonation state of selectively ^{15}N-labeled histidines directly within H3K(+H)4b by using ^{1}H-^{15}N heteronuclear single quantum coherence (HSQC) NMR (Fig. 2.8). It has been shown that ^{15}N chemical shifts of the imidazole ring are sensitive to hydrogen bond formation (Roberts, Chun et al. 1982; Bachovchin 1986; Van Dijk, Scheek et al. 1992; Farr-Jones, Wong et al. 1993). We recorded ^{1}H-^{15}N HSQC spectra of free HK peptides to measure J-coupling between two carbon-attached, non-exchangeable protons (Hε1 and Hδ2) and two nitrogens of the imidazole ring (Nδ1 and Nε2) at pH values from 3.9 to 7.9 (Fig. 2.9). The three-bond $^{3}J_{N\delta1H\delta2}$ coupling results in a relatively weak cross-peak in HSQC spectra (Pelton, Torchia et al. 1993) whose intensities are diagnostic for histidine tautomer populations. The chemical shifts of histidine nitrogens are classified with three possible protonation types: deprotonated, type-β nitrogen, 249.5 ppm; protonated, type-α nitrogen, 167.5 ppm; charged and protonated, type-α+ nitrogen, 176.5 ppm (Bachovchin 1986; Van Dijk, Scheek et al. 1992; Pelton, Torchia et al. 1993). At pH 7.3, the nitrogen protonation states identified two predominant tautomeric states of histidines among four labeled histidines. The histidines that were more highly protonated were designated His 1, the other histidine signals His 2.

The pH dependence of ^{1}H chemical shift of Nε2-Hδ2 was then determined to calculate the pKa of each histidine residue using the Henderson-Hasselbalch

equation. A pH titration of the ^{1}H and ^{15}N chemical shifts of Nε2-Hδ2 was performed to obtain the pKa of each histidine signal, showing that His 1 and His 2 have pKa values of 6.3 and 5.3-5.8, respectively (Fig. 2.9). Notably, His 1 differentiated into three individual cross peaks at low pH (Fig. 2.8 right panel). Because of its repetitive sequence, however, we were not able to assign residue types to individual histidine residues. Assuming the extent of proton transfer is linearly correlated to the difference of Nδ1 and Nε2 chemical shift, the tautomeric equilibrium of histidines can be quantified (Bachovchin 1986; Van Dijk, Scheek et al. 1992). At pH 7.3, the protonation level of Nδ1 of His 1 and His 2 were 25% and 13.5%, and while at pH 5.0, the protonation level of Nδ1 of His 1 and His 2 were increased to 35% and 20%, respectively.

A titration of H3K(+H)4b by siRNA was also similarly monitored by ^{1}H-^{15}N HSQC spectra to determine whether peptide siRNA binding altered the tautomeric forms of His residues. To increase the resolution and efficiency of signal acquisition, siRNA titration experiments were performed with a narrow sweep width (160 to 190 ppm, Fig. 2.8, middle and right pane). Compared with the normal full-width spectrum, Nδ1-H signals of His 1 and 2 aliased by 36 ppm (negative phase, orange) and 72 ppm (positive phase, black) in the ^{15}N dimension at pH 7.3, respectively. Upon the addition of siRNA, Nδ1-H of both histidines shifted downfield (towards the direction of deprotonation (Farr-Jones, Wong et al. 1993), (Fig. 2.10)) while the predominant Nε2-H remained unchanged. His 1 and 2 shifted by 0.5 to 1 ppm, respectively, at a peptide:siRNA molar ratio 4:1. Moreover, this peak shift was similar to that in the

buffer containing 100 mM NaCl (Fig. 10) demonstrating its nonionic in nature. The siRNA titration experiment shoed that as the peptide:siRNA molar ratio decreased to 2:1 (data not shown), cross-peaks were broadened due to polyplex formation (Fig. 2.10). The Nδ1 peak shifts induced by siRNA binding were enhanced by two fold (1-2.5 ppm) at pH 5.0. The perturbations of Nδ1 chemical shift of HK/siRNA polyplexes were positively correlated with the numbers of hydrogen bonds. Thus, the results of the HSQC are consistent with the thermodynamic behavior, which showed increase heat release as the pH decreased.

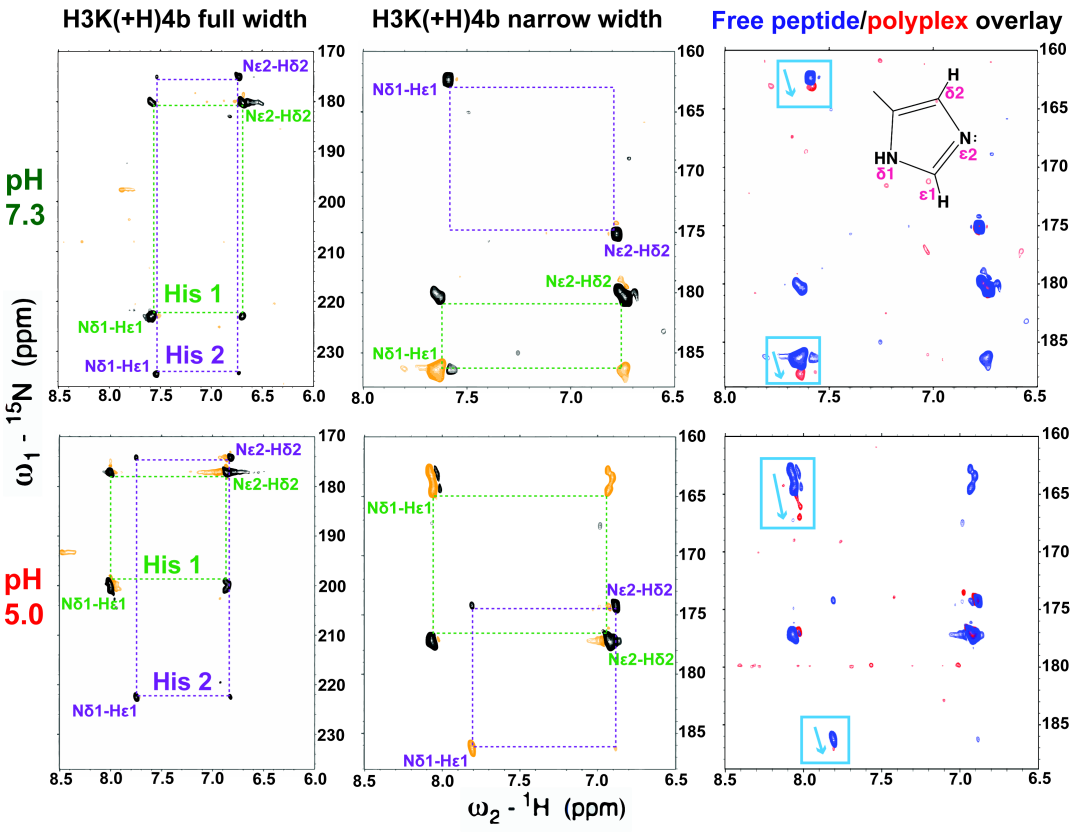

Fig. 2.8. Protonated nitrogen shifted toward the direction of deprotonation.

Representative ^{1}H-^{15}N spectra (72 and 36 ppm, ^{15}N width) of H3K(+H)4b (blue) at pH 7.3 (upper panel) and 5.0 (lower panel). Two imidazole ring sets of cross peaks were observed (His 1 and 2). siRNA was added at a peptide:siRNA molar ratio 4:1 (red, right panel). The black and orange peaks at left and middle panels represent unfolded and folded peaks, respectively. Upon siRNA binding, both Nδ1-H tautomers shifted downfield by 0.5 ppm at pH 7.3. The peak shift upon addition of siRNA demonstrates hydrogen bond formation. The complex-induced peak shift was increased to 2.0 ppm when the pH was lowered to 5.0.

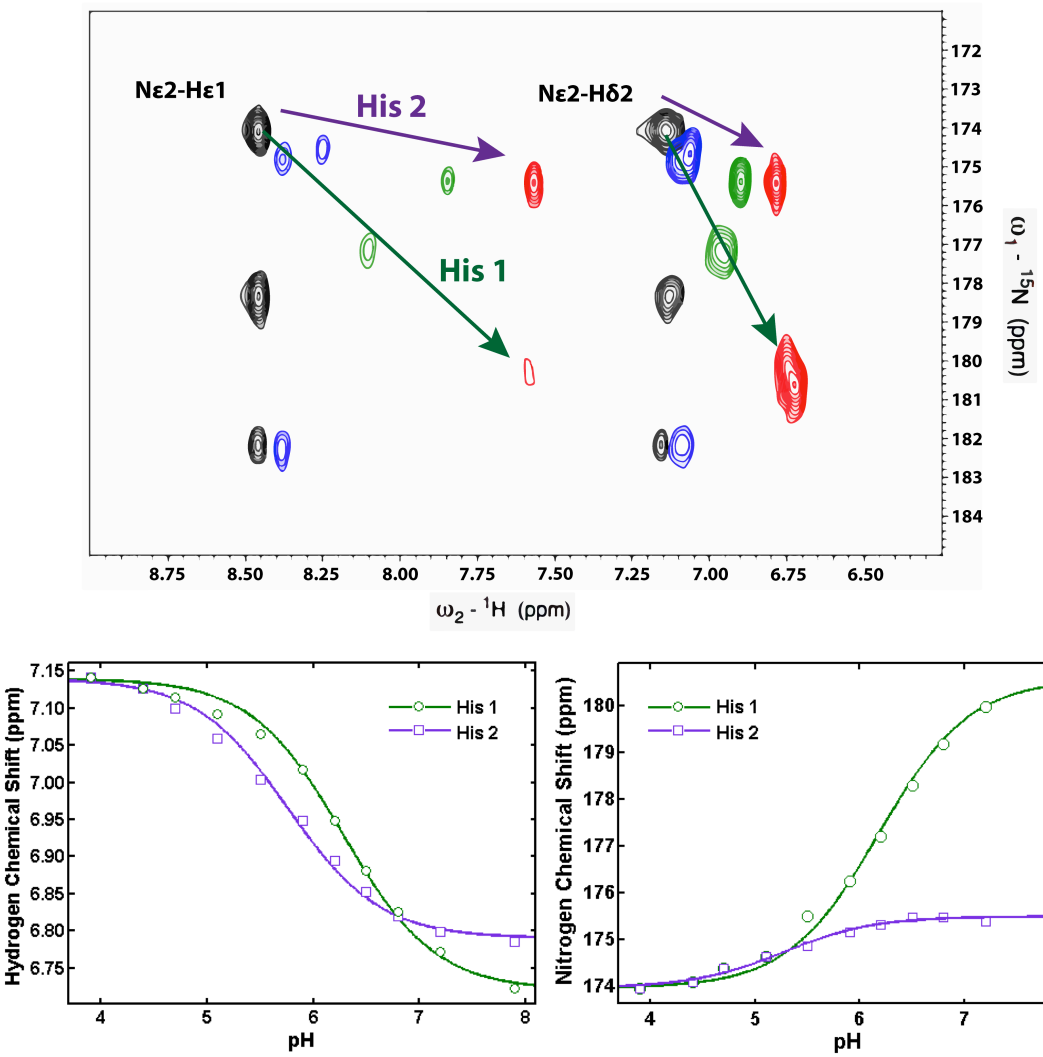

Fig. 2.9. pH titration spectra and curves for the ^{15}N-labeled histidine proton and nitrogen resonances in HSQC experiments.

Representative ^{1}H-^{15}N spectra of free H3K(+H)4b at pH 3.9 (black), 5.1 (blue), 6.2 (green), and 7.9 (red) is presented on the upper panel. The solid line (lower panel) represents the least-square fit of the data to the Henderson-Hasselbalch equation. pKa values of 6.3 and 5.8 for His 1 and His 2 were derived from proton resonance curve fits; 6.2 and 5.3 from nitrogen resonance curve fits. $R^2 > 0.99$.

2.5 Discussion

The binding mechanism and interaction between cationic polymers and siRNA are likely to have a critical role in the stability and delivery efficacy of the polyplexes. The goals of this work were to identify the contributions of purely ionic vs. non-electrostatic interactions, to characterize hydrogen bonding patterns in the siRNA and peptides, and to identify the molecular origin of the enhanced stability and biological activity of the HK peptides.

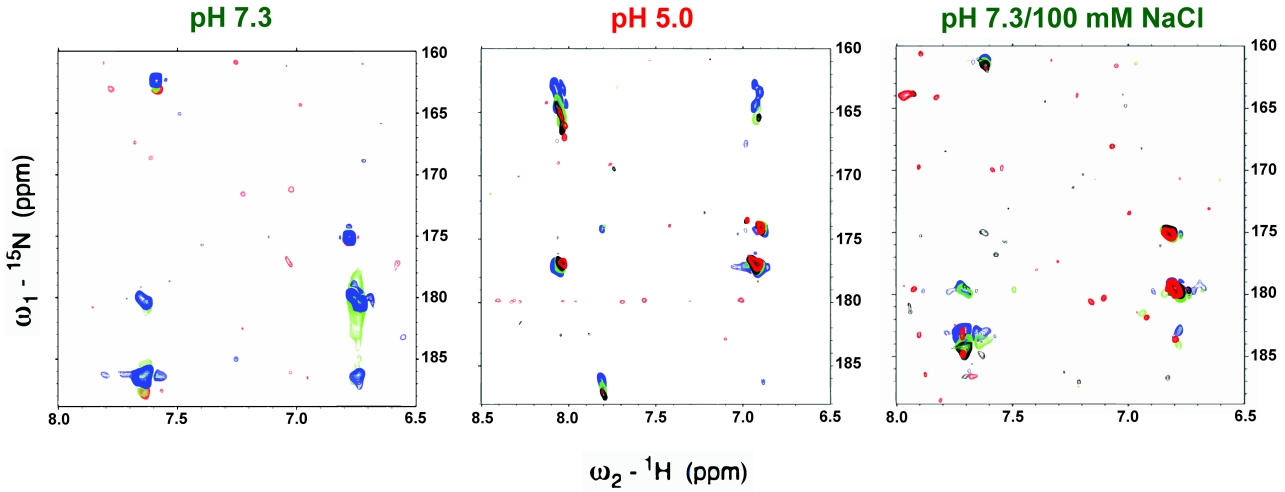

Fig. 2.10. NMR titration of H3K(+H)4b with siRNA.

Representative ^{1}H-^{15}N spectra of free H3K(+H)4b and H3K(+H)4b/siRNA polyplexes at pH 7.3 (left), pH 5 (middle), and pH 7.3 buffer with added 100 mM NaCl (right). The colors represent several peptide/siRNA molar ratios of 13/1 (green), 6/1 (black), and 4/1(red) or the "free peptide" (blue). As the amount of siRNA added to the peptides increased, the perturbation of Nδ1 resonance increased whereas Nε2 remained unshifted.

Polyplexes in which ionic interactions are dominant can be sensitive to physiological salt concentration and charged blood components such as albumin, thus reducing the ability to silence target genes *in vitro* and *in vivo*. Serum destabilization of cationic liposome:plasmid DNA complexes may be inhibited with a high positive/negative

charge ratio (Yang and Huang 1997), but excess polymers can be problematic for siRNA delivery. For example, Mixson's laboratory has demonstrated that higher HK to siRNA ratios are associated with poorly formed or small polyplexes that were less effective in gene silencing *in vivo* (Chou, Leng et al. 2011). Moreover, an increased charge density of polycations may damage cell membranes, which results in cytotoxicity (Fischer, Li et al. 2003). Nevertheless, the increased charge density of an ionizable polyplex upon protonation within acidic endosomes may lead to unpacking of the polyplexes with increased delivery of siRNA to the cytosol.

In addition to electrostatic interactions, a number of studies have reported that non-ionic interactions including hydrogen bonding may contribute significantly to binding of cationic carriers and DNA plasmids (Prevette, Kodger et al. 2007; Ma, Lavertu et al. 2009). Hydrogen bond formation enhances the stability of polyplexes without the use of excess cationic polymers, thereby reducing cytotoxicity induced by excess positive charges. Allen *et al*. have developed a hydroxyl-containing polymer in which intermediate binding and putative hydrogen bonding with DNA resulted in higher transfection (Allen, Green et al. 2011). Hydrogen bond formation also plays a pivotal role in maintaining the condensed state of the polyplex in combination with electrostatic interactions, particularly when exposed to the disruptive effects of serum (Buyens, Meyer et al. 2010). Despite the importance of hydrogen bonds in the stability of polyplexes, prior studies with histidine-containing polyplexes have focused on the role of histidine in buffering endosomes and not on its ability to stabilize polyplexes. In this study, we investigated the potential binding and

intermolecular forces between HK peptides and siRNA by gel electrophoresis analysis, ITC, and NMR. Together, the data indicate that hydrogen bonds formed between histidine residues and nucleic acids enhance the stability, silencing activity, and transfection efficacy of polyplexes.

Isothermal titration calorimetry is a sensitive technique that has been used to determine the predominant factors critical for binding interactions. Previous studies have suggested that charge-charge interaction of polycations and nucleic acids is often accompanied by the depletion of counterions and the disruption of the hydration layer, greatly increasing entropy and driving an enthalpically unfavorable reaction (Matulis, Rouzina et al. 2000; Korolev, Berezhnoy et al. 2012). In my data, exclusively entropy-driven binding was observed with the titration of K4b or A2K with siRNA, demonstrating that lysines interact primarily with negatively charged phosphate backbone of nucleic acids. In contrast, peptides containing histidines, H3K(+H)4b or H2K, release a significant amount of heat in the initial phase of binding to siRNA. This initial binding event probably represents a monomeric interaction between siRNA and HK peptide with minimal polyplex formation. In contrast to the ionic interaction between K4b and siRNA, exothermic HK siRNA binding appears to be stabilized primarily by non-ionic interactions (Mascotti and Lohman 1997). Furthermore, these non-ionic interactions were shown to be hydrogen bonds, as determined by diagnostic changes in NMR spectra under conditions that minimized polyplex formation.

The transition from the exothermic to the endothermic phase of binding, as described in Results, was correlated with the aggregation of polyplexes. The endothermicity is presumably due to strain energy or steric conflicts upon aggregation. Similar thermodynamic results have been obtained for polyethylenimine binding to nucleic acids (Utsuno and Uludag 2010; Zheng, Pavan et al. 2012). Polyplex formation is likely to involve multiple interactions, including ionic interaction, hydrogen bonding, π-π stacking, and/or hydrophobic interaction. Interestingly, H3K(+H)4b and N3K4b shared similar binding patterns in which peptide siRNA interaction was initially an exothermic reaction, followed by two transitions. Considering that both histidines and asparagines have amine groups compatible with formation of hydrogen bonds, it is anticipated that hydrogen bonding, rather than stacking, is the major source of exothermicity.

Several studies have shown that the substitution of histidines with asparagines does not necessarily interrupt the binding and biological activity of proteins (Lowe, Fersht et al. 1985; Narayan, Chou et al. 2007). However, the initial exothermicity of H3K(+H)4b binding to siRNA is 5 times greater than that of N3K4b (-80 vs. -15 kcal/mole, Fig. 2.4) binding to siRNA. The thermodynamic difference can be correlated with the serum stability of the polyplex determined by gel electrophoresis. The enthalpy of H3K(+H)4b siRNA initial binding is pH-dependent. At pH 5.0, 6.0, and 7.3, the first exothermic peaks were -120, -90, and -80 kcal/mole, respectively. The results of HSQC also showed that Nδ1-H peaks of both histidines had a greater change in chemical shift at pH 5.0 than at 7.3. Therefore, the exothermic binding that

we assign to hydrogen bonding by histidines is enhanced by protonation to give $HisH^+$, and protonation of histidine primarily enhanced the interactions of Nδ1-H protons with siRNA. Furthermore, the hydrogen bond length of N-H donors of imidazole rings is generally shorter than N-H of amide groups on asparagines because of neighboring electron-withdrawing effects (Steiner 2002). Thus, in addition to increased protonation level of Nδ1-H and charge potential, delocalization of electrons on the imidazole ring may also be responsible for the enhanced exothermic level, when siRNA binding of HK is compared with NK.

Because unprotonated histidines serve as both hydrogen bond donors and acceptors, hydrogen bonds may not necessarily form between histidines and nucleic acids. To determine the orientation of the hydrogen bond, we increased the protonation of histidines by lowering the pH to disrupt potential hydrogen bond interfaces of histidine-histidine (his-his) or histidine-lysine (his-lys) between HK peptides. If his-his or his-lys hydrogen bonding was dominant, protonation of histidines would decrease the number of hydrogen bond acceptors and therefore reduce hydrogen bonding and the exothermic level. The enhanced exothermic interaction at lower pH (Fig. 2.6), however, provided evidence that hydrogen bond pairs were predominantly at the interface of H3K(+H)4b and siRNA. Importantly, pH-dependent thermodynamic patterns correlated with the chemical shift perturbation in HSQC. Moreover, the addition of siRNA to H3(+H)4b gave rise to greater shift of Nδ1 peaks at lower pH as assessed with HSQC. Whereas multiple lines of evidence indicate that hydrogen bonds have an important role in augmenting the binding of HK with siRNA

and stabilizing the polyplex, the present studies do not support improved siRNA protection of siRNA by formation of his-his hydrogen bonds.

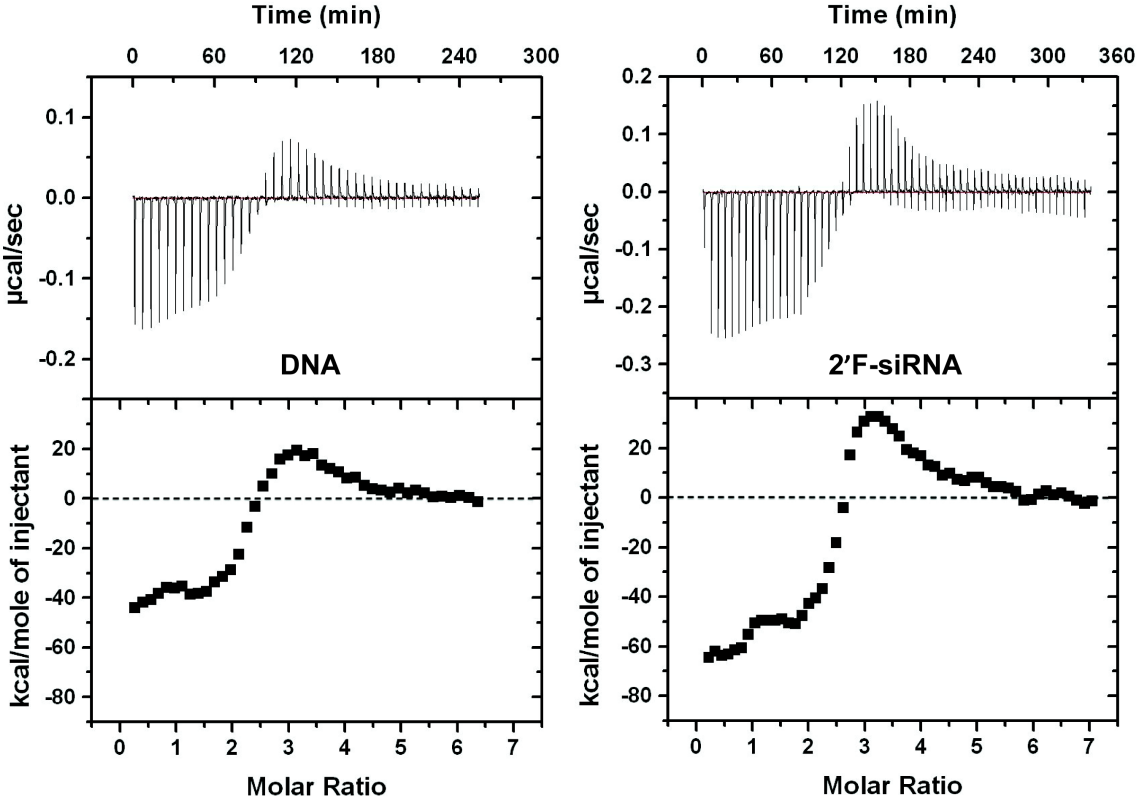

Fig. 2.11. Isothermal titration calorimetry of H3K(+H)4b binding to DNA and 2'-fluoro-siRNA.

The binding of H3K(+H)4b to DNA resembles its binding to 2'-fluoro-siRNA. The initial binding saturates at a reduced rate until the first transition point compared with unmodified siRNA, suggesting that 2'-hydroxl groups play a role in hydrogen bond formation.

The ITC data also shows that branched HK peptides have multiple binding stages upon titration into siRNA. As previously described, the transition from exothermic to endothermic reaction is attributed to aggregation induced by the charge neutralization. Nonetheless, the origin of the double peaks in the exothermic phase remained unclear. By replacing the branched HK with linear peptides or replacing

the siRNA with DNA oligonucleotides (Fig. 2.11), double exothermic peaks either regressed to one peak or became less significant. Therefore, we speculate that the complicated binding patterns are correlated with charge heterogeneity in the branched structure of peptides and/or the response of the siRNA duplex. Compared with DNA, dsRNA has narrow, deep major grooves and wide, shallow minor grooves, which differ in solvent accessibility. The second stage of binding may be initiated when hydrogen bond donors and acceptors buried in the major groove are exposed to branched HK peptides once the binding sites in the minor groove are saturated or the A-form structure is altered by initial binding event.

The HSQC spectroscopy established the involvement of histidines as potential hydrogen bond donors. Although the current technique does not allow us to identify the exact hydrogen bonds involving building blocks on siRNA, a study has shown that phosphate oxygens, hydroxyl groups of riboses, and oxygens or nitrogens of nucleobases of nucleic acids provide potential hydrogen bonds acceptors to the side chain of histidines (Chen, Kortemme et al. 2004). In a DNA- and RNA- binding protein-nucleic acids X-ray crystal structure database (Chen, Kortemme et al. 2004), the most common hydrogen bond acceptors are the phosphate oxygens. When we replaced the siRNA with a 19-mer DNA with similar sequence, however, the thermodynamic profile of H3K(+H)4b and DNA binding showed reduced exothermicity (initially -40 kcal/mol) and binding affinity. Even though H3K(+H)4b does not bind specifically to double stranded RNA, the energetic difference between RNA and DNA recognition suggests that, in addition to phosphates, minor grooves

and/or 2'-hydroxyl groups also form hydrogen bonds (Schmedt, Green et al. 1995; Bevilacqua and Cech 1996). In addition to DNA, a 2'-fluoro-modified siRNA was used to compare with unmodified siRNA binding to H3K(+H)4b to determine the role of 2'-hydroxyl groups. The binding patterns of 2'-fluoro-modified siRNA was indistinguishable from DNA duplex (Fig. 2.11), suggesting that hydrogen bond formation between H3K(+H)4b and the 2'-hydroxyl groups of unmodified siRNA. We speculate that the polyplex is stabilized by hydrogen bond networks that occupy potential binding sites of ribonucleases or competing binding proteins.

Both the ITC and HSQC data indicated that the overall contribution of hydrogen bonding increases at a pH below 7.3 (physiological), which leads us to explore how the siRNA escapes from polyplexes and endosomes. With the pKa of histidines being 6.3 or lower, we speculate that electrostatic repulsion between the histidines upon protonation in the acidic endosomes plays the dominant role in disrupting and/or unpacking the polyplexes (Fig. 2.12). Furthermore, various charged proteins in the cytosol interacting with the loosely-packed HK polyplex may have a complementary role in promoting decomposition of polyplexes. Unpacking of the polyplex could occur with further polyplex disruption into smaller and less dense smaller polyplexes, with monomeric HK siRNA units as part of the continuum. Upon unpacking of the polyplex, regardless of the extent of disruption, the protonated HK peptides would likely interact with negatively charged endosomal membranes, which would thus act similarly to detergents to aid in the escape of siRNA. This model is consistent with the data provided in this manuscript, as well as previous observations from Mixson's

laboratory and others (Chen, Zhang et al. 2002; Rehman, Hoekstra et al. 2013). Moreover, if the electrostatic repulsion in the acidic endosomes disrupts polyplexes to the extent of releasing "free" peptide, the secondary structure of H3K(+H)4b may enhance the membrane lytic activity (Medina-Kauwe, Xie et al. 2005). Accordingly, we propose a model in which the complexation of H3K(+H)4b and siRNA involves electrostatic interaction and hydrogen bonding, whereas decomplexation of polyplexes is induced by overcharging, disruption of the polyplex, and interaction of the peptide with the endosomal membranes (Fig. 2.12).

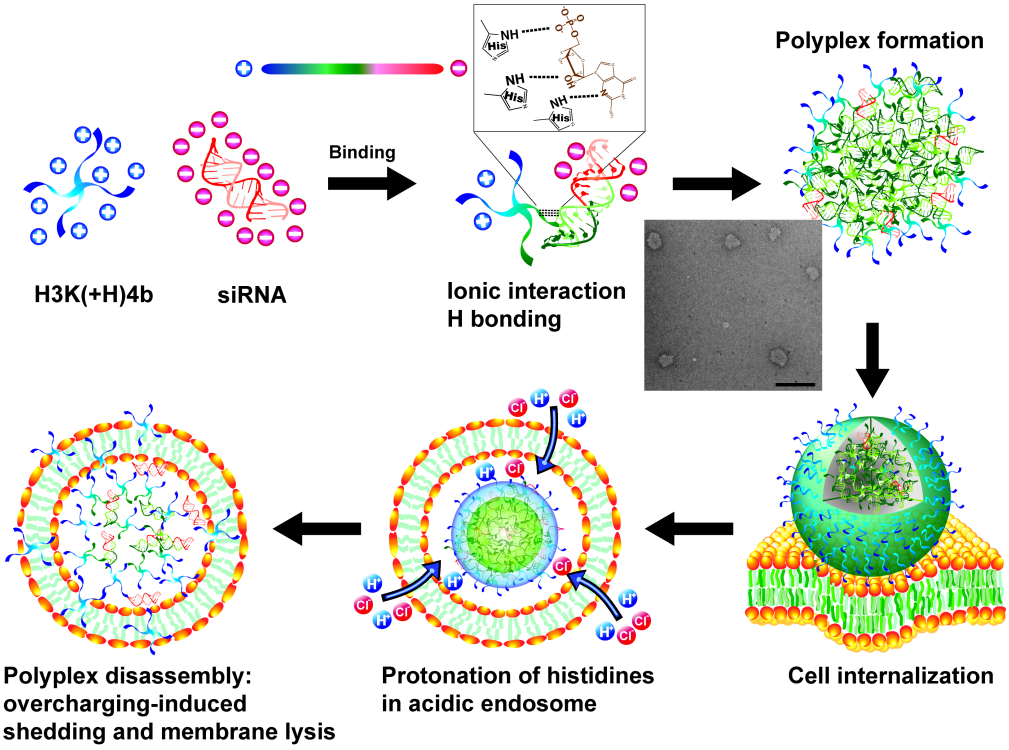

Fig. 2.12. Model of HK and siRNA binding illustrating compactness in serum and release (or partial release) in endosomes.

The colors blue, green, and red represent positive, neutral, and negative electrostatic potential, respectively. Hydrogen bonds are shown as dashed lines. Scale bar in the TEM figure, 500 nm.

2.6 Conclusion

Characterization of polyplex stability is considered one of the most important properties to understand for more effective carriers to be developed. My study demonstrates that non-ionic interactions between HK peptides and siRNA is essential for increased stability of HK polyplexes in serum compared to polylysine polyplexes. In particular, spectral shifts in the NMR established that the histidine component of HK formed hydrogen bonds with siRNA. Thus, in addition to the role of buffering endosomes by histidines, their formation of hydrogen-bonds with siRNA is likely a key reason why histidine-containing polyplexes are effective transfection and silencing agents. Moreover, the distinguishing features derived from structural and biophysical studies with HK peptides may be shared by other hydrogen-forming peptides and synthetic polymers, even those without imidazole groups. A fundamental understanding of vector-cargo interactions may establish evidence-based approaches to assess the potential of carriers for siRNA delivery.

Chapter 3: Selective Modification of HK Peptides Enhances siRNA Silencing of Tumor Targets *In Vivo*

3.1 Abstract

My research has focused on systemic delivery of small interference RNA (siRNA) by branched peptides composed of histidine and lysine, called HK peptides. After studying several histidine-lysine (HK) peptides, one four-branched peptide, H3K(+H)4b, with a predominant repeating pattern of -HHHK-, was found to be an effective carrier of siRNA in vitro and in vivo. Although the unmodified H3K(+H)4b carrier of siRNA targeting an oncogene was previously shown to have promise in a tumor-bearing mouse model, we sought to develop a more effective HK carrier of siRNA in the current study. My primary goal was to determine whether different ligand (cyclic RGD)-PEGylation patterns on the H3K(+H)4b peptide affect siRNA delivery *in vitro* and *in vivo*. We compared the unmodified H3K(+H)4b with two modified H3K(+H)4b peptides for their ability to deliver siRNA in a tumor-bearing mouse model; one modified HK peptide, $(RGD\text{-}PEG)^4$H3K(+H)4b, had four cyclic RGD polyethylene glycol (cRGD-PEG) conjugates per molecule, whereas the other peptide, (RGD-PEG)H3K(+H)4b, had one cRGD-PEG per molecule. Although the modified HK peptides by themselves did not form stable polyplexes with siRNA, combination of a highly charged unmodified HK peptide, H2K4b, with either of the modified HK peptides did form stable siRNA polyplexes. For *in vitro* experiments

with MDA-MB-435 cells that expressed luciferase, the H3K(+H)4b/siRNA polyplexes targeting luciferase decreased its activity by 90% compared with negligible down-regulation by the modified H3K(+H)4b polyplexes ($P < 0.01$). In contrast, the two modified H3K(+H)4b/siRNA polyplexes administered intravenously were more effective than the H3K(+H)4b polyplexes in silencing luciferase in a tumor xenograft model. The luciferase activity in tumor lysates of mice administered H3K(+H)4b, (RGD-PEG)H3K(+H)4b, and $(RGD\text{-}PEG)^4$H3K(+H)4b polyplexes decreased by 18%, 35%, and 75%, respectively. Thus, the siRNA polyplex incorporating the highly modified peptide, $(RGD\text{-}PEG)^4$H3K(+H)4b, was the most effective at silencing its target *in vivo* ($P < 0.01$). These studies demonstrate that selectively modified HK polymers are promising candidates for targeting oncogenes with siRNA.

3.2 Introduction

RNAi is a promising research and therapeutic strategy, utilized to down-regulate aberrant disease-causing genes and to study genes important for signal transduction pathways. The RNAi process is activated by incorporation of a 19 to 23-mer double stranded RNA fragment (siRNA) into the RISC complex (Fire, Xu et al. 1998). Together with the Argonaut 2 endonuclease that is part of the RISC complex, the siRNA recognizes and cleaves the target mRNA in a catalytic manner (Hammond, Bernstein et al. 2000; Bernstein, Caudy et al. 2001; Hammond, Boettcher et al. 2001;

Reynolds, Leake et al. 2004). To realize the potential of siRNA as a therapeutic agent, an effective delivery system for siRNA is essential to facilitate specific targeting and cellular uptake in the target tissue, particularly for systemic diseases such as cancer. Indeed, the development of an efficient delivery system for nucleic acids including siRNA has proved elusive and has been the rate-limiting step in developing siRNA-based therapeutics.

Nevertheless, there are many promising carriers for siRNA in various stages of pre-clinical and clinical trials, including synthetic polymers, aptamers, neutral and cationic liposomes, and peptides (Schiffelers, Ansari et al. 2004; Morrissey, Lockridge et al. 2005; Song, Zhu et al. 2005; Bartlett and Davis 2008; Kim, Jeong et al. 2008; Merritt, Lin et al. 2008; Peer, Park et al. 2008; Dassie, Liu et al. 2009; Mu, Nagahara et al. 2009). Currently, no systemic carrier of siRNA has fully been proven effective for clinical use against cancer, but evidence points to a need for ligand-mediated tissue targeting and a preference for polyplex forms. Moreover, it is likely that non-viral carriers will continue to evolve for the foreseeable future, with progressive improvements. To this end, Mixson's lab has focused on developing an effective *in vitro* and *in vivo* vehicle for small interference RNA. To accomplish this, we have synthesized and screened a number of histidine-lysine rich peptides (HK)(Chen, Zhang et al. 2001; Chen, Zhang et al. 2002; Leng and Mixson 2005; Leng, Scaria et al. 2005) testing their ability to carry and deliver siRNA to give effective gene inhibition. While lysines are essential for binding siRNA, histidines are important for buffering and may aid in the release of siRNA from endosomes.

Altering the sequence of histidines and lysines within the branches of the HK polymer can affect its ability to transport siRNA within the cell. After studying several HK peptides, one 4-branched form, H3K(+H)4b, with predominant repeating patterns of -HHHK-, was determined to be an effective carrier of siRNA; the H3K(+H)4b/siRNA polyplexes targeting the Raf-1 oncogene inhibited tumor growth by 60% (Leng, Scaria et al. 2008).

In the current study, we sought to develop a more effective ligand targeted form of the H3K(+H)4b/siRNA polyplex, particularly for use *in vivo*. In order to prevent aggregation and to selectively target the tumor with the polyparticle, the H3K(+H)4b was modified by varying the number and location of cRGD-PEG conjugates. Two modifications of H3K(+H)4b were made: one highly modified HK polymer in which an cRGD-PEG was attached to each branch (four cRGD-PEG per molecule) and the other, a more limited HK modification in which the cRGD-PEG was attached to the $(Lys)_3$ core that generates the branched polypeptide (one cRGD-PEG per molecule). Compared to the unmodified H3K(+H)4b, both modified HK peptides when combined with an unmodified HK peptide were markedly more effective carriers of siRNA to tumors in a murine model. Moreover, the siRNA polyplex containing the highly modified HK was the most effective in silencing the target gene in tumor xenografts.

3.3 Materials and Methods

3.3.1 Animals

Female athymic mice (4-8 wk old) were purchased from NCI (Frederick, MD). The experiments were done in accordance with regulations by the Institutional Animal Care and Use Committee of the University of Maryland Baltimore.

3.3.2 Cell line

A human malignant cell line MDA-MB-435, stably expressing Firefly luciferase, was cultured in Dulbecco's minimal essential medium (DMEM) containing 10% fetal calf serum (FCS) and 20 mM glutamine.

3.3.3 Synthesis, sequences, and chemical modification of HK peptides

The branched HK polymer was synthesized on a Rainin Voyager synthesizer (PTI, Tucson, AZ) by the biopolymer core facility at the University of Maryland, as previously described. The unmodified four branched H3K(+H)4b and H2K4b polymers, with dominant repeating patterns of -HHHK- and -HHK-, respectively, were synthesized as described previously (Leng, Scaria et al. 2005). The four terminal branches of the HK polymers emanate from the 3-lysine core: for H3K(+H)4b, the branch sequence is KHHHKHHHKHHHHKHHHK and for H2K4b, the branch sequence is KHKHHKHHKHHKHHKHHKHK. For modified

H3K(+H)4b, a cysteine was added to each of the four N-terminal branches or to the C-terminal end of the lysine core. Cyclic (c)RGD-PEG was conjugated to the HK polymer using a synthesis procedure similar to one previously described (Schiffelers, Ansari et al. 2004). Briefly, cyclic RGD peptide with the sequence c(RGDfK) (purchased from Peptides International, Louisville, KY) was coupled to 3.4 kD PEG using a heterobifunctional PEG, SCM-PEG-VS, from Nektar Therapeutics (Huntsville, AL), in dry DMSO in equimolar ratio. The cRGD-PEG conjugate was precipitated from DMSO by adding 10 fold excess of anhydrous cold ether. The resulting solid material was dried, characterized and used for coupling to H3K(+H)4b. The cRGD-PEG-VS conjugate obtained was then reacted with H3K(+H)4b consisting of cysteine at the N-terminus of each of the four branches (for $(RGD\text{-}PEG)^4$-H3K(+H)4b) or C-terminus (for (RGD-PEG)H3K(+H)4b) at pH 7.3 (HEPES buffer), to obtain the cRGD-PEG modified polypeptides. The modified H3K(+H)4b peptides were purified by dialysis and characterized by amino acid analysis. The resulting conjugates on average had one (for (RGD-PEG)H3K(+H)4b) or four (for $(RGD\text{-}PEG)^4$H3K(+H)4b)) cRDG-PEG moieties, based on amino acid analysis of the purified conjugates.

3.3.4 siRNA

The siRNA duplex targeting luciferase (Luc) was as follow: sense, 5'-CUG-CAC-AAG-GCC-AUG-AAG-A-dTdT-3'; antisense, 5'-UCU-UCA-UGG-CCU-UGU-GCA-G-dTdT-3', targeting 5'-CUG-CAC-AAG-GCC-AUG-AAG-A-3'. The 2-O-methyl (2'OMe) siRNA for the luciferase was similar to the unmodified siRNA

except that the uridines in the sense strand had 2-OMe modifications. The control siRNA was siGENOME Non-Targeting siRNA #3, sense 5'-AUG-UAU-UGG-CCU-GUA-UUA-G-dTdT-3'; antisense, 5'-CUA-AUA-CAG-GCC-AAU-ACA-C-dTdT-3' (Dharmacon, Lafayette, CO).

3.3.5 Gel retardation assay

The amount of HK polymer (modified and/or unmodified) to neutralize siRNA was determined by the gel retardation assay. Varying amounts of HK peptides were mixed with 1 μg of siRNA and incubated for 30 minutes at room temperature. Specifically, the following HK:siRNA ratios (w/w or w/w/w) were prepared in water: 1) H3K(+H)4b:siRNA (1:1; 1.5:1; 2:1; 2.2:1; 2.5:1); 2) (RGD-PEG)H3K(+H)4b/H2K4b:siRNA and 3) $(RGD\text{-}PEG)^4$H3K(+H)4b)/H2K4b:siRNA (3/0.6:1; 4/0.6:1; 6/0.6:1; 3/0.8:1; 4/0.8:1; 6/0.8:1). After the HK/siRNA polyplex was loaded onto the gel (3 % agarose), electrophoresis was carried out at a constant voltage of 75 V for 45 minutes in TBE buffer containing ethidium bromide. The siRNA band densities were then visualized under a UV transilluminator at a wavelength of 365 nm. On the basis of fluorescence (UN-SCAN-IT; Silk Scientific, Orem, UT) of siRNA that had migrated into each lane, the stability of HK/siRNA polyplex was determined. A gel retardation assay was also done on each *in vivo* HK siRNA preparation injected into the mice. Gel retardation assays similar to those described above were also carried out with HK polyplexes after exposing them to various concentrations of serum to assess their stability.

3.3.6 Particle size and surface charge analysis

Particle size was measured on all HK polyplexes by dynamic light scattering (DLS) with the N4 plus particle size analyzer on HK polyplexes (Beckman Coulter Corp., Miami, FL). The zeta potential was measured by Delsa 440 SX instrument (Coulter) on HK/siRNA polyplexes that were used for *in vivo* studies.

3.3.7 HK siRNA nanoparticle preparation

For *in vitro* experiments, HK/siRNA polyplexes were prepared as previously described (Leng, Scaria et al. 2005; Leng, Scaria et al. 2008) by briefly mixing siRNA (1 μg) in 50 μl of OptiMEM (Invirtrogen, Carlsbad, CA) with various amounts of HK peptides. The siRNA polyplexes were maintained at room temperature for 30 min prior to size measurements and/or incubation with cells or serum. The ratios for HK to siRNA were based on gel retardation assays with additional ratios tested for *in vitro* bioluminescent assays.

For tumor xenografts experiments *in vivo*, mice were treated by injection in the tail vein with HK polyplexes containing 40 μg of luciferase or control siRNA. After the polymers were mixed with the siRNA, the resulting polyplex formed at room temperature for 40 minutes. Each mouse was then treated by i.v. injection with 300 μl of the polyplexes. The ratios of polymers to siRNA for *in vivo* bioluminescent studies were based on the gel retardation and particle size measurements.

3.3.8 Stability of HK polyplexes in serum

With one microgram of siRNA in complex with the optimal amount of unmodified H3K(+H)4b or the two modified cRGD-PEG H3K(+H)4b peptides, the polyplexes (2 ml) were incubated with increasing concentrations (0%, 10%, 50% and 75%) of mouse serum (total volume 10 μl) for 1 h at room temperature. The gel retardation assay was used to test the stability of the polyplexes in serum.

3.3.9 Cellular uptake

Cells (1×10^5) were incubated with different carriers (H3K(+H)4b, (RGD-PEG)-H3K(+H)4b/H2K4b, or $(RGD\text{-}PEG)^4$H3K(+H)4b/H2K4b) in complex with Cy3 labeled-siRNA (IDT, Coralville, IA). After 4 h, cells were fixed in formaldehyde for 5 min; the nuclei were stained with chromatin dye Hoechst 33342 (Invitrogen, Carlsbad, CA) in PBS for 5 min. Confocal images were obtained with a Zeiss LSM510 laser scanning confocal microscope (Carl Zeiss, Thornwood, NY).

3.3.10 *In vitro* bioluminescence assays

MDA-MB-435 cells expressing luciferase were plated in a 24-well plate (0.5 ml of DMEM, 10% serum) at a density of 3×10^4 cells/well. Various peptides and peptide combinations (H3K(+H)4b, (RGD-PEG)H3K(+H)4b, $(RGD\text{-}PEG)^4$H3K(+H)4b, (RGD-PEG)H3K(+H)4b/H2K4b, and $(RGD\text{-}PEG)^4$H3K(+H)4b/H2K4b, in complex with Luc-siRNA (1 μg), were prepared as described previously, and polyplexes were incubated with MDA-MB-435 cells for 48 h. The HK to siRNA ratios that were

tested for *in vitro* bioluminescent experiments were as follows: H3K(+H)4b:siRNA, 2.2:1, 4:1, 6:1; (RGD-PEG)H3K(+H)4b:siRNA, 2:1, 4:1, 6:1; $(RGD\text{-}PEG)^4$-H3K(+H)4b:siRNA, 2:1, 4:1, 6:1; (RGD-PEG)H3K(+H)4b/H2K4b:siRNA, 2/0.8:1, 3/0.8:1; 6/0.8:1; $(RGD\text{-}PEG)^4$H3K(+H)4b/H2K4b:siRNA, 2/0.8:1, 4/0.8:1, 6/0.8:1.The cells were then exposed to lysis buffer (200 μl) (Promega, Madison, WI) followed by centrifugation at 12,500 rpm for 5 min. The luciferase activities in the supernatant fraction were measured by a Turner TD 20/20 luminometer (Promega).

3.3.11 *In vivo* bioluminescence experiments

a. Tumor lysates: MDA-MB-435 xenografts that stably expressed luciferase were established by injecting 2 x 10^6 cells into midclavicular line of female nude mice (NCI Frederick). After tumor reached about 50 mm^3, mice were separated into five treatment groups: untreated, H3K(+H)4b/Luc siRNA (w/w, 2.2/1), (RGD-PEG)H3K(+H)4b/H2K4b/Luc siRNA (w/w/w, 3/0.8/1), and $(RGD\text{-}PEG)^4$H3K(+H)4b/H2K4b/Luc siRNA or control siRNA (w/w/w, 4/0.8/1). These HK polyplexes containing 40 μg of siRNA were administered via the tail veins. Forty-eight hours after inoculation of the polyplexes, the mice were euthanized and luciferase activity was then measured in tumor homogenates. After determining the most effective carrier, time course and 2'OMeLuc siRNA experiments were performed in a similar manner. Tumor volume was determined using the formula 1/ 2 × length × $width^2$.
b. Bioluminescence Imaging: The protocol for preparation and inoculation of

HK/siRNA polyplexes in tumor- bearing mice was similar to tumor lysate experiments except that the IVIS-200 optical imaging system (Xenogen Corp., Almeda, CA) measured tumor luciferase activity in real-time in living mice. At the time of imaging, mice were anesthetized with a 2.5% isofluorane/oxygen mixture and injected i.p. with 150 mg/kg of D-Luciferin (Caliper LifeSciences, Hopkinton, MA); photon emission was measured 15 min after the administration of luciferin. To standardize the photon emission (i.e., RLU), the region of interest at times 0 and 48 h were of equal size.

3.3.12 Cytokine measurements

A multiplex bead-based assay using Luminex technology was used to measure serum levels of mouse INF-α, INF-γ, TNF-α, and IL-6 as described by manufacturer (Upstate Waltham, MA). Levels of mouse INF-α were measured with an ELISA kit as described by the manufacturer (PBL Biochemical Laboratories, Piscataway, NJ). These assays were done by the cytokine core facility at the University of Maryland School of Medicine.

3.3.13 Statistics

Since the number of observation is too small to be assumed a normal distribution, results comparing multiple groups were analyzed by Kruskal Wallis one-way analysis of variance on ranks (GraphPad Prism 6.0, La Jolla, CA). Wilcoxon rank-sum test was used, where appropriate, for pair-wise comparisons. Values shown represent

means, and error bars represent standard deviation. In all cases, differences were considered to be statistically significant when the *P* values were < 0.05.

3.4 Results

3.4.1 Optimization of HK/siRNA polyplexes

To determine appropriate HK and siRNA ratios for *in vivo* studies, gel retardation assays (Kim, Jeong et al. 2006; Huh, Lee et al. 2010; Ofek, Fischer et al. 2010) and particle size measurements using dynamic light scattering (DLS) were used to facilitate development of siRNA polyplexes. Moreover, we have previously found that plasmid polyplexes formed with HK peptides that were approximately 100 to 150 nm in size were effective in transfection of tumor xenografts (Leng, Scaria et al. 2006). Therefore, we examined various ratios of HK to siRNA to determine the minimal amount of HK that would form polyplexes retaining approximately 90% or more of the siRNA in the loading well and that would result in a polyplex with a diameter of 150 nm or less (Fig. 3.1). For H3K(+H)4b, the lowest ratio to retard siRNA and still be associated with the smallest particle size was 2.2/1 (w/w) (ratio, 4/1). At this ratio, about 92% of the siRNA was retarded and the size of the siRNA polyplex was 149 ± 41 nm. In contrast to the unmodified H3K(+H)4b, both modified HK were unable to retard siRNA, even at very high ratios (i.e., 7/1, N/P). Moreover, at any ratio of the modified HK polymers to siRNA, the particle size of the siRNA polyplex could not be determined by DLS (data not shown). As a result, we

combined an unmodified H2K4b peptide that has a high lysine content and greater condensing properties with the modified H3K(+H)4b polymers to enable greater siRNA binding. For the modified polymer with only one cRGD-PEG conjugated to its core, the optimal (RGD-PEG)H3K(+H)4b/H2K4b/siRNA ratio was 3/0.8/1 (w/w/w; N/N/P ratio, 4/1/1); this ratio resulted in 99% retardation of the siRNA and a nanoparticle size of 147±51 nm. For the highly modified HK, the selected $(RGD\text{-}PEG)^4$H3K(+H)4b/H2K4b/siRNA ratio was 4/0.8/1 (w/w/w; N/N/P ratio 3/1/1), the minimum amount of HK polymer to produce a stable polyplex. These selected ratios for unmodified and modified polymers to siRNA were used in subsequent experiments although additional ratios were also evaluated for *in vitro* gene silencing experiments. At these selected ratios, polyplexes containing the H3K(+H)4b, (RGD-PEG)H3K(+H)4b, and $(RGD\text{-}PEG)^4$H3K(+H)4b had zeta potentials of 37, 17.3, and 16.7 mV, respectively. Notably, the amount of H2K4b used in siRNA polyplexes that also incorporated modified H3K(+H)4b was not sufficient to neutralize the negatively charged siRNA; the H2K4b/siRNA ratio of 0.8/1 (w/w) retained only 35% of the siRNA in the gel retardation assay (data not shown).

3.4.2 *In vitro* evaluation of HK peptides as carriers of siRNA

We also tested the ability of unmodified and modified HK/siRNA polyplexes to down- regulate luciferase stably expressed in MDA-MB-435 cells. Of note, MDA-MBA-435 cells have elevated levels of the $\alpha_V\beta_3$ integrin, the receptor for cRGD (Felding-Habermann, O'Toole et al. 2001). The unmodified H3K(+H)4b or the two modified H3K(+H)4b with and without H2K4b were used as carriers of a luciferase-

targeting siRNA *in vitro*. Unmodified H3K(+H)4b polyplexes inhibited luciferase activity by approximately 90%, while the polyplexes containing only modified HK peptides had minimal activity (Fig. 3.2A). In addition, the polyplexes with the modified HK combined with H2K4b had no activity across several HK:siRNA ratios. These functional siRNA assays correlated with fluorescent uptake studies. That is, significant numbers of large intracellular particles from the unmodified H3K(+H)4b/siRNA polyplexes accumulated intracellularly after four hour of incubation while the modified HK/siRNA polyplexes showed a diffuse fluorescence pattern similar to the siRNA control (Fig. 3.2B). Similar fluorescence patterns were observed at different time points (data not shown).

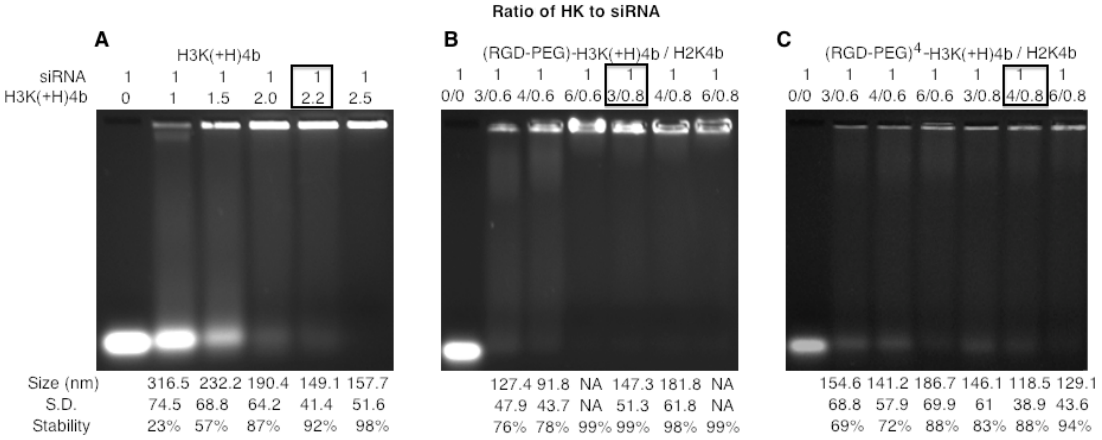

Fig. 3.1. Gel retardation assay

To determine the amount of HK that retards siRNA migration, various ratios of unmodified H3K(+H)4b (A) or modified HK combinations (B, (RGD-PEG)-H3K(+H)4b/H2K4b; C, $(RGD\text{-}PEG)^4$H3K(+H)4b/H2K4b) in complex with siRNA (1 μg) were prepared and then subjected to gel electrophoresis for 30 minutes (3% gel). Different ratios of HK polymers to siRNA are represented above the gel and the particle size is shown below the gel. For the modified HK groups (b,c), modified and unmodified polymers (H2K4b) were mixed for more complete retardation of siRNA. The ratio enclosed in the box represents the selected *in vitro* and *in vivo* silencing conditions based on the size of the particle (less than 150 nm) and siRNA retardation. NA represents polyplexes in which the size could not be determined by dynamic light scattering.

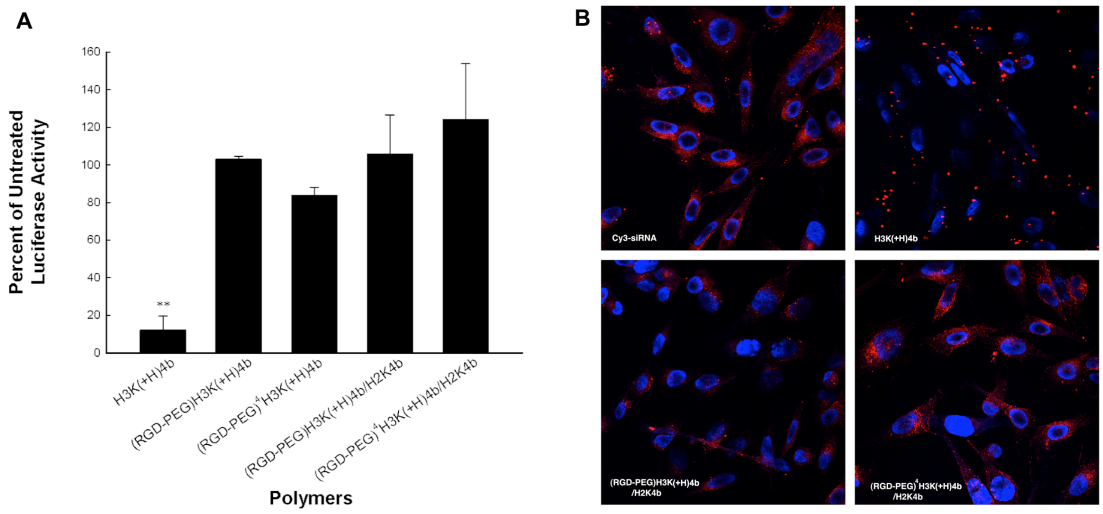

Fig. 3.2. *In vitro* comparison of HK polymers as carriers of siRNA

(A) Several HK or combination of HK carriers (H3K(+H)4b, (RGD-PEG)H3K(+H)4b, (RGD-PEG)^{4}H3K(+H)4b, (RGD-PEG)H3K(+H)4b/H2K4b, (RGD-PEG)^{4}H3K(+H)4b/H2K4b) of Luc siRNA were tested for their abilities to inhibit luciferase expression in MDA-MB-435 cells compared with the untreated group. H3K(+H)4b was the most effective carrier down- regulating expression by nearly 90%, whereas inhibition by other carriers was negligible. The data represent the mean ± SD of luciferase of six determinations for each carrier. **, $P < 0.01$; H3K(+H)4b vs. modified HK carriers. (B) Comparison of uptake of different HK/siRNA polyplexes. A number of discrete intracellular fluorescent particles of siRNA were observed with unmodified H3K(+H)4b carriers, whereas the combination of modified and unmodified HK/siRNA polyplexes showed diffuse intracellular fluorescence- similar to the fluorescence pattern observed with the siRNA alone. Images were obtained by a Zeiss LSM510 laser scanning confocal microscope. The HK to siRNA ratios were as follows: H3K(+H)4b:siRNA, 4:1; (RGD-PEG)H3K(+H)4b, 4:1; (RGD-PEG)^{4}H3K(+H)4b, 4:1; (RGD-PEG)-H3K(+H)4b/H2K4b, 3/0.8:1; (RGD-PEG)^{4}H3K(+H)4b/H2K4b, 4/0.8:1.

3.4.3 *In vivo* evaluation of HK peptides as carriers of siRNA

Similar to the *in vitro* study, we screened numerous HK polymers in complex with Luc siRNA for their ability to inhibit luciferase in tumor xenografts. After MDA-MB-435 tumors expressing luciferase grew to approximately 50 mm^3, the mice were divided into various treatment groups and treated by injection with the different HK

Luc siRNA polyplexes. After 48 h, the mice were euthanized and the tumor lysates were evaluated for luciferase activity. The group treated with (RGD-PEG)^{4}H3K(+H)4b/H2K4b in complex with Luc siRNA was the most effective in silencing the tumor luciferase activity (Fig. 3.3), with activity reduced by about 75% ($P < 0.01$; (RGD-PEG)^{4}H3K(+H)4b/H2K4b vs. other carriers and control groups). The unmodified H3K(+H)4b and (RGD-PEG)H3K(+H)4b/H2K4b polyplexes reduced tumor luciferase activity by 18 and 35%, respectively ($P < 0.05$; (RGD-PEG)-H3K(+H)4b/H2K4b vs. unmodified H3K(+H)4b or untreated). Thus, the highly modified HK polyplex formulation was the most effective. To determine whether reduction of tumor luciferase was based on the specificity of the siRNA mechanism, a non-targeting siRNA in complex to the most effective carrier, (RGD-PEG)^{4}H3K(+H)4b/H2K4b, was used as the negative control *in vivo*. There was approximately 20% inhibition for the non-targeting siRNA polyplex, suggesting that the Luc siRNA specifically inhibited luciferase expression.

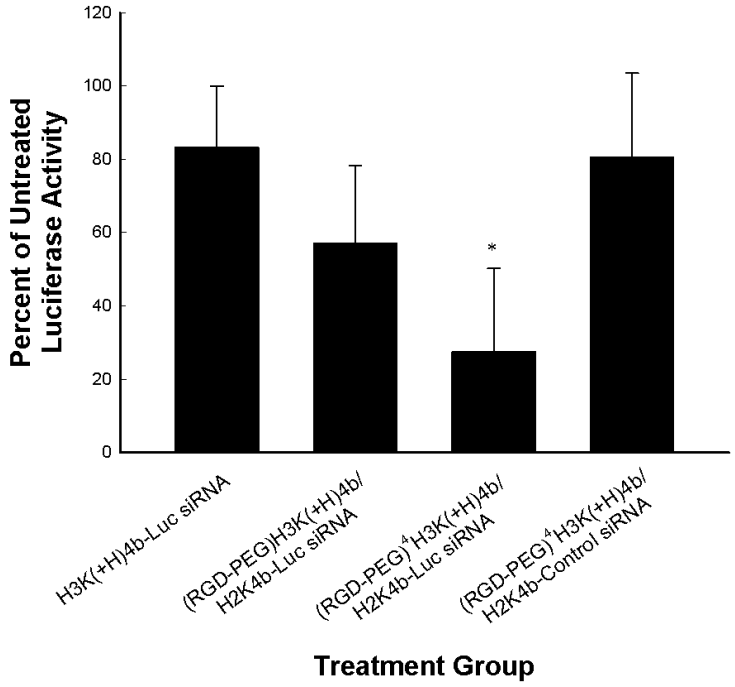

Fig. 3.3. *In vivo* evaluation of HK polymers to determine most effective carrier for Luc-siRNA

Four HK siRNA preparations (three HK-Luc siRNA; one HK-control siRNA) were compared for their ability to silence luciferase expression in MDA-MB-435 xenografts. The modified HK peptide, $(RGD\text{-}PEG)^4H3K(+H)4b/H2K4b$, of Luc siRNA was the most effective, reducing luciferase expression in tumor xenografts by 75%. HK:siRNA ratios used in this experiment were chosen based on the gel retardation assays. The data represent the mean ± SD of luciferase of six determinations for each carrier. *, $P < 0.05$; $(RGD\text{-}PEG)^4H3K(+H)4b/H2K4b$ carrier vs. other carriers and control groups.

We also confirmed the tumor lysate studies with the Xenogen optical imaging system and demonstrated that highly modified H3K(+H)4b polyplexes significantly suppressed luciferase activity in tumor xenografts (Fig. 3.4). Mice treated with the highly modified H3K(+H)4b/H2K4b combination in complex with Luc-siRNA had decreased luciferase activity in tumors of 63 ± 15% compared to luciferase activity of tumors in untreated mice (P = 0.01, n = 3). For untreated mice, the RLU was 7.47

$\pm 1.71 \times 10^5$ at time 0, and $9.43 \pm 2.33 \times 10^5$ 48 h later, whereas for treated mice, the RLU was $7.78 \pm 1.90 \times 10^5$ at time 0, and $3.08 \pm 0.59 \times 10^5$ at 48 h. The regions of interest at time 0 and 48 h for RLU determinations were equal in size.

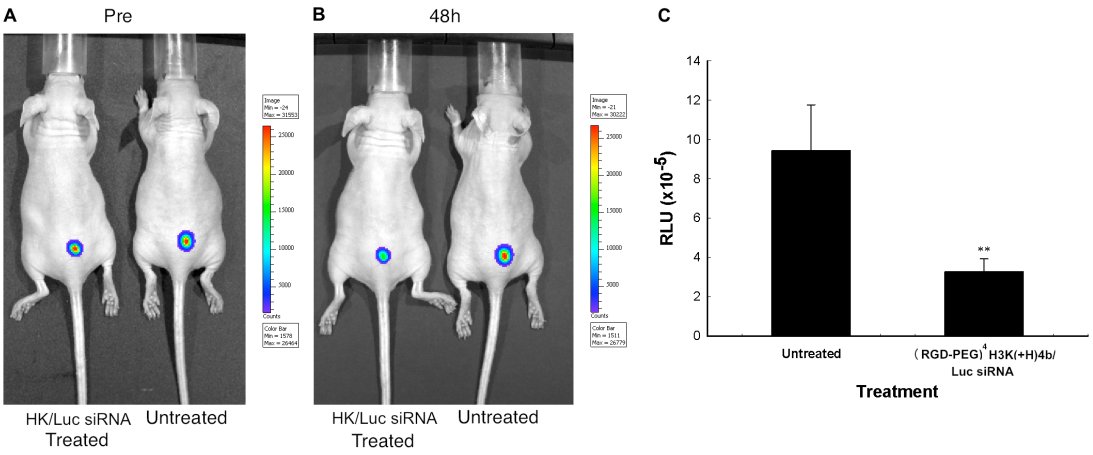

Fig. 3.4. Bioluminescence imaging

Bioluminescence imaging was performed with the Xenogen IVIS 200 system. Mice bearing tumor xenografts were separated into two groups after the tumor size reached 50 mm^3 and this experiment was repeated three times. (A) and (B) show tumor images of representative mice taken before treatment and 48 h after treatment, respectively. The mouse on the right in (A) and (B) was untreated; the mouse on the left of (A) and (B) was treated with $(RGD\text{-}PEG)^4$H3K(+H)4b/H2K4b/Luc siRNA polyplex (designated HK/Luc siRNA) by tail vein injection. The mouse treated with siRNA showed a marked down-regulation of luciferase. (C) This shows the mean of the experiments comparing untreated mice with treated mice (n=3). In mice treated with luciferase siRNA, luciferase activity was reduced by 63.14 ± 15.18%. **, P = 0.01; siRNA treated vs. untreated.

3.4.4 Time course of siRNA-mediated luciferase inhibition *in vivo*

To determine the duration of Luc silencing in the MDA-MB-435 xenografts, a time course was done with the most effective polyplex, $(RGD\text{-}PEG)^4$-H3K(+H)4b/H2K4b/Luc siRNA. After HK/siRNA polyplex injection, inhibition of luciferase activity was 71% at 24 h, 75% at 48 h, and 46% at 72 h compared to untreated controls (Fig. 3.5). These findings suggest that the optimal time interval for

dosing may be about 3 days for rapidly dividing tumor cells to obtain maximum tumor growth inhibition (Bartlett and Davis 2006; Bartlett, Su et al. 2007; Bartlett and Davis 2008).

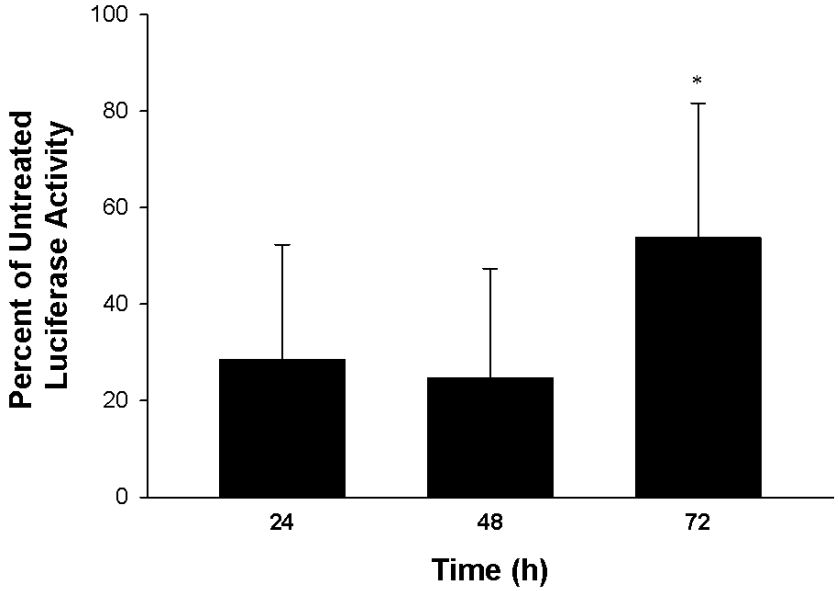

Fig. 3.5. Time course of siRNA induced luciferase activity reduction

Tumor-bearing mice were injected with the optimal HK/Luc siRNA polyplex and luciferase activity was determined from tumor lysates at 24, 48, or 72 h. Compared to activity before treatment, luciferase activity was down-regulated by 71%, 75% and 46% at 24 h, 48 h, and 72 h respectively. *, $P < 0.05$; 72 h vs. 24 and 48 h time point. The data for each time point represent the mean ± SD of luciferase.

3.4.5 Cytokine induction by HK/siRNA polyplexes

Cationic carriers in complex with siRNA can induce cytokines which in turn can result in cellular toxicity and/or inhibit gene expression in tumors by an indirect mechanism (Hornung, Guenthner-Biller et al. 2005; Judge, Sood et al. 2005; Kim, Choung et al. 2007; Zamanian-Daryoush, Marques et al. 2008). Thus, luciferase activity may be reduced due to intra-tumoral cytokine induction and tumor cell

apoptosis, non-specific mechanisms other than siRNA-mediated gene silencing. To minimize cytokine induction by the siRNA polyplex *in vivo*, the sense strand of the siRNA can be modified by cautious addition of a methyl group to the 2'-hydroxyl group of the ribose without significantly affecting the biological activity of the siRNA (Robbins, Judge et al. 2007). In $(RGD\text{-}PEG)^4$H3K(+H)4b/H2K4b polyplexes, a 2'O-methylated Luc siRNA was compared to unmodified Luc siRNA. If cytokine induction resulted in a non-specific cytotoxic effect from the polyplexes, then the unmodified siRNA polyplex would likely be more effective at reducing luciferase activity compared to the 2'-OMe luciferase polyplex. As shown in Fig. 3.6A, however, there were no significant differences between the unmodified and 2'-OMe siRNA tumor-bearing treatment groups; the decrease in luciferase activity was 80% in the 2'-OMe siRNA group vs. 75% in the unmodified siRNA group. Furthermore, the HK in complex with siRNA (unmodified or 2'-OMe modified) did not induce higher cytokine levels (IL-6, INF- α, INF-γ, and TNF-α) compared to the untreated groups (Fig. 3.6B). The cytokine levels in three groups were very low in comparison to DOTAP liposomal siRNA complexes, particularly for INF-α (INF-α, 754 pg/ml). Together, these data indicate that modified HK/siRNA polyplexes administered i.v. did not increase the level of cytokines in mice and cytokine induction by the HK/siRNA polyplex did not have a significant role in decreased expression of luciferase in the tumors.

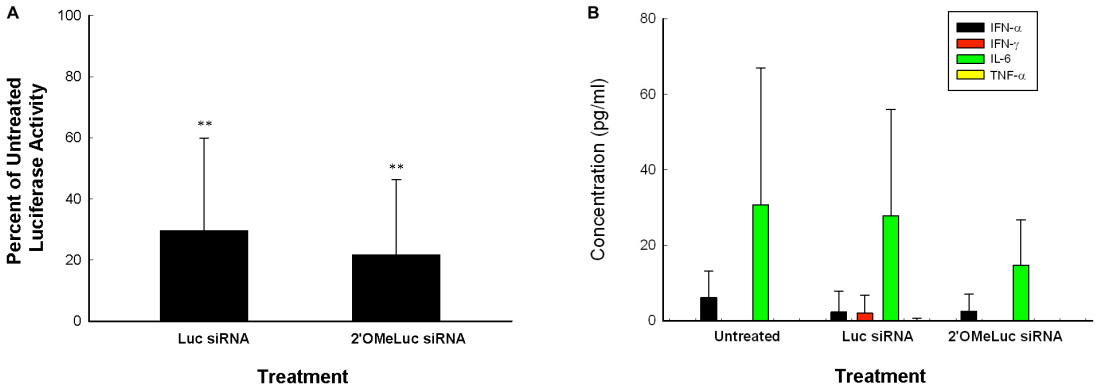

Fig. 3.6. Effect of induced cytokines on luciferase activity.

(A) Unmodified and 2'OMeLuc siRNA in complex with the optimal HK combination were compared for their ability to reduce luciferase activity in tumor xenografts. The reduction in luciferase activity was similar in the two groups (75% with unmodified vs. 80% with 2'OMeLuc siRNA), indicating that silencing was not due to induction of cytokines. The data represent the mean ± SD of luciferase activity of five determinations for each carrier. **, $P < 0.01$; siRNA treated vs. untreated. (B) Serum cytokine levels in MDA-MB-435 bearing mice were measured in untreated, optimal HK-Luc siRNA and optimal HK-2'OMe-Luc siRNA treatment groups. No differences were detected in the cytokine levels among the different treatment groups.

3.4.6 Nuclease stability of HK/siRNA polyplexes

The integrity of HK/siRNA polyplex may be sensitive to the serum components *in vivo* (Buyens, Meyer et al. 2010). PEGylated polymers may augment the stability of the polyplex, by reduced binding of serum components. To investigate their stability in mouse serum, HK polyplexes were incubated in the presence of varying amounts of serum for one hour at room temperature and then analyzed by gel electrophoresis (3% agarose). As shown in Table 1, increased dissociation of siRNA was observed from all carriers as the serum concentration was increased to 50% and above. Among the polyplexes, the unmodified H3K(+H)4b/siRNA polyplexes were less stable than the modified HK polyplexes. There was little difference in the stability in serum between the two modified HK polyplexes.

Table 3.1. Stability of HK/siRNA polyplexes in serum

[Serum] Peptides	0%	10%	50%	75%
H3K(+H)4b	89.99% ± 0.77%	87.18% ± 1.39%	64.62% ± 3.38%**	51.46% ± 3.20%**
(RGD-PEG)H3K(+H)4b/H2K4b	94.93% ± 0.26%	92.89% ± 2.21%	83.58% ± 2.46%	73.32% ± 2.18%
$(RGD\text{-}PEG)^4$H3K(+H)4b/H2K4b	88.09% ± 3.33%	95.12% ± 0.42%	84.09% ± 0.43%	75.41% ± 3.37%

Unmodified H3K(+H)4b and modified H3K(+H)4b/H2K4b carriers in complex with siRNA were incubated at various concentrations of mouse serum (0%, 10%, 50% and 75%) for 1 hr. Gel retardation was then used to measure the stability of the polyplexes as described in the Methods section. Compared to unmodified H3K(+H)4b/siRNA polyplexes, the two PEGylated HK polyplexes had greater stability at high serum concentration (50%, 75%); **, $P < 0.01$. The data represent the mean ± SD of measurement of 3 determinations for each carrier.

3.5 Discussion

To develop more effective carriers of siRNA, we compared two ligand modified HK peptides with an unmodified HK peptide. The two cRGD-PEG HK peptides differed in the number and location of cRGD-PEG conjugates on the polymer. One highly modified HK polymer with a cRGD-PEG conjugated to each branch was made that we thought would have greater tumor uptake and selectivity. Nevertheless, we were concerned that such a modification on each branch might interfere with binding to siRNA. To investigate this, an HK peptide with only one cRGD-PEG attached to its core was prepared and was expected to bind siRNA more effectively because the branching arms were not modified. Surprisingly, neither modified HK polymers by themselves effectively retarded siRNA, even at elevated N/P ratios (7:1). This data,

together with the inability to determine their particle size by DLS, suggest that a stable nanoparticle was not formed.

Nevertheless, combining modified H3K(+H)4b with unmodified H2K4b when mixed with siRNA did form stable nanoparticles that could effectively silence their target *in vivo*. Because H2K4b alone previously was not an effective carrier of siRNA in silencing its targets (Leng, Scaria et al. 2005) and reduced amounts of H2K4b were used to form the polyplex, it is likely that H2K4b has a supportive role in forming the polyplex, but not a primary role in the siRNA polyplex silencing role of the target. H2K4b was selected as a helper peptide because of its high content of lysines and its greater ability to condense nucleic acids compared to other HK peptides. It will be interesting to test polyplexes using other unmodified HK peptides (i.e., H3K(+H)4b) that are significantly more effective as carriers of siRNA, even though they are less efficient in condensing nucleic acids compared with H2K4b. The data in this study are consistent with the notion that H2K4b binds tightly with siRNA and provides a central nidus to which the modified H3K(+H)4b then binds. Such a model is similar to what the results shown by Kim *et al.* with their carrier/siRNA complexes. In that model, although the PEGylated siRNA did not effectively silence its cellular target, a combination of PEI with the targeted PEGylated siRNA was effective; PEI was posited to form the central core and stabilize the siRNA polyplex (Kim, Jeong et al. 2006; Kim, Jeong et al. 2008). Although the modified and unmodified HK peptides were mixed together before addition of the siRNA, we plan in future studies to

determine whether sequential addition of H2K4b first to the siRNA, followed by the modified H3K(+H)4b might increase the efficacy of the carrier.

Moreover, since both cRGD-PEG modifications of H3K(+H)4b did not form an effective or a defined siRNA polyplex without the addition of an unmodified HK polymer (i.e., H2K4b), it is unclear whether any PEG modifications to the H3K(+H)4b polymer will result in a stable siRNA polyplex. We initially anticipated that singly modified H3K(+H)4b would bind more tightly with siRNA and form a more stable and defined particle compared to the highly modified H3K(+H)4b. Nevertheless, utilizing fluorescent quenching assays we determined that limited and highly modified HK peptides had markedly reduced binding with siRNA (data not shown). Limited modification of the branches has been considered but we have not determined a synthetic approach for site specific addition of cRGD-PEG to one or more branches. Alternatively, smaller molecular weight PEG conjugated to HK peptides than the 3400 MW PEG that we have used in this data may enable HK to bind more effectively with siRNA and form stable HK/siRNA polyplexes.

In contrast to most carriers *in vivo* that were identified from the most promising carriers *in vitro*, we found in this study that the most effective HK carrier *in vitro* was not the optimal carrier *in vivo*. Of the HK investigated, unmodified H3K(+H)4b was the most effective carrier *in vitro*, whereas the modified H3K(+H)4b/H2K4b carrier of siRNA had no observed silencing activity in cell culture experiments. In contrast, the silencing efficiency by siRNA in tumor xenografts was significantly greater with

the modified HK polyplexes *in vivo* and correlated with the number of cRGD-PEG per HK. Increased multivalency based on the ligand conjugated to the drug or complex is known to augment internalization (Schraa, Kok et al. 2002; Boturyn, Coll et al. 2004) and this provides the likely rationale for greatest activity by the highly modified H3K(+H)4b polyplex *in vivo*. It is not at all clear why efficient silencing of luciferase was observed *in vivo* but not *in vitro* with the modified HK polyplexes. Although the literature is consistent with my results that PEGylation of the polyplex may decrease uptake *in vitro* and enhance accumulation of the polyplex within the tumor tissue, addition of cell-specific ligands such as cRGD to PEG usually augments uptake of polyplexes not only *in vivo* but also *in vitro* (Hood, Bednarski et al. 2002; Schiffelers, Ansari et al. 2004; Kim, Yockman et al. 2005; Kim, Yockman et al. 2006; Li and Huang 2006; Li, Chen et al. 2010). Indeed, previous groups have found that cRGD conjugated nanoparticles (with or without PEG) selectively targeted $\alpha_v\beta_3$ integrins on the cell surfaces of MDA-MB-435 cells *in vitro* and *in vivo* (Arap, Pasqualini et al. 1998; Kim, Yockman et al. 2005; Kim, Yockman et al. 2006; Yoshimoto, Ogawa et al. 2008; Lee, Lee et al. 2009). Although modification of H3K(+H)4b with cRGD-PEG did not enhance uptake or silencing with siRNA *in vitro*, the *in vivo* results demonstrating down-regulation of luciferase in tumors formed by MDA-MB-435 cells suggest that modification of HK greatly augmented silencing activity of the siRNA polyplex. This is further bolstered by my finding that similarly modified HK were effective and specific carriers of luciferase-expressing plasmids to MDA-MB-435 tumor xenografts compared to other tissues (data not shown). Although it is common to observe carriers that are ineffective *in vivo* that

were effective *in vitro*, there are few other studies (Solodin, Brown et al. 1995; Lee, Marshall et al. 1996; Love, Mahon et al. 2010) demonstrating that more efficient carriers *in vivo* were ineffective *in vitro*. The importance of this observation is that it suggests that until alternative screening methods to evaluate carriers are developed for *in vivo* models, it is likely many other carriers that are particularly effective *in vivo* will never be identified.

Delivery remains the major obstacle to achieving meaningful RNAi silencing. Consequently, my primary goal in this study was to develop a more effective carrier of siRNA to tumor xenografts. On the basis of the current results, we anticipate that the (RGD-PEG)^{4}H3K(+H)4b/H2K4b combination will be significantly more effective carrier than the unmodified carrier for siRNA in targeting oncogenes of tumor xenografts. Furthermore, the silencing of luciferase by the cRGD-targeted HK/siRNA polyplex appears to be specific, as evidenced by the minimal silencing by the control siRNA and low induction of cytokines by the HK/siRNA polyplex. Indeed, $\alpha_v\beta_3$ integrins are expressed not only by tumor cells but also endothelial cells. The conjugation of cRGD peptide as a targeting agent for $\alpha_v\beta_3$ integrins advances the HK polymer selective for both tumor and endothelial cells. However, it requires more effort for the cRGD modified HK polymers to permeate leaky tumor vasculatures and specifically silenced the target in tumor xenografts. Although the efficacy of cRGD-PEG targeted HK as a carrier of siRNA targeting tumors and angiogenesis requires further validation, the studies thus far have indicated that modified HK is a promising candidate for systemic delivery of siRNA.

My silencing tumor xenograft model examined whether targeted HK/siRNA polyplexes could effectively traversed the endothelial cell barrier to silence Luc expressed by tumor cells. Nevertheless, it is likely that the cRGD-HK/siRNA polyplexes will also target the more readily accessible $\alpha_V\beta_3$-expressing endothelial cells of tumors. In addition to cyclic RGD peptides, other tumor-selective ligands could be conjugated to the HK peptides to target tumor cells and silence their oncogenes (Sugahara, Teesalu et al. 2009). Although the efficacy of cRGD-PEG targeted HK as a carrier of siRNA targeting tumors and angiogenesis requires further validation, the studies thus far have indicated that modified HK is a promising candidate for systemic delivery of siRNA.

Chapter 4: Surface Modified HK/siRNA Polyplexes with Enhanced Pharmacokinetics and Tumor Growth Inhibition

4.1 Abstract

We characterized in this study the pharmacokinetics and antitumor efficacy of histidine-lysine (HK)/siRNA polyplexes modified with PEG and a cyclic RGD (cRGD) ligand targeting αvβ3 and αvβ5 integrins. Using non-invasive imaging, systemically administered surface modified HK/siRNA polyplexes exhibit nearly 4-fold higher blood levels, 40% higher accumulation in tumor tissue, and 60% lower luciferase activity than unmodified HK/siRNA polyplexes. A surface modified HK/siRNA polyplex with an siRNA targeting Raf-1 was also found to be more effective in reducing MDA-MB-435 tumor growth. Repeated systemic administration of the selected surface modified HK/siRNA polyplexes targeting Raf-1 showed 35% greater inhibition of tumor growth than unmodified HK/siRNA polyplexes and 60% inhibition of tumor growth compared to untreated mice. Thus, improved blood pharmacokinetic results and tumor localization observed with the integrin-targeting surface modification of HK/siRNA polyplexes correlated with greater tumor growth inhibition. This investigation reveals that through control of targeting ligand surface display in association with a steric PEG layer, modified HK/siRNA polyplexes show promise to advance RNAi therapeutics in oncology and potentially other critical diseases.

4.2 Introduction

RNAi silencing of oncogenes via siRNA has a great potential for cancer treatment, but its application is limited by several substantial obstacles. For example, necessary advances include avoiding siRNA degradation by nucleases in blood and tissues, minimizing side effects of the siRNA or delivery system, transport of the highly negative charged siRNA to target tissue and then across cellular membranes, and shifting intracellular trafficking away from lysosomal degradation to endosomal lysis. After considerable exploration of a wide range of approaches, including chemically protective analogues alone, antibody-carrier chimerae and cell-penetrating peptide conjugates, most efforts to achieve these milestones are now focused on developing target-specific and biologically metastable nanoparticle carriers for siRNA oligonucleotides (Song, Zhu et al. 2005; Bartlett and Davis 2008; Peer, Park et al. 2008; Yang, Dou et al.).

Whereas there have been no FDA-approved siRNA carriers for systemic treatment, a few have advanced to clinical trials (clinicaltrials.gov) (Brower 2010; Davis, Zuckerman et al. 2010; Alsina, Tabernero et al. 2012; Strumberg, Schultheis et al. 2012). These early clinical trials with different carriers encourage testing other pre-clinical carriers siRNA that have therapeutic efficacy in animal models, including synthetic polymers, peptides, siRNA aptamers, neutral and cationic liposomes (see review (Leng, Woodle et al. 2009)). To investigate siRNA-mediated gene silencing in tumor cells, Mixson's lab has synthesized a number of branched histidine-lysine (HK)-rich peptides (Leng, Scaria et al. 2005). While lysines presumably bind and

protect siRNA via electrostatic interaction, pH-sensitive histidines play an important role in buffering the acidic endosomes and may interact with the endosomal membrane, aiding the endosomal escape of siRNA. Many other investigators have reported on the use of histidine-containing peptides for DNA plasmid or siRNA delivery (Midoux and Monsigny 1999; Putnam, Gentry et al. 2001; Hatefi, Megeed et al. 2006; Kichler, Mason et al. 2006). By varying the amino acid sequence and number of branches, a four-branched polymer, H3K(+H)4b, with repeating patterns primarily of –HHHK-, was found to be the most effective and least toxic carrier of siRNA *in vivo* (Leng, Scaria et al. 2008).

Although *in vitro* and *in vivo* tumor growth inhibition indicative of therapeutic efficacy has been achieved with non-ligand targeted HK polyplexes, a more stable and targeted delivery system is thought necessary to improve the therapeutic index and range of siRNA gene targets. To improve the stability of the siRNA polyplex, surface coatings with hydrophilic polymers such as polyethyleneglycol (PEG) or carbohydrates such as hyaluronic acid and oligo-maltose have been studied (Jiang, Park et al. 2008; Li and Huang 2008). Such modifications shield the polyplex surface to prevent protein binding, reduce reticuloendothelial uptake, and/or extend the circulation time *in vivo*. On the other hand, such hydrophilic coated polyplexes can also exhibit a decrease in cellular uptake due to steric hindrance of the surface layer.

To circumvent steric hindrance leading to decreased cellular uptake, ligands for receptors can be conjugated to the polyplex and displayed on its surface, giving

improved cellular uptakes in a wide array of delivery systems (Kircheis, Wightman et al. 2001; Hood, Bednarski et al. 2002; Schiffelers, Ansari et al. 2004; Li and Huang 2008). In this chapter, the cRGD-PEG conjugate was attached to the N-terminal lysine on each branch of H3K(+H)4b to target selectively $\alpha_v\beta_3$ and $\alpha_v\beta_5$ integrins that are overexpressed on the cell surfaces of MDA-MB-435 tumor xenografts (Fig. 4.1).

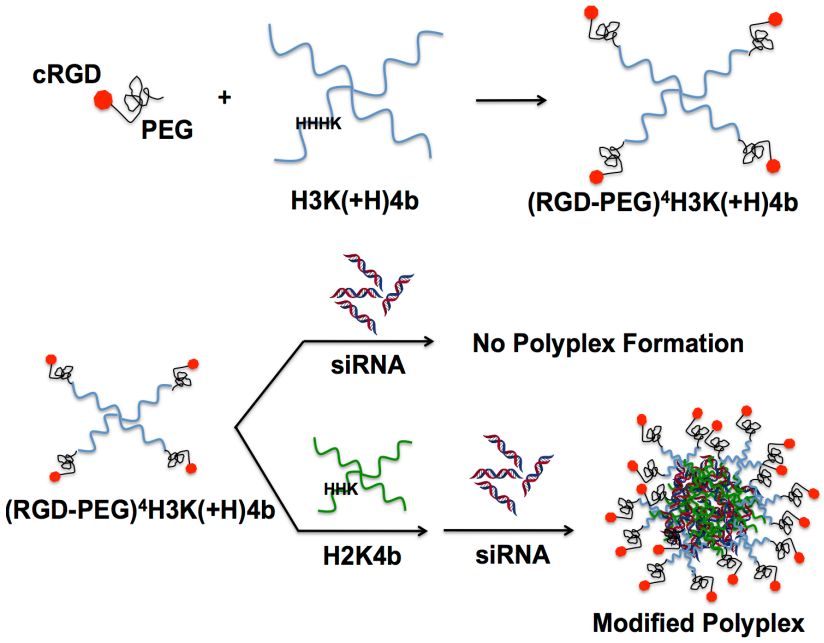

Fig. 4.1. Schematic illustration of (cRGD-PEG) modification patterns and HK/siRNA polyplex formation.

Each of four N-terminal branches was conjugated to a single (cRGD-PEG). A two-step mixing was utilized to prepare modified polyplexes: $(cRGD\text{-}PEG)^4H3K(+H)4b$ was first added to a helper peptide, H2K4b. The resulting mixture was then mixed with siRNA at room temperature for 30 min to form HK/siRNA polyplexes.

We previously determined the optimal cyclic RGD and PEGylation patterns on H3K(+H)4b (Fig. 3.3) for systemically administered siRNA targeting the luciferase gene in a bioluminescence mouse model. To increase binding with siRNA and form stable siRNA polyplexes, an unmodified H2K4b (H2K indicating that the

predominant repeating groups is –HHK–) was combined with the ligand-PEG modified HK peptide $(RGD\text{-}PEG)^4$H3K(+H)4b and with siRNA, resulting in HK/siRNA polyplexes that provided effective gene silencing without cytokine induction *in vivo* (Chou, Leng et al. 2011). In the current study, we further investigate the cRGD targeted HK/siRNA polyplexes in terms of pharmacokinetics, biodistribution and antitumor efficacy and compare them to unmodified HK/siRNA polyplexes. The cRGD-PEG modification of HK/siRNA polyplexes extended the half-life in the blood and showed greater tumor accumulation, resulting in reduction of luciferase activity by more than 70%. Consistent with these effects on pharmacokinetics and biodistribution, the ligand-targeted HK/siRNA polyplex showed enhanced antitumor efficacy with an siRNA targeting the Raf-1 oncogene. It reduced Raf-1 mRNA and protein expression and it suppressed growth of MDA-MB-435 subcutaneous xenograft tumors in mice.

4.3 Materials and Methods

4.3.1 Animals

Female athymic mice (4 to 8 weeks old, body weight ~20 g) were purchased from NCI Frederick. All experiments were performed in accordance with the regulations of the Institutional Animal Care and Use Committee of the University of Maryland School of Medicine.

4.3.2 Cell line

A human malignant cell line MDA-MB-435, stably expressing Firefly luciferase (stable transformation by electroporation with the linearized pCpG-Luc plasmid), was cultured and maintained in Dulbecco's minimal essential medium (DMEM) containing 10% fetal calf serum (FCS) and 20 mM glutamine. The pCpG-Luc plasmid was made by ligating the luciferase gene (digested from pMOD-Luc plasmid, InvivoGen, San Diego, CA) into the multiple cloning site of pCpG-mcs (InvivoGen). This cell line is identical to the cell line involved in chapter 2 and 3.

4.3.3 Synthesis, sequences, and chemical modification of HK peptides

Branched peptides, H2K4b and H3K(+H)4b with predominant repeating groups, –HHK– and –HHHK–, respectively were synthesized on a Rainin Voyager synthesizer (PTI, Tucson, AZ) by the biopolymer core facility at the University of Maryland, as previously described (Leng and Mixson 2005). Each of four terminal branches emanates from the 3-lysine core: for H3K(+H)4b, the branch sequence is KHHHKHHHKHHHHKHHHK; for H2K4b, the branch sequence is KHKHHKHHKHHKHHKH-HKHK. For modified H3K(+H)4b, cyclic (c)RGD and PEG (3.4 kD) were conjugated to each N-terminal branch as described in 3.3.3, resulting in four (cRGD-PEG) conjugates per HK peptide, $(RGD\text{-}PEG)^4$H3K(+H)4b (Chou, Leng et al. 2011).

4.3.4 siRNA

Sequences of siRNA targeting luciferase (siLuc) were as follows: sense, 5'-CUG-CAC-AAG-GCC-AUG-AAG-A-dTdT-3'; antisense, 5'-UCU-UCA-UGG-CCU-UGU-GCA-G-dTdT-3', targeting 5'-CTG-CAC-AAG-GCC-ATG-AAG-A-3'. siLuc was also used as the control siRNA for studying inhibition of tumor growth. Raf-1 siRNA duplex (siRaf-1) was as follows: sense, 5'-GCA-UCA-GAU-GAU-GGC-AAA-C-dTdT-3'; antisense, 5'-GUU-UGC-CAU-CAU-CUG-AUG-CdTdT-3', targeting 5'-GCA-TCA-GAT-GAT-GGC-AAA- C-3' (Dharmacon, Lafayette, CO). Luciferase siRNA was conjugated to Alexa Fluor 546 (Dharmacon) or a near infrared dye, Cy5.5 (Sigma-Aldrich, St. Louis, MO), on the 5' end of the sense strand. Each siRNA was maintained in siRNA buffer (Dharmacon) for 30 min at RT for annealing the duplex.

4.3.5 Preparation and biophysical properties of HK polyplexes

The ternary $(RGD\text{-}PEG)^4$H3K(+H)4b/H2K4b/siRNA and H3K(+H)4b polyplexes were prepared as described in chapter 3 for experiments *in vivo* . As defined by gel retardation assays and the biophysical characteristics, the optimal N/P ratios for H3K(+H)4b/siRNA and $(RGD\text{-}PEG)^4$H3K(+H)4b/ H2K4b/siRNA were about 2.2/1 (w/w) (N/P ratio, 4/1) and 4.0/0.8/1 (w/w/w; N/N/P ratio 3/1/1) used in this study.

For these ratios of HK/siRNA polyplexes, the size and zeta potential were determined with the Zetasizer (Malvern, Westborough, MA) prior to their injection. The size is reported as the average size obtained from unimodal analysis of dynamic light

scattering of the particles at a 90° angle carried out with software provided by the instrument manufacturer. Each particle size and zeta potential data point represents the mean ± S.D. of four measurements on separate preparation.

4.3.6 Fluorescence quenching assay

The relative binding affinity between various HK polymers and siRNA was studied with Alexa 546-labeled siRNA (λ_{ex} = 550 nm, λ_{em} = 570 nm, Dharmacon, Lafayette, CO). Fluorescent-labeled siRNA (0.14 μM, 100 μl) in phosphate buffer (10 mM, pH 7) was added to a 96-well plate, and changes in fluorescence were then measured by adding 0.033 μM increments of H3K(+H)4b, H2K4b, (RGD-PEG)^{4}H3K(+H)4b, or (RGD-PEG)^{4}H3K(+H)4b/H2K4b. After incubation of HK and siRNA at room temperature for 20 min, the fluorescence intensity was measured by a Wallac Victor 3 1420 multilabel counter (Perkin Elmer, Boston, MA), and the relative fluorescence intensity was normalized after subtracting background levels.

4.3.7 Preparation of HK/siRNA polyplexes for treatment of tumor xenografts

HK/siRNA polyplexes were prepared as previously described (Chou, Leng et al. 2011). Briefly, for unmodified polyplexes, H3K(+H)4b peptide (88 μg in 150 μl of water) was rapidly added to the siRNA (40 μg in 150 μl water) and mixed with a Vortex mixer. For the modified HK combination, the (RGD-PEG)^{4}H3K(+H)4b peptide (160 μg in 150 μl of water) or PEG^{4}H3K(+H)4b (152 μg in 150 μl of water) was mixed with unmodified H2K4b (32 μg in 75 μl of water) and maintained for 30

min at room temperature before siRNA was added. The polyplexes were allowed to form for 40 min at room temperature following by injection and biophysical characterization.

4.3.8 Biodistribution, pharmacokinetics, and bioluminescence

MDA-MB-435 cells (2 x 10^6 cells) expressing luciferase were injected into the mid-clavicular line of female nude mice (NCI Frederick). After tumors grew to about 180 mm^3, mice were separated into three siRNA treatment groups: aqueous siLuc, H3K(+H)4b/siLuc (w/w, 2.2/1), and $(RGD\text{-}PEG)^4$H3K(+H)4b/H2K4b/siLuc (w/w/w, 4/0.8/1). The aqueous siRNA or HK/siRNA polyplexes containing 40 μg of siLuc (including 5% (2 μg) of Cy5.5-labeled siLuc) were administered in the tail vein. For biodistribution studies, the mice were imaged by the IVIS-200 optical imaging system (Xenogen Corp., Alameda, CA) at 0, 15, 30, and 60 min, and 2, 4, 6, and 24 h post-injection. Fluorescence emission at the tumor location, given as relative units after normalization of maximal and minimal intensities (Lee, Veiseh et al. 2010), was measured with regions of interest of equal size at specified time points. Biodistribution imaging and tumor luciferase activity were measured by IVIS-200 before and 48 h after siRNA treatment targeting luciferase (Chou, Leng et al. 2011).

Similarly, to determine the effects of PEG and cRGD modifications, the PEG^4H3K(+H)4b/H2K4b/siLuc polyplexes (w/w/w, 3.8/0.8/1) were compared with $(RGD\text{-}PEG)^4$H3K(+H)4b/H2K4b and H3K(+H)4b polyplexes for their ability to

silence luciferase in tumor xenografts of about 60 mm^3. Tumor imaging with IVIS-200 imaging was done 48 h after injection of the polyplexes.

For pharmacokinetic experiments, tumor-bearing mice were treated with Cy5.5-labeled Luc siRNA (5% of total Luc siRNA) in complex with different formulations of HK peptides as described above for the biodistribution study. At several time points (2, 5, 10, 15, 25, 45, 60, and 120 min), blood (100 μl) was collected and serum was isolated (Li, Chen et al. 2008). The serum (30 μl) was then mixed with PBS (20 μl) in a 96-well clear bottom plate, and the fluorescence signal was imaged by the IVIS-200 system. The concentration of the polyplexes were calculated from a standard curve of fresh aqueous siRNA or polyplexes (Lee, Veiseh et al. 2010). As described previously (Merkel, Librizzi et al. 2009; Rowland and Tozer 2011), the pharmacokinetic analysis of the data was performed using a two-compartment model ($f = A*exp(-\alpha t) + B*exp(-\beta t)$) with first order adsorption and elimination from the central compartment by using Sigma Plot, 11.0. After curve fitting of the data, the PK parameters were calculated based on the following expressions:

Terminal half-life: $\ln 2/\beta$

Clearance (CL): $1/(\frac{A}{\alpha}+\frac{B}{\beta})/Mouse\ body\ weight$

Mean residence time (MRT): $\frac{1}{\alpha}+\frac{1}{\beta}$

Area under curve 2 h (AUC_{2h}): $\sum_{i=0}^{n-1}\frac{t_{i+1}-t_i}{2}(C_i+C_{i+1})$ where *t* and *C* represent time of sampling and concentration of siRNA, respectively.

4.3.9 Inhibition of tumor growth and Raf-1 expression

Mice with MDA-MB-435 xenografts (about 25 mm^3 in size) were separated into four treatment groups: untreated, H3K(+H)4b/Control siLuc, H3K(+H)4b/siRaf-1, and $(RGD\text{-}PEG)^4$H3K(+H)4b/H2K4b/siRaf-1. HK/siRNA polyplexes with same w/w ratios as described above were injected intravenously three times a week for a total of 6 or 7 treatments depending on the experiment. Tumor volume was determined before each treatment with skin calipers by using the formula $1/2 \times \text{length} \times \text{width}^2$. Two days after the last injection, the mice were euthanized and total RNA was isolated from excised tumor xenografts using the RNeasy mini kit (Qiagen, Hilden, Germany). Expression of Raf-1 (368 nt) and β-actin (294 nt) mRNA was assessed by reverse transcriptase-polymerase chain reaction (RT-PCR) as described previously (Leng and Mixson 2005). RT-PCR products were then loaded onto a 3% agarose and subjected to electrophoresis at a constant voltage of 100 V for 90 minutes in TBE buffer containing ethidium bromide. The band density was visualized on a UV transilluminator with a wavelength of 365 nm and the image was digitized and analyzed by UN-SCAN-IT (Silk Scientific, Orem, UT).

4.3.10 Immunohistochemical detection of Raf-1 and Ki67, and analysis of apoptosis using the TUNEL assay

Tumors were fixed in 10% formalin for 24 h and processed as paraffin-embedded tissue sections. Immunostaining was performed according to the manufacturer's protocol (Vector, Versatile ABC, Burlingame, CA). Briefly, tumor sections were deparaffinized in xylene and rehydrated in graded ethanol. Antigens were retrieved

by maintaining tissue in 10 mM citrate buffer, pH 6.0, at boiling point for 40 min. Endogenous peroxidase and non-specific binding were blocked by 3% H_2O_2 for 10 min and 5% goat serum for 30 min, respectively. For detection of Raf-1 and Ki67, tissue sections were incubated with rabbit anti-human polyclonal antibody (Raf-1: 1:50 dilution, Ab-259, Genscript, Piscataway, NJ, USA; Ki67: 1:50 dilution, Chemicon, Ramona, CA, USA) at 4 °C overnight and secondary horseradish peroxidase-labeled antibody was added for 30 min. The chromogen diaminobenzidine (DAB) was applied for 5 min to permit color development. Finally tissue was dehydrated and mounted with glass coverslips. Four arbitrarily picked brightfield images were converted to normalized blue images (Brey, Lalani et al. 2003) allowing automatic classification (quantification) of positive DAB staining. The TUNEL assay was performed on paraffin-embedded tissue according to the manufacturer's instruction (FragEL DNA Fragmentation Detection Kit, Calbiochem, San Diego, CA). The tissue sections were incubated with terminal deoxynucleotidyl transferase for 90 min after specimen permeabilization and endogenous peroxidase inactivation. The labeling reaction was then terminated and tumor sections were stained with DAB substrate.

Table 4.1. Size and zeta potential of HK/siRNA polyplexes

Peptide	Size (nm)[a]	Zeta potential (mV)[a]
H3K(+H)4b	166.7 ± 24.8[b]	41.5 ± 5.5
PEG-HK	68.6 ± 11.3	17.3 ± 1.3
RP-HK	82.4 ± 5.4	22.7 ± 4

[a]The size and zeta potential of polyplexes were measured before their systemic administration to mice. [b]Each data point represents the mean ± S.D. of four measurements.

4.4 Results

4.4.1 Polyplexes formed with the combination of modified and unmodified HK peptides

Relative binding affinities of HK peptides to siRNA were determined by titration of Alexa 546-labeled siRNA with different peptides. When the peptide binds siRNA, fluorescence intensity is attenuated due to polyplex formation. These results of these quenching studies corroborated a previous study that used a gel retardation assay (Chou, Leng et al. 2011), confirming that a combination of unmodified H2K4b and $(RGD\text{-}PEG)^4$H3K(+H)4b was required to form the ternary polyplexes (Figs. 4.1 and 4.2). The unmodified HK peptides, H2K4b and H3K(+H)4b, had high affinity for siRNA to form polyplexes (as evidenced by decreased fluorescence at N/P ~ 1), the modified $(RGD\text{-}PEG)^4$H3K(+H)4b peptide alone showed negligible binding to siRNA. A combination of unmodified H2K4b peptide, with a greater charge density, and the RGD-PEG modified H3K(+H)4b peptide showed quenching of the siRNA that was intermediate between the modified alone and unmodified peptides, suggesting that both peptides are present in the polyplex (Fig. 4.2). The size and zeta potential of the unmodified or combined $(RGD\text{-}PEG)^4$H3K(+H)4b/H2K4b/siRNA polyplexes used for *in vivo* experiments are shown in Table 4.1. To simplify the nomenclature, the combination of $(RGD\text{-}PEG)^4$H3K(+H)4b and H2K4b will be designated RP-HK.

4.4.2 Enhanced pharmacokinetics with modified HK/siRNA polyplexes

The concentration of polyplexes in blood was determined by measuring near infrared (NIR) fluorescence from Cy5.5-labeled siRNA, alone or incorporated within the polyplexes (Fig. 4.3). The advantage of the near infrared based methodology is its high sensitivity and low background, thereby requiring only small amounts of blood to detect the Cy5.5 signal. At indicated time points up to 2 hours, blood was drawn and the amount of siRNA in the serum was measured. Fifteen minutes after injection, the concentrations of the siRNA, alone or as polyplexes, decreased to less than 10% of the injected dose. As shown in figure 4.3, aqueous siRNA and unmodified HK/siRNA polyplexes were eliminated substantially faster than the modified RP-HK/siRNA polyplexes. The key pharmacokinetic parameters were determined by fitting the data with a bi-compartment model (Table 4.2) (Rowland and Tozer 2011) and the results of curve fitting were shown in figures 4.4-4.6 and table 4.3. The sterically stabilized and ligand-targeting polyplexes had a 3-fold greater terminal half-life ($t_{1/2b}$) and mean residence time (MRT), and a 4-fold increase in the area under the curve compared to unmodified HK polyplexes. In addition, the surface modification of the polyplexes markedly reduced elimination clearance (CL) by 10-fold. Thus, all pharmacokinetic parameters indicated that surface modification of the HK/siRNA polyplexes greatly increased its residence time in the bloodstream which suggests that the modified polyplexes will have greater tumor uptake and siRNA silencing of the targeted oncogene.

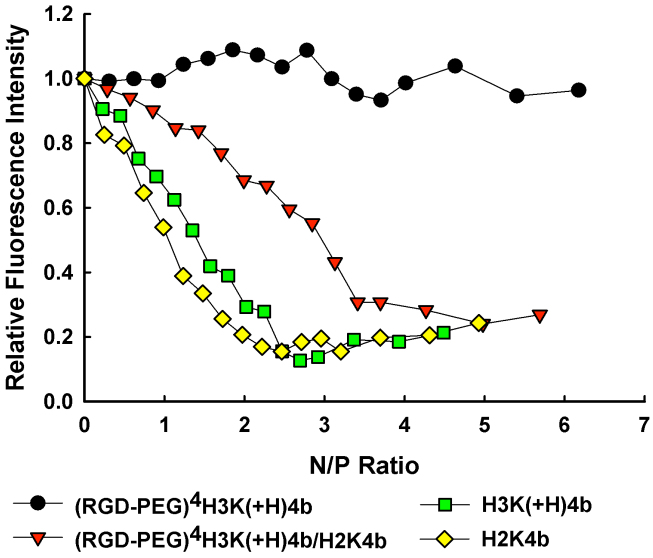

Fig. 4.2. Relative binding affinity of HK peptide formulations with siRNA.

Relative binding affinity of four HK peptide formulations (H3K(+H)4b; H2K4b; $(RGD\text{-}PEG)^4H3K(+H)4b$; $(RGD\text{-}PEG)^4H3K(+H)4b/H2K4b$ (RP-HK)) for Alexa 546-labeled siRNA was studied in 10 mM phosphate buffer, pH 7.0. Relative fluorescence intensity is the percentage of unbound siRNA after subtraction of background fluorescence. See Results section for further details.

4.4.3 Increased localization of cRGD-PEG modified HK/siRNA polyplexes

The tumor-specific targeting efficacy was assessed by NIR fluorescence imaging of Cy5.5-conjugated siRNA with a non-invasive imaging system, IVIS-200, before and at specified times after injection (Fig. 4.7A). Autofluorescence was observed in the abdomen, but this did not interfere with measurement of the polyplex levels within tumors. As soon as 15 min after injection, the modified RP-HK/siRNA polyplexes gave higher fluorescence in tumor tissue than that of the unmodified HK/siRNA polyplexes. In contrast, administration of aqueous siRNA resulted in minimal tumor fluorescence, indicative of negligible siRNA uptake. The amount of targeted RP-HK/siRNA polyplexes within tumors was quantified by measuring intratumoral

fluorescence (Fig. 4.7B). While unmodified HK/siRNA polyplexes rapidly reached maximal accumulation within the tumor 30 min after injection, the modified RP-HK/siRNA polyplexes required 60 to 120 min after injection to achieve maximal levels. Compared to accumulation of unmodified HK polyplexes within tumors, accumulation of modified RP-HK polyplexes was 40% higher ($P < 0.01$) at 60 min. Although the polyplex distribution in the major organs was difficult to assess due to autofluorescence in the abdominal region, significant accumulation of fluorescence with the aqueous siRNA-treated group occurred earlier in the spleen compared to the HK/siRNA polyplex groups. Not surprisingly, fluorescence in aqueous siRNA-treated mice was observed in the bladder with the first image (15 min), whereas siRNA of the polyplexes was not detected at a significant level in the bladder until 2 h after injection. There was little difference in organ fluorescence accumulation between the modified RP- and unmodified HK polyplexes except that accumulation in the liver occurred earlier with unmodified polyplexes.

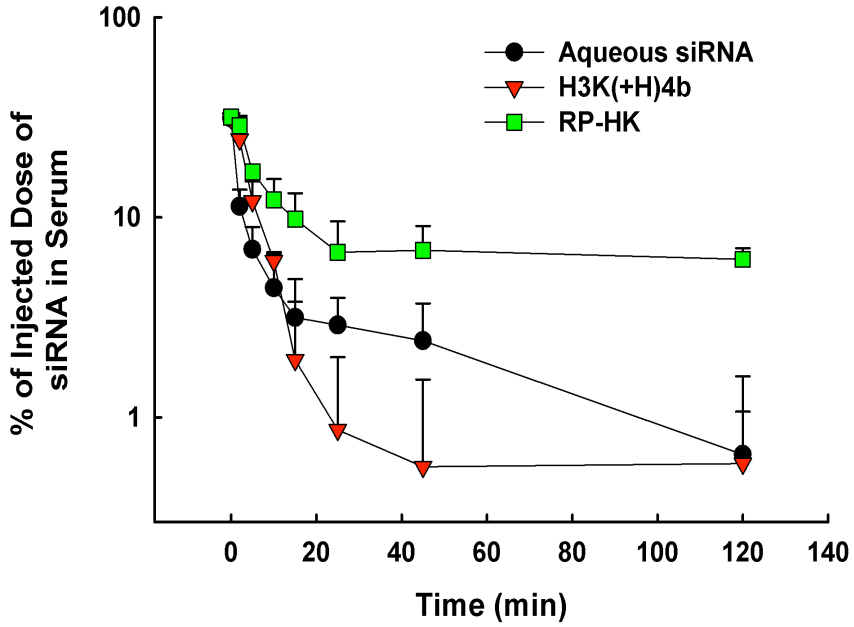

Fig. 4.3. Serum pharmacokinetics of Cy5.5 labeled siRNA and polyplexes.

A semilogarithmic plot of serum concentration vs. time for up to 2 h after intravenous injection of siRNA alone or in complex with the unmodified HK or modified RP-HK peptides. The data represent the mean ± SD of %ID/ml (n = 4 per carrier) where % ID/ml is the percentage of injected dose per milliliter of serum.

Table 4.2. Pharmacokinetic parameters for siRNA formulations

	$t_{1/2\beta}$ [a] (min)	CL[b] (ml/min/kg)	AUC_{2h}[c] (μg/ml×min)	MRT[d] (min)
Aqueous siRNA	27.7	18.50	126.3 ± 52.7	41.4
H3K(+H)4b: siRNA	86.6	16.62	98.0 ± 58.6	129.5
RP-HK: siRNA	256.7	1.57	385.0 ± 92.4	374.7

[a]$t_{1/2\beta}$, terminal half-life; [b]CL, clearance; [c]AUC_{2h}, area under curve from 0 to 2 h; [d]MRT, mean residence time

Curve fitting results of aqueous siRNA or polyplex concentration in the serum using two-compartment model:

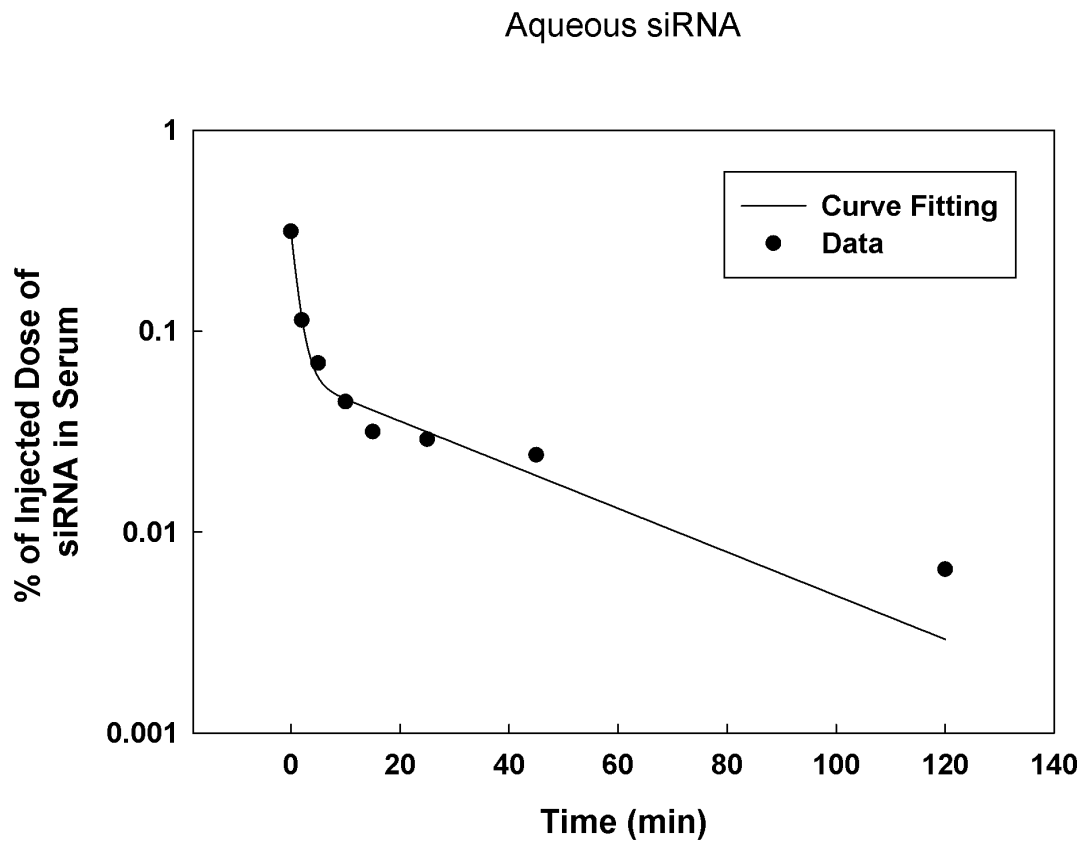

Fig. 4.4. Curve fitting of the concentration of aqueous siRNA in serum

$R^2 > 0.99$

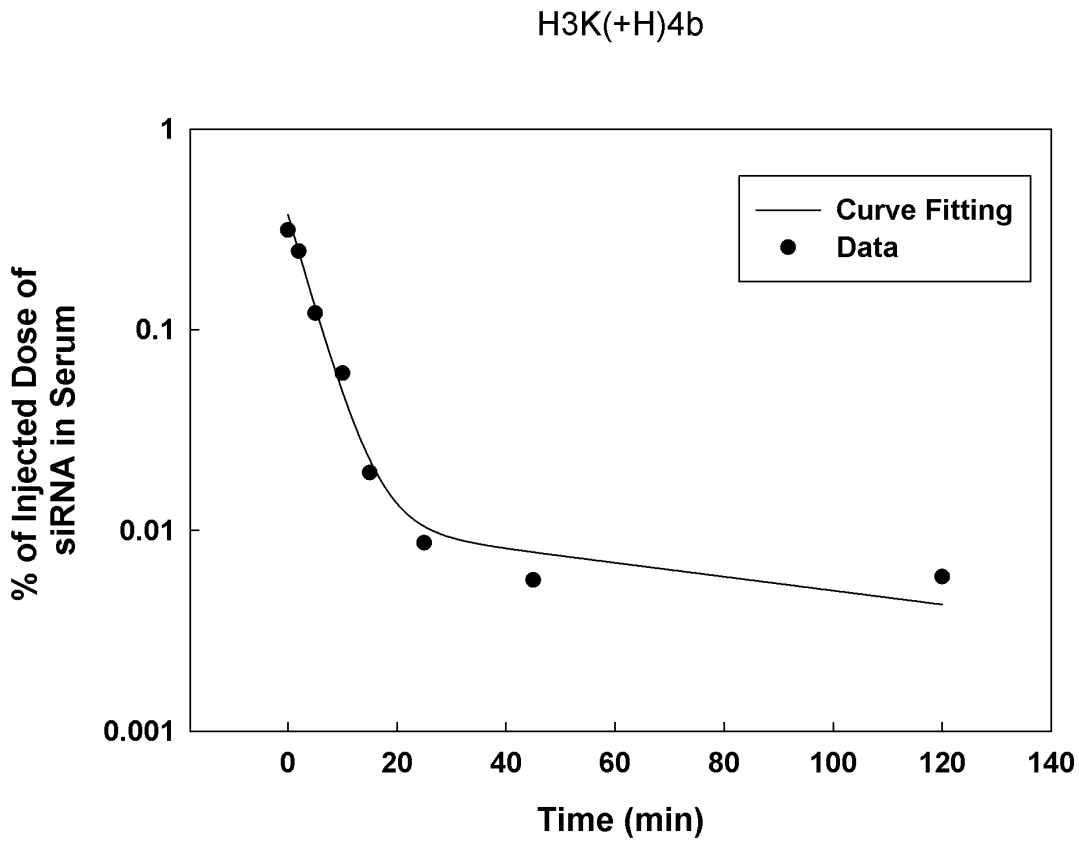

Fig. 4.5. Curve fitting of the concentration of unmodified polyplexes in serum

$R^2 > 0.98$

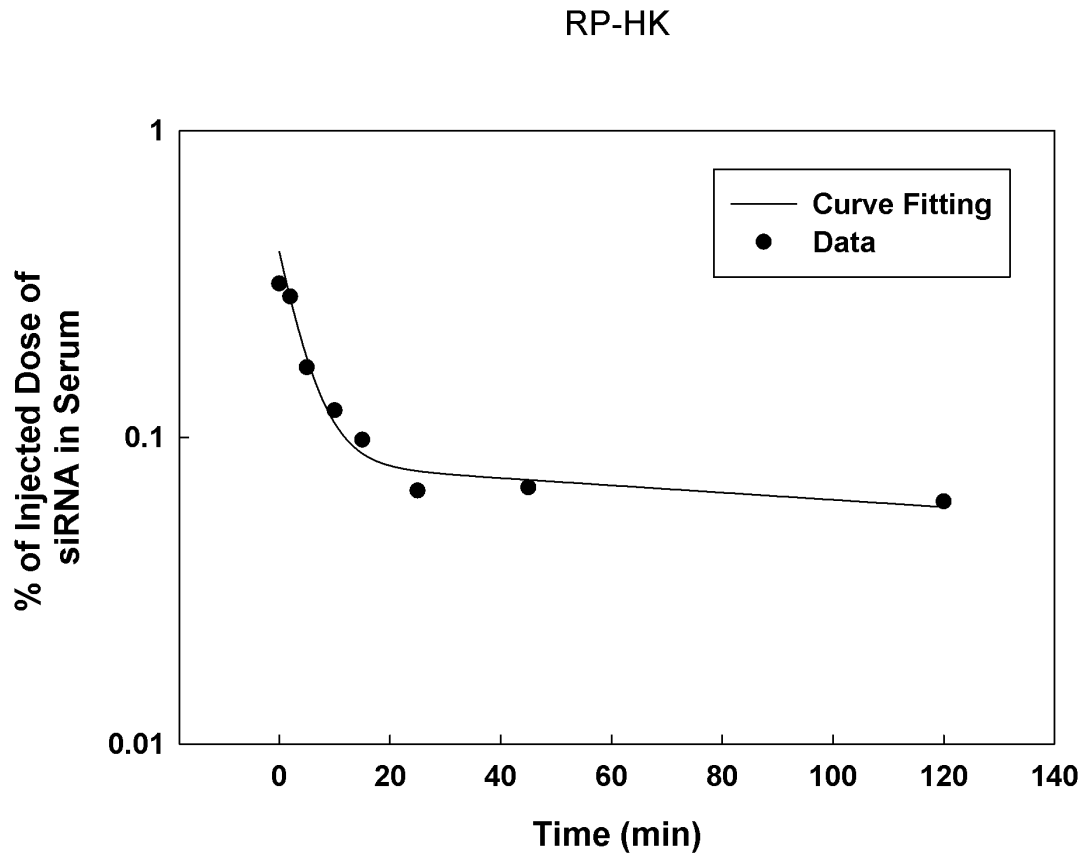

Fig. 4.6. Curve fitting of the concentration of modified polyplex in serum

$R^2 > 0.99$

Table 4.3. The coefficients of two-compartment model derived from curve fitting.

	A	B	α	β
Aqueous siRNA	0.2542	0.0587	0.718	0.025
H3K4b	0.3631	0.0111	0.224	0.008
RP-HK	0.3208	0.082	0.2326	0.0027

$f = A*exp(-\alpha t) + B*exp(-\beta t)$

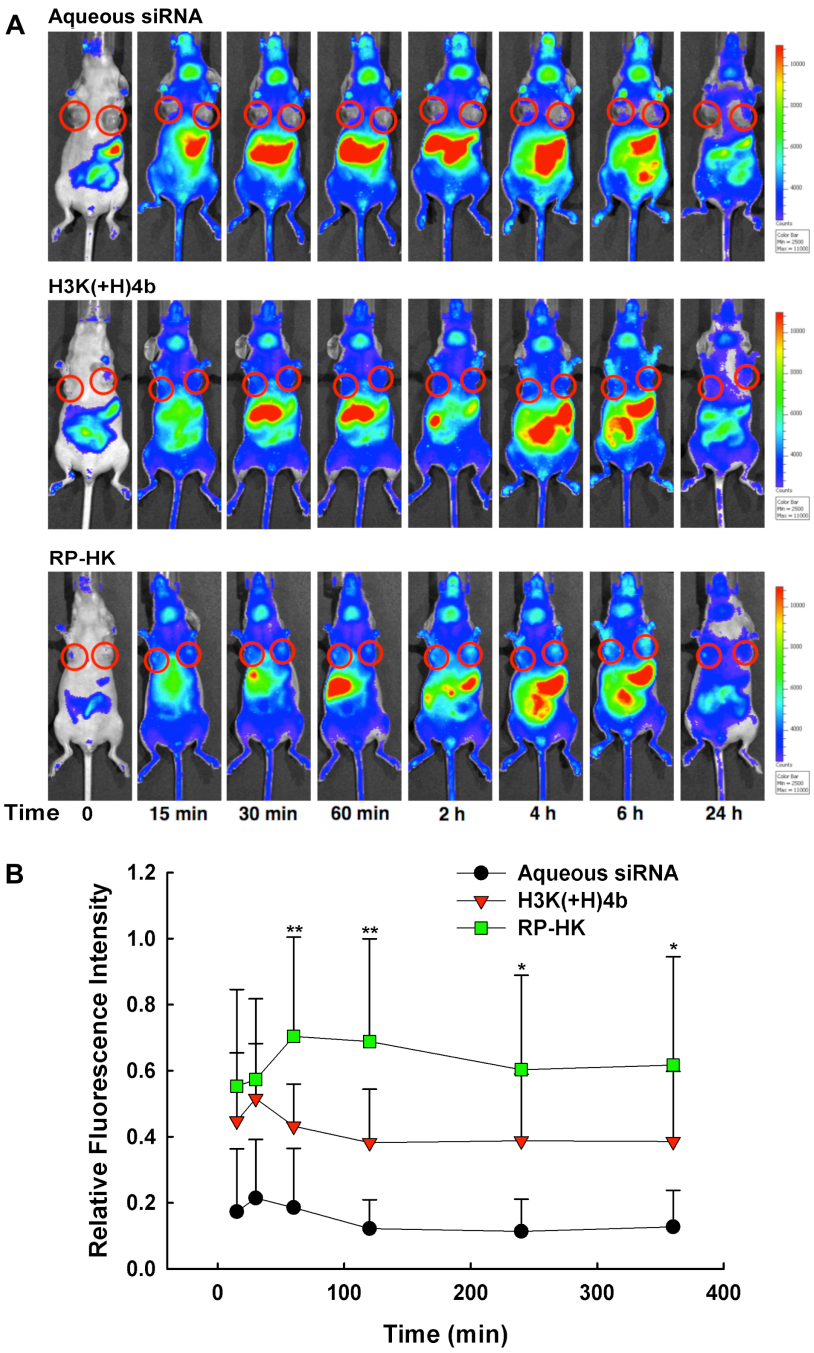

Fig. 4.8. Real-time biodistribution of Cy5.5 labeled siRNA and polyplexes.

(A) Representative biodistribution of Cy5.5-labeled siRNA in a mouse, with the siRNA administered as an aqueous solution, unmodified HK polyplex or RP-HK polyplex. Times 15, 30, 60, 120 min, and 4, 6, and 24 h are shown. Red circles encircle the tumors (B) Fluorescence emission localized at the tumor was measured for the different siRNA groups. The data represent the mean ± SD of fluorescence of four determinations for each carrier. **, $P < 0.01$; RP-HK carrier vs. unmodified HK carriers and control groups.

4.4.4 The correlation between tumor luciferase silencing and pharmacokinetics

The correlation between PK/biodistribution and target gene silencing of the different polyplexes was determined with same group of mice, which had tumors expressing luciferase. Luciferase activity was measured by the IVIS imaging system before and 48 h after treatment (Fig. 4.8). Compared to aqueous siLuc, the modified RP-HK siLuc polyplexes inhibited luciferase expression by about 70%, whereas the unmodified HK siLuc polyplexes only inhibited luciferase activity by about 10%. These results with the labeled siRNA were consistent with my previous results with unlabeled siRNA (Chou, Leng et al. 2011). Thus, the labeled siRNA apparently does not interfere with the functional characteristics or activity of the HK polyplexes in silencing its target. Consequently, down-regulation of luciferase activity correlated with increased blood circulation time and tumor tissue accumulation of polyplexes.

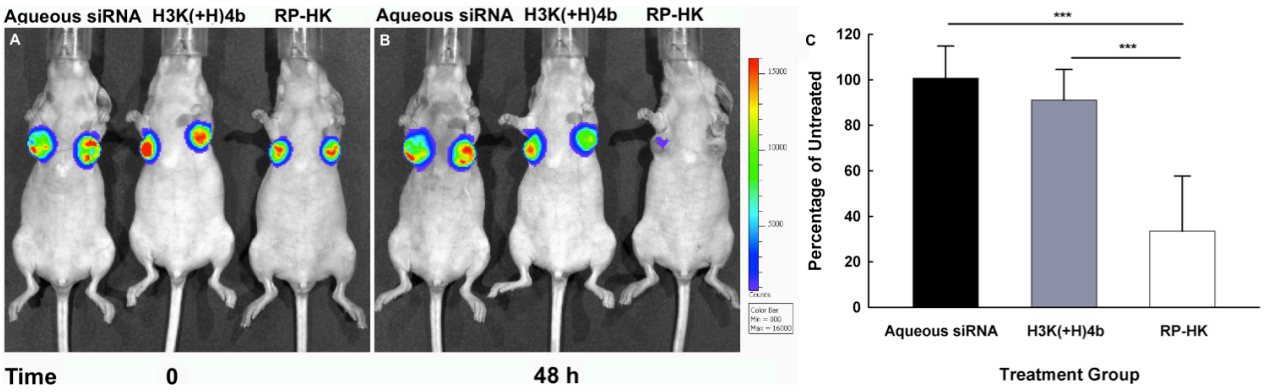

Fig. 4.8. Bioluminescence assay for silencing of luciferase expression.

The representative mice were from the same treatment groups used for the biodistribution study. Panel A and B show tumor bioluminescence images of representative mice taken before and 48 h after treatment, respectively. The treatment groups in A and B were as follows (from the left to right): aqueous siRNA, H3K(+H)4b, and RP-HK polyplexes respectively. (C) The percent silencing of luciferase activity by different treatment groups compared to the untreated control group represents the mean ± SD of fluorescence of four determinations. ***, $P < 0.001$.

We were particularly interested in determining the contribution of the cRGD targeting ligand to the tumor-tissue gene silencing by RP-HK polyplexes. Consequently, the ability of RP-HK polyplexes to reduce the luciferase activity of the tumor was compared to HK polyplexes with the same PEGylation but with the cRGD absent (Fig. 4.9). The PEGylated alone HK (PEG-HK) polyplexes silenced luciferase activity within tumor xenografts more effectively than unmodified HK but less effectively than RP-HK polyplexes. Moreover, the PEG and cRGD appeared to have approximate additive contributions. The PEG-HK siLuc polyplexes were 60% more effective than the unmodified HK siLuc polyplexes ($P < 0.05$) whereas the RP-HK siLuc polyplexes were 50% more effective than PEG-HK siLuc polyplexes ($P < 0.01$).

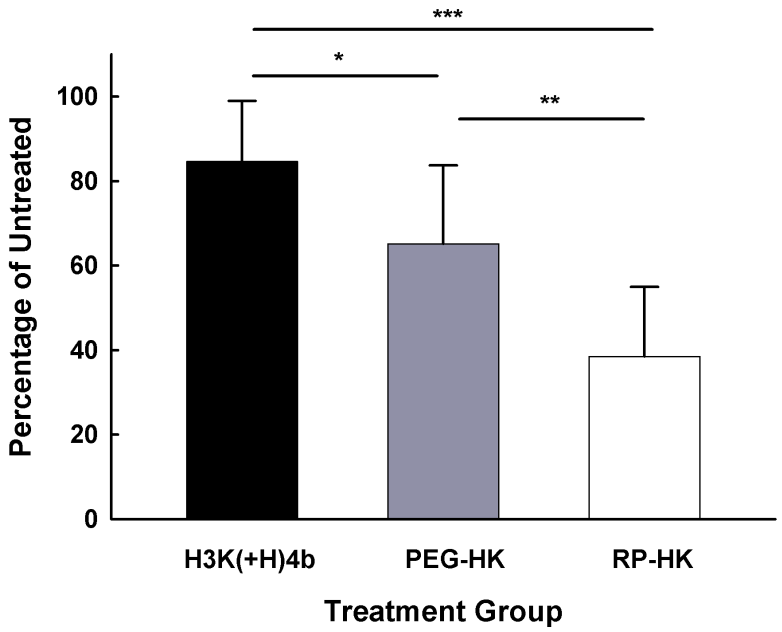

Fig. 4.9. PEG and cRGD modifications of HK enhance gene silencing in tumor xenografts.

Luciferase siRNA polyplexes with unmodified, PEG or cRGD-PEG (RP) modified H3K(+H)4b were systemically administered to tumor xenografts bearing mice. Before and 48 h after treatment, luciferase activity was determined by an IVIS 200 system. The data represent the mean ± SD of luciferase of four determinations for each carrier. *, $P < 0.05$; **, $P < 0.01$; ***, $P < 0.001$.

4.4.5 Inhibition of tumor tissue gene expression and growth by targeting Raf-1

In addition to silencing the luciferase marker, we evaluated the ability of different carriers to deliver siRNA targeting the Raf-1 oncogene *in vivo*. We examined inhibition of MDA-MB-435 tumor growth by modified or unmodified HK/siRNA polyplexes with siRaf-1. Six systemic injections were given via tail vein, three times a week for 2 weeks. As early as the second injection, the modified RP-HK siRaf-1 polyplexes showed 30% greater reduction in tumor size compared to the untreated mice ($P < 0.01$) (Fig. 4.10A). In contrast, there was no statistical difference in tumor growth for treatment with the unmodified HK siRaf-1 polyplex compared to the

untreated groups. After the last injection, the modified RP-HK polyplexes reduced tumor size 33% more effectively than the unmodified HK polyplexes ($P < 0.01$) and nearly 60% more than tumors of untreated mice ($P < 0.01$). Tumor volumes of mice treated with the modified RP-HK carrier in complex with a negative control siLuc were similar to those of untreated mice.

To evaluate whether reduction in tumor growth rate was dependent on reduction in the expression of the Raf-1 oncogene, we determined the Raf-1 mRNA in the various treatment groups by RT-PCR. Compared to the untreated group (Fig. 4.10B), the modified HK polyplexes down-regulated Raf-1 mRNA expression by 90% (lane 3), whereas the unmodified treatment group decreased the RNA by 60% (lane 2). The correlation between Raf-1 mRNA expression and luciferase activity clearly indicated that the target gene silencing was significantly enhanced by ligand-targeting modification of the HK peptides.

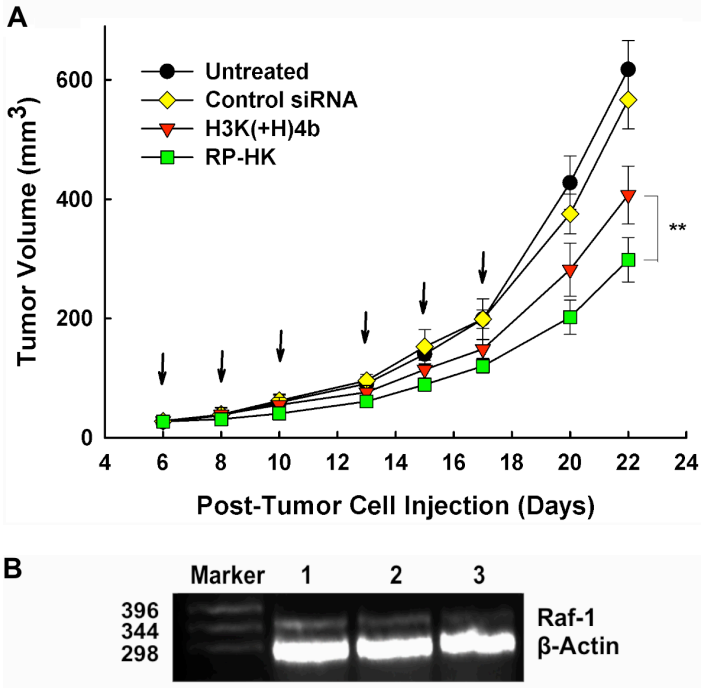

Fig. 4.10. MDA-MB-435 tumor growth and Raf-1 mRNA inhibition.

(A) MDA-MB-435 tumor-bearing mice were separated into four groups when tumor size was about 25 mm^3: untreated, H3K(+H)4b/siLuc control, H3K(+H)4b/Raf-1 siRNA, and RP-HK/Raf-1 siRNA. Treatment was given three times a week for two weeks (arrows). Data for each time point represent the mean ± SD of tumor volume of five determinations for each treatment group. **, $P < 0.01$. (B) Raf-1 and β-actin mRNA expression was determined by RT-PCR analysis of RNA isolated from tumor tissue at day 22. Lanes 1, 2, and 3 represent untreated, unmodified, and modified polyplexes treatment group, respectively.

4.4.6 Immunohistological analysis of treated tumor tissue

Down-regulation of Raf-1 and its downstream effects in tumor tissue of mice treated systemically with HK siRaf-1 polyplexes was evaluated by immunohistochemistry. Tumors from treated mice were sectioned and stained for Raf-1 and Ki67 as well as for apoptosis (with the TUNEL assay) (Fig. 4.11A). Non-necrotic areas of tumor were examined histologically from mice 2 days after the last treatment. DAB-stained

cells were identified (by brown staining) and quantified by analysis of four arbitrarily selected normalized blue images (Brey, Lalani et al. 2003). In viable areas of tumors, Raf-1 protein was down-regulated by nearly 40% and 80% in the unmodified and modified HK siRaf-1 polyplex treatment groups, respectively, compared to untreated groups (Fig. 4.11; $P < 0.01$, modified vs. unmodified or untreated). Notably, reduction of Raf-1 protein with immunostaining was consistent with Raf-1 mRNA suppression determined by RT-PCR. Furthermore, as evidenced by the cell proliferation marker Ki67 (Fig. 4.11), the modified polyplex treatment reduced cell proliferation more effectively (50%) than did unmodified treatment or untreated ($P < 0.01$, modified vs. unmodified, untreated).

The TUNEL assay was used to assess cellular areas of apoptosis (Fig. 4.11). Quantification of staining was not appropriate with TUNEL assay since apoptosis region was sporadically distributed (Fig. 4.11B). Qualitatively, modified RP-HK siRaf-1 polyplexes generally induced larger areas of apoptosis than unmodified HK siRaf-1 polyplexes. In conclusion, immunohistological analysis showed greater reduction of Raf-1 protein and cellular proliferation as well as increased apoptosis with the RP-HK treatment, consistent with enhanced anti-tumor efficacy.

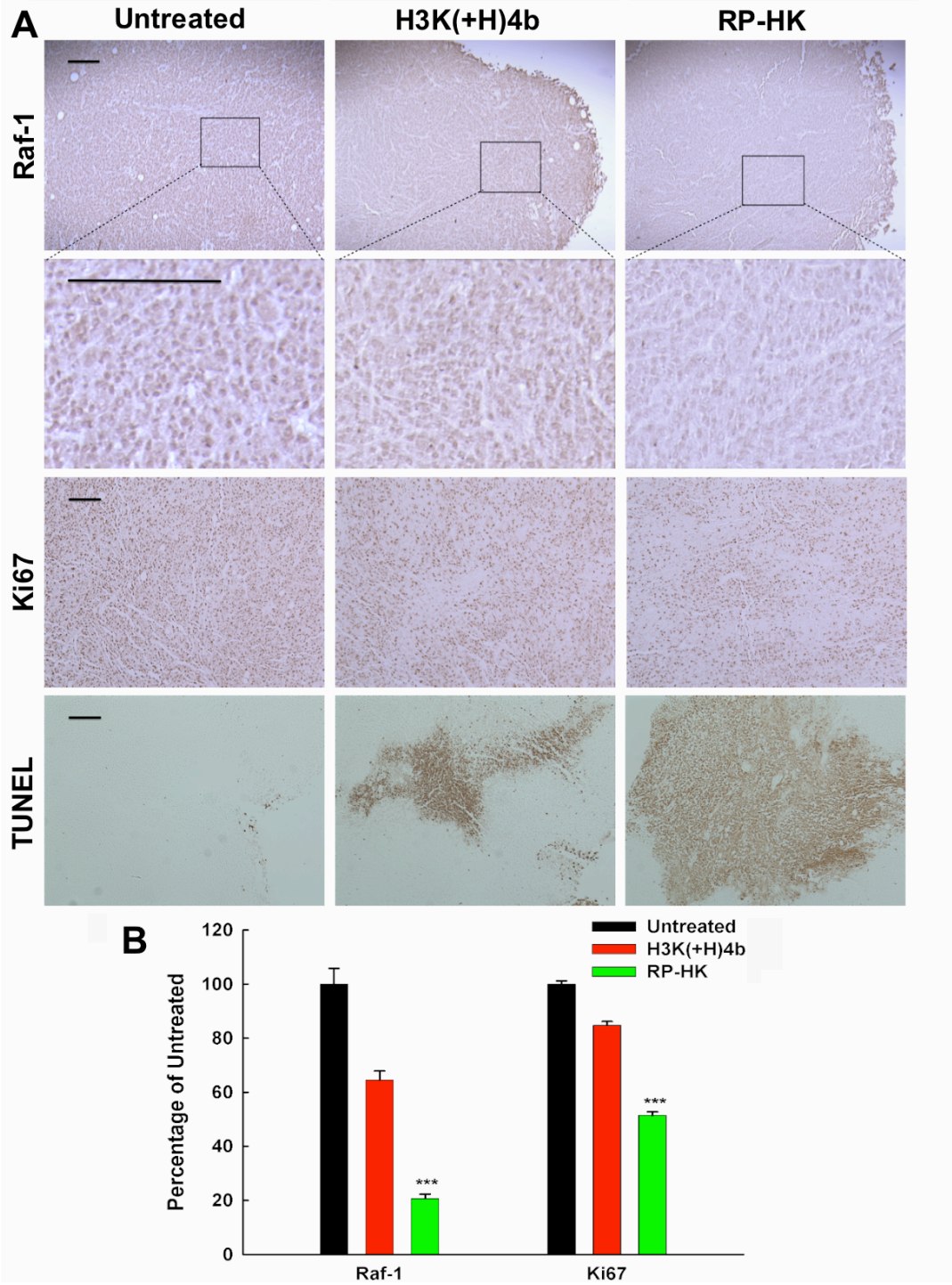

Fig. 4.11. Histochemical analysis of Raf-1, Ki67, and apoptosis.

(A) Scale bars equal 10 μm. (B) Quantification of cells staining positive for Raf-1 and Ki67 with different treatments is shown, expressed as the percentage of untreated control. The data represent the mean ± SD of percentage of four images for each treatment. ***, $P < 0.001$.

4.5 Discussion

The potential of RNAi to provide a substantial advance in therapeutics, especially for cancer treatment, has been limited due to lack of an efficient carrier. Mixson's group has methodically investigated improvements in a family of branched histidine-lysine peptides carriers of siRNA by altering their sequence and number of branches (Leng, Scaria et al. 2008). While the H3K(+H)4b peptide was demonstrated to be an effective carrier of siRNA both *in vitro* and *in vivo*, modification of H3K(+H)4b with a cRGD targeting ligand, in concert with PEGylation, was found to provide a more effective carrier, using an *in vivo* bioluminescence assay (Chou, Leng et al. 2011). Although PEGylation and addition of a tumor-specific ligand were expected to increase accumulation of the polyplexes within the tumor, the mechanisms for the improved carrier were never investigated nor whether the tumor targeting activity of the RP-HK/siRNA polyplexes could translate into greater tumor reduction. We established in this study that the half-life in the bloodstream correlates with increased accumulation of the modified HK polyplexes within the tumor. The improved pharmacokinetics of the modified HK polyplexes resulted in significantly greater reduction of targeted oncogene expression with a marked decrease in tumor size.

PEGylation can provide tumor targeting by facilitating the enhanced permeability and retention (EPR) effect due to an increased blood circulation half-life (Tanaka, Shiramoto et al. 2004). We show here that PEGylation alone of HK/siRNA polyplexes enhances siRNA activity in tumor tissue. The reduction of intratumoral

luciferase was further enhanced using targeted RP-HK/siRNA polyplexes (Fig. 4.9). Thus, it appears that the cRGD and PEG modifications have important and additive contributions. PEG has been used in numerous studies to increase the hydrophilicity of polyparticles including polyplexes, minimize clearance by phagocytic cells, and increase the half-life of the polyparticle *in vivo* (Brannon-Peppas and Blanchette 2004). The improved tumor tissue siRNA activity by the PEGylated-only HK/siRNA polyplexes was likely the result of surface steric stabilization by PEG, which reduced the zeta potential due to an increase in hydrodynamic radius (Woodle, Collins et al. 1992). The reduction in zeta potential (Table 4.1) by nearly 50% for RP-HK/siRNA polyplexes (23 mV) compared to unmodified HK/siRNA polyplexes (41 mV) is attributable to PEG, since the zwitterionic cRGD peptide is not known to alter the hydrodynamic surface properties. Reduction of the surface charge with sterically stabilized polyplexes would be expected to inhibit their non-specific attachment and internalization by cells, prolong their half-life in the circulation, and importantly enhance their ligand receptor-mediated cellular uptake (Levchenko, Rammohan et al. 2002; Bartlett, Su et al. 2007). Without steric stabilization, non-selective attachment to cell surfaces by highly positively charged unmodified HK/siRNA polyplexes may contribute to a larger fractional α clearance and thus slightly lower blood levels (AUC) than that of aqueous siRNA.

It may be possible to increase blood circulation and EPR tumor targeting of HK/siRNA polyplexes further by conjugation with even higher molecular weight PEG (e.g., 5.1 kDa). For example, Sato and colleagues showed that the molecular

weight of PEG as well as the degree of PEGylation significantly influenced the circulation time of polylysine/siRNA polyplexes. By increasing the weight ratio of PEG (to polylysine) from 70% to 90%, the circulatory half-life of polyplexes in the bloodstream was enhanced by 100-fold (Sato, Choi et al. 2007). Consequently, increasing or modifying the PEGylation of HK/siRNA polyplexes might further improve the pharmacokinetic properties and therapeutic window by this mechanism.

An important contribution to tumor tissue targeting appears to be provided by the cyclic RGD peptide ligand, attributable to selective binding to the $\alpha_v\beta_3$ and $\alpha_v\beta_5$ integrins that are over-expressed and activated on cell surfaces of both MDA-MB-435 cancer cells and tumor tissue neovasculature (Wong, Mueller et al. 1998; Hood, Bednarski et al. 2002). The NIR optical fluorescence biodistribution studies on RP-HK:siRNA demonstrated that ligand-targeted polyplexes accumulated at higher levels in the tumor tissue than unmodified polyplexes (Fig. 4.9). With combined cRGD ligand and PEGylation, the RP-HK/siRNA polyplexes gave the greatest improvement in pharmacology, biodistribution and tumor tissue targeting siRNA activity, both for a constitutively expressed reporter gene and a therapeutic gene, Raf-1. Perhaps surprisingly, the modified RP-HK/siRNA polyplexes resulted in an improved pharmacokinetic profile distinct from that observed with a transferrin targeted cyclodextrin-based siRNA polyplexes. In those studies, the blood circulation half-life of aqueous siRNA and targeted cyclodextrin/siRNA polyplexes were similar (Zuckerman, Choi et al.). Moreover, accumulation of the targeted cyclodextrin/siRNA polyplexes occurred in kidneys within 20 minutes of intravenous

administration, whereas targeted RP-HK/siRNA polyplexes showed a substantial delay: fluorescent siRNA was not observed in the bladder until 2 hours after administration. It is unclear why this difference in renal clearance between the two polyplexes occurred, since the particle size of the targeted RP-HK/siRNA polyplexes should enable their passing readily through the endothelial fenestrations of the glomerulus. Although several studies, including my results with unmodified HK/siRNA polyplexes, have demonstrated a rapid decrease in blood levels of polymeric polyplexes within 20 minutes of intravenous administration (Bartlett, Su et al. 2007; Merkel, Librizzi et al. 2009), the targeted RP-HK/siRNA polyplexes were detected in the blood for up to 2 hours. The prolong b-phase by which serum levels of RP-HK polyplex nearly levels off between 20 minutes and two hours is somewhat surprising and may in part represent polyplex absorption to serum proteins. To date, no reported studies of PEGylated polyplexes have achieved the prolonged blood circulation observed with PEGylated liposomes (Woodle and Lasic 1992), such as wrapsomes (Yagi, Manabe et al. 2009) in which PEG extended the blood half-life in mice up to 17 hr.

Inhibition of the target gene was consistent with pharmacokinetics and distribution in that luciferase expression was markedly down-regulated by the modified polyplexes. Nevertheless, it was still surprising that a single treatment would give rise to over 70% of gene silencing of luciferase, particularly since many cells expressing luciferase are several layers removed from the vasculature. We corroborated this striking down-regulation of luciferase activity with both xenogen imaging and

measurement of the luciferase activity from extracts of tumor xenografts. This silencing effect by RP-HK/siRNA polyplexes was nearly identical over a wide range of tumor sizes (50 to 180 mm^3) (Fig. 4.8) (Chou, Leng et al. 2011), indicating that targeting mechanisms such as EPR remained similar (Heneweer, Holland et al.). Moreover, the decrease in luciferase activity was homogeneous throughout the tumor, further validating the results. Perhaps more importantly, the reduction of Raf-1 mRNA and protein expression by 90% and 80%, respectively, further confirms the results of luciferase activity. Several other investigators have also found that non-viral carriers of siRNA have unexpectedly high rates of silencing their targets (Takeshita, Minakuchi et al. 2005; Bartlett and Davis 2006; Ofek, Fischer et al. 2010; Yang, Dou et al. 2011). Taken together, these results strongly suggest that the siRNA can selectively silence their targets in the tumor xenograft very efficiently, but the mechanisms for this high efficiency remain to be elucidated.

This high efficiency of siRNA delivery to subcutaneous xenograft tumors, observed with the RP-HK/siRNA polyplexes, is in marked contrast to other stabilized and targeted nucleic acid delivery systems. It has been suggested that effective siRNA delivery to tumor xenografts may be aided by membranous exosomal vesicles, which are derived from multivesicular bodies (MVB) and subsequently released from the cell (Mears, Craven et al. 2004; Meckes, Shair et al. 2010). The 40 to 100 nm exosomes, which contain specific proteins and RNA including RNA-induced silencing complex (RISC), P body component GW182, mRNA, and microRNA, have been speculated to have an important role in intercellular communication between

tumor cells (Valadi, Ekstrom et al. 2007; Lakhal and Wood). Importantly, the exosomal mRNA retains its function after transfer to the recipient cell. Although there is yet no evidence that siRNA entrapped within exosomes can shuttle intercellularly to target mRNA, exosome-mediated gene transfer has been exploited for targeted siRNA delivery across the bloodbrain barrier resulting in 60% gene inhibition (Alvarez-Erviti, Seow et al. 2011). Thus, exosome-mediated intercellular communication within tumor cells may have a role in efficient luciferase or Raf-1 knockdown within the tumor. Despite the possibility of a biologically mediated mechanism having a role in the knock-down of the targeted gene, the importance of increasing transfection efficiency of polyplexes and the underpinning mechanisms that increase this efficiency should not be minimized.

Although tumor growth was inhibited more effectively with the modified HK polyplexes, reduction in tumor size was not equivalent to Raf-1 gene inhibition; that is, we did not observe a 90% reduction in tumor size corresponding to the 90% knockdown we observed with the Raf-1 gene. Because tumor proliferation and apoptosis are mediated by multiple and complex signal transduction pathways regardless of the oncogene targeted, there may be cross-talk and compensatory responses between pathways that facilitate the development of resistance to therapeutics. For example, Hoeflich and colleagues have indicated that diminished mitogen-activated protein kinase (MEK), downstream of Raf-1, activates PI3K pathway driving tumor development in basal-cell like breast cancers (Hoeflich, O'Brien et al. 2009). Depending on the malignant cell and its compensatory

responses, oncogenes such as survivin can be targeted, which may result in greater tumor inhibition; for example, siRNA targeting survivin decreased MDA-MB-435 cellular growth significantly more than targeting Raf-1 (data not shown). Regardless of the oncogene targeted, it will be important to block additional signal pathways to suppress tumor growth more effectively. Moreover, there have been a number of studies showing that blocking multiple pathways in malignant tumor cells gives a synergistic reduction in tumor size (Spankuch, Kurunci-Csacsko et al. 2007; Sun, Du et al. 2011; Xiong and Lavasanifar 2011). Consequently, future work in Mixson's laboratory will focus on enhancing siRNA delivery systems in combination with synergistic inhibitory therapies that target interactive signal pathways.

4.6 Conclusion

We investigated the pharmacokinetics, biodistribution, and therapeutic activity of RP-HK/siRNA polyplexes targeting Raf-1 gene expression in a subcutaneous xenograft tumor model in mice. Consistent with greater silencing of the reporter gene in tumor xenografts, the pharmacokinetics showed that RP-HK/siRNA polyplexes have an increased half-life in the bloodstream and greater accumulation of siRNA within the tumor. Consequently, translational studies were undertaken with a therapeutic siRNA candidate targeting Raf-1. The results show that targeted HK/siRNA polyplexes gave a significantly greater reduction of the targeted tumor tissue gene expression, at both mRNA and protein levels. This resulted in a marked decrease in tumor growth rate,

with histochemistry measurements of downstream effects supporting an siRNA-mediated mechanism of action for the observed efficacy.

Chapter 5: Conclusion and future work

5.1 Conclusion

The most looming hurdle of siRNA-based therapeutics has been the lack of a reliable carrier. The overall goal of this dissertation is to develop more effective carriers for systemic delivery of siRNA to the tumors. As a result, I have investigated biophysical properties that are critical for stable polyplex formation. Furthermore, the HK peptide was modified with PEG and ligand cRGD to enhance the recognition and specificity at target tissues. The physical characterizations and chemical modifications were utilized to investigate and optimize HK peptide carriers.

Histidines of HK peptides were initially viewed as buffering agents that would aid the release of siRNA. However, previous studies suggested that histidines might play a role in stabilization against serum-induced degradation. In chapter 2, we analyzed thermodynamic binding of siRNA and peptides differing in sequences or number of branches. The exothermicity of histidine-containing peptides suggested the presence of non-ionic interaction. Using a ^{15}N selectively labeled peptide, we determined that histidines mediate hydrogen bonding with siRNA and enhance the stability of polyplexes.

To enhance the pharmacokinetics of polyplex, the most effective carrier H3K(+H)4b determined in previous studies was conjugated to PEG and cRGD peptide. In chapter

3, *in vitro* and biophysical characteristics of these modified HK/siRNA polyplexes (delayed migration on gel, size, surface charge, morphology and cell culture studies) have been determined and correlated with silencing tumor targets in a mouse model. It was observed that PEGylation inhibited binding of the peptide to siRNA. To produce stable polyplexes with PEGylated H3K(+H)4b and siRNA, we showed that it is important to incorporate an unmodified H2K4b that has greater charge density in the two-step mixing procedure. With an *in vivo* bioluminescence assay, we found that unmodified peptide was the most effective carrier *in vitro*, whereas the polyplex containing $(RGD\text{-}PEG)^4$H3K(+H)4b down-regulated luciferase expression most effectively by 75% *in vivo*. Moreover, we found that the enhanced gene silencing activity was correlated to the number of cRGD-PEG per peptide molecule and was not a result of cytokine induction. Notably, the commonly used practice of utilizing only effective carriers *in vitro* for *in vivo* study may not result in identification of effective carriers.

In chapter 4, we continued studying the pharmacokinetics and biodistribution of the most effective carrier, $(RGD\text{-}PEG)^4$H3K(+H)4b (RP-HK), determined in chapter 3. Pharmacokinetic parameters such as serum half-life, area under curve, and tumor localization of RP-HK polyplex are enhanced by 3 to 5 times compared to unmodified polyplexes. Importantly, the improved pharmacokinetics were correlated to greater gene silencing in tumor xenograft models. Whereas tumor size was inhibited by 60%, Raf-1 target gene was inhibited by 90%, showing that RP-HK is a promising carrier for systemic delivery of siRNA. To further improve antitumor

efficacy, it is important to target alternative oncogenes (e.g., survivin) or block additional pathways with the combination of chemotherapeutics (e.g., PI3K and Bcl2).

In conclusion, this dissertation provides insights in characterization of biophysical properties that are critical to the biological activity of peptide/siRNA polyplexes. We also synthesized chemically modified HK peptide in which siRNA could be delivered *in vivo* more effectively.

5.2 Future work

The ultimate goal of work like this is to establish an evidence-based approach to screen carrier candidates. Experimental investigation of the binding mechanism and dynamic structural adjustments of siRNA polyplex self-assembly are expected to dictate silencing activity. For example, we have found correlations between the entropy-driven process in the ITC profile and *in vitro* transfection efficiency (data not shown): the condensing process with an enthalpy greater than 20 kcal/mol may prevent the decomplexation and reduce release of siRNA. Furthermore, this endothermic binding is likely to correlate with the content of lysines. Therefore, lysines not only provide an electrostatic driving force to promote histidine-mediated hydrogen bonding, they also play an important role in electrostatic polyplex aggregation. To determine optimal binding, peptides differing in the length of histidine spacers between two lysine residues will be synthesized and studied with

ITC to correlate their hydrogen bonding potentials and thermodynamic profiles with transfection results *in vitro* and *in vivo*. This study is expected to open the door for reorientation of current procedures for the evaluation of transfection agents.

One of the unanswered questions left in the chapter 2 is the nature of the assembled structure of HK/siRNA polyplexes and the change induced by electrostatic versus nonelectrostatic interactions. The molecular origin of peptide/siRNA binding may provide more insight into the design of peptide sequence. To gain the information of binding interface, we will collaborate with Dr. Jana Shen at School of Pharmacy to develop computer simulation tools. Using a coarse-grained polymer model and the constant pH molecular dynamics technique (Wallace and Shen 2012; Fu, Markegard et al. 2013), accurate electrostatic calculations and large-scale molecular dynamic simulations for peptide/siRNA self-assembly process can be performed. We will also synthesize singly labeled linear HK peptide, corresponding to a branch of the branched peptide, to obtain residue-specific characterizations with NMR. The information obtained from ITC, NMR, and simulations will be systemically analyzed to identify the correlation between biophysical properties and biological activities. Moreover, through the collaboration with Dr. Seog and Dr. Kahn, the peptide/siRNA condensation and decomplexation process may be studied at a single molecule level, and the morphology and mechanical properties of polyplexes may be investigated with atomic force microscopy.

In chapter 2, we discovered that although the unmodified peptide is a more effective carrier for siRNA delivery *in vitro*, the cRGD-PEG modified peptide shows significantly greater delivery efficiency *in vivo*. Contradictory results between *in vitro* and *in vivo* studies have also been observed by other groups (Whitehead, Matthews et al. 2012). To improve *in vitro/in vivo* translatability, the effects of different routes of delivery to the trafficking of siRNA polyplexes will be elucidated. Anderson's group has recently shown that the kinetics of assembly and disassembly of siRNA complexes can be tracked by FRET-labeled siRNA (Alabi, Love et al. 2012). Although this approach is currently limited to cell culture experiments, it will be interesting to study unpackaging of nucleic acids *in vivo* to correlate with complexation properties of polyplexes derived from biophysical experiments. A fundamental understanding of polyplex disassembly *in vivo* may also reveal whether other factors such as polyplex-serum interaction or specific tumor type responses are involved.

In the antitumor efficacy experiment, it appears that even though the Raf-1 oncogene was downregulated by 90%, tumor growth inhibition was not as significant as target gene silencing. As discussed in the chapter 4, cross-talk and feedback compensation between oncogenic signal transduction pathways may play an important role in tumor cell proliferation. To reduce the tumor growth more effectively, alternative genes and pathways should be targeted. Preliminary data has shown that at least *in vitro*, siRNA targeted to survivin reduces viability of cancer cells more effectively than Raf-1 siRNA (60% vs. 30%, unpublished data). I will compare the antitumor efficacy of

surivin siRNA with Raf-1 in a xenograft model with cRGD-PEG modified HK peptides.

In addition to replacing Raf-1 with survivin siRNA, the combination of chemotherapy and siRNA therapy will also be further examined to promote synergistic tumor suppression. Docetaxel is an FDA approved anti-mitotic chemotherapeutic agent which has been used for treatment of breast, ovarian, prostate, and lung cancer (Clarke and Rivory 1999; Lyseng-Williamson and Fenton 2005; Michael, Syrigos et al. 2009). The goal of combining docetaxel and siRNA is to inhibit the tumor growth more effectively and to lower the dosage of docetaxel to minimize the side effects. This delivery platform and strategy may increase the applicability of these therapies for clinical trials.

To advance the HK/siRNA polyplex towards clinical trials, it is important to improve the stability of the polyplex. As discussed in the chapter 4, increasing the level of PEGylation of polyplexes may significantly prolong the serum half-life. However, it may be difficult for heavily PEGylated peptides to form polyplexes with siRNA. Moreover, heavily PEGylated polyplexes may also reduce the interaction with the cell membrane and thus, decrease cellular uptake. Post-PEGylation of HK/siRNA polyplexes may be an alternative approaches to minimize influence of PEG to peptide/siRNA binding and polyplex formation. In addition to shielding the polyplex with PEG, there are alternative approaches to enhance the stability. For example, as I discussed in the Introduction, Kataoka's group has shown that the serum stability of

the polymeric micelles structure can be enhanced through disulfide cross-linking (Christie, Matsumoto et al. 2012). As for HK peptides, cysteines added to the terminals of branched peptides can be oxidized to cross-link RP-HK peptides. The preliminary data shows that the cross-linked RP-HK polyplex down-regulates 50% of the luciferase expression in the tumor xenografts compared with untreated groups. It will be interesting to determine whether the cross-linked RP-HK polyplex maintains gene silencing ability with long-term enzymatic stress.

Most of the efficacious polyplexes or lipoplexes are prepared by mixing and self-assembly of carriers and siRNA. A further challenge of RNAi therapeutics is the scale-up of the production of nanoplexes from small doses for mice to larger doses in humans. Incomplete mixing may result in heterogeneity in the biophysical properties of nanoparticles which are likely to create variance in their biological activity. The use of microfluidic devices for mixing may be a scalable technique to produce monodisperse polyplexes or lipoplexes (Belliveau, Huft et al. 2012; Chen, Love et al. 2012). Precisely controlled mixing process with microfluidic bioreactors has the advantage of preparing reproducibly homogenous nanomaterials that are sensitive to the concentration upon mixing. It is anticipated that microfluidic devices will facilitate the production of HK/siRNA polyplexes at the clinical scale.

To advance the HK/siRNA polyplex towards clinical trials, it is important to improve the stability of the polyplex. As discussed in the chapter 4, increasing the level of PEGylation of polyplexes may significantly prolong the serum half-life. However, it

may be difficult for heavily PEGylated peptides to form polyplexes with siRNA. Moreover, the uptake and the release of payloads may also be potential problems for heavily PEGylated polyplexes. Post-PEGylation of HK/siRNA polyplexes may be an alternative approaches to minimize influence of PEG to peptide/siRNA binding and polyplex formation. In addition to shielding the polyplex with PEG, there are alternative approaches to enhance the stability. For example, as discussed in the Introduction, Kataoka's group has shown that the stability of the polymeric micelles structure can be enhanced through disulfide cross-linking (Christie, Matsumoto et al. 2012). As for HK peptides, cysteines added to the terminals of branched peptides can be oxidized to cross-link RP-HK peptides. The preliminary data shows that the cross-linked RP-HK polyplex down-regulates 50% of the luciferase expression in the tumor xenografts compared with untreated groups. It will be interesting to determine whether the cross-linked RP-HK polyplex maintains gene silencing ability with long-term enzymatic stress.

Most of the efficacious polyplexes or lipoplexes are prepared by mixing and self-assembly of carriers and siRNA. A further challenge of RNAi therapeutics is the scale-up of the production of nanoplexes from small doses for mice to larger doses in humans. Incomplete mixing may result in heterogeneity in the biophysical properties of nanoparticles which are likely to create variance in their biological activity. The use of microfluidic devices for mixing may be a scalable technique to produce monodisperse polyplexes or lipoplexes (Belliveau, Huft et al. 2012; Chen, Love et al. 2012). Precisely controlled mixing process with microfluidic bioreactors has the

advantage of preparing reproducibly homogenous nanomaterials that are sensitive to the concentration upon mixing. It is anticipated that microfluidic devices will facilitate the production of HK/siRNA polyplexes at the clinical scale.

Appendix

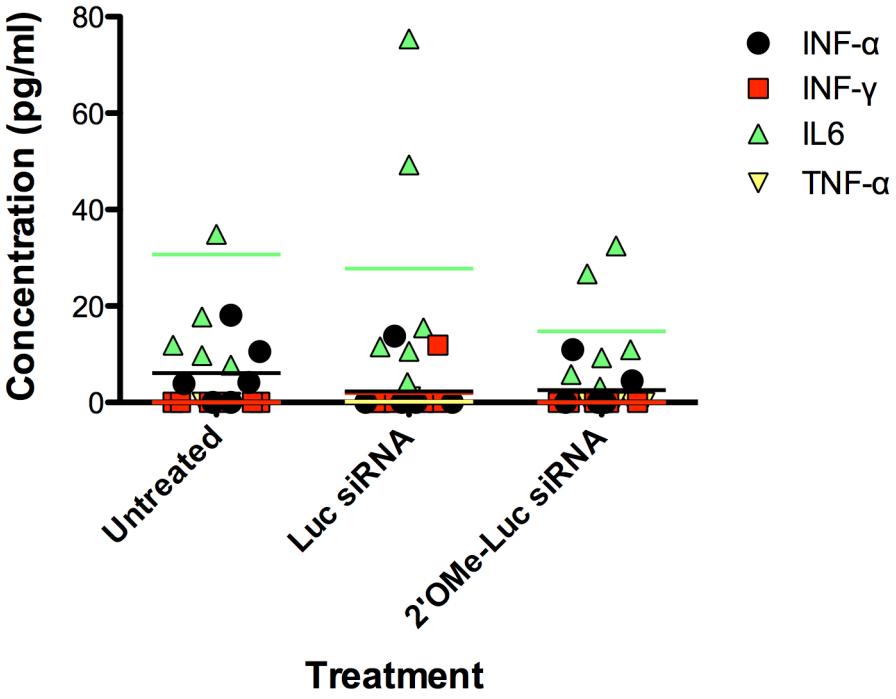

Fig. A1. All data points of cytokine induction corresponding to Fig. 3.6.

Bibliography

Aigner, A. (2008). "Cellular delivery in vivo of siRNA-based therapeutics." Curr Pharm Des **14**(34): 3603-19.

Alabi, C. A., K. T. Love, G. Sahay, T. Stutzman, W. T. Young, R. Langer and D. G. Anderson (2012). "FRET-labeled siRNA probes for tracking assembly and disassembly of siRNA nanocomplexes." ACS Nano **6**(7): 6133-41.

Allen, M. H., M. D. Green, H. K. Getaneh, K. M. Miller and T. E. Long (2011). "Tailoring charge density and hydrogen bonding of imidazolium copolymers for efficient gene delivery." Biomacromolecules **12**(6): 2243-50.

Alsina, M., J. Tabernero, G. Shapiro, H. Burris, J. R. Infante, G. J. Weiss, C. Cervantes-Ruiperez, M. M. Gounder, L. Paz-Ares, R. Falzone, J. Hill, J. Cehelsky, A. Vaishnaw, J. Gollob and P. LoRusso (2012). Open-label extension study of the RNAi therapeutic ALN-VSP02 in cancer patients responding to therapy. 2012 ASCO Annual Meeting, Chicago, Illinois, Journal of Clinical Oncology.

Alvarez-Erviti, L., Y. Seow, H. Yin, C. Betts, S. Lakhal and M. J. Wood (2011). "Delivery of siRNA to the mouse brain by systemic injection of targeted exosomes." Nat Biotechnol **29**(4): 341-5.

Arap, W., R. Pasqualini and E. Ruoslahti (1998). "Cancer treatment by targeted drug delivery to tumor vasculature in a mouse model." Science **279**(5349): 377-80.

Bachovchin, W. W. (1986). "15N NMR spectroscopy of hydrogen-bonding interactions in the active site of serine proteases: evidence for a moving histidine mechanism." Biochemistry **25**(23): 7751-9.

Bartlett, D. W. and M. E. Davis (2006). "Insights into the kinetics of siRNA-mediated gene silencing from live-cell and live-animal bioluminescent imaging." Nucleic Acids Res **34**(1): 322-33.

Bartlett, D. W. and M. E. Davis (2008). "Impact of tumor-specific targeting and dosing schedule on tumor growth inhibition after intravenous administration of siRNA-containing nanoparticles." Biotechnol Bioeng **99**(4): 975-85.

Bartlett, D. W., H. Su, I. J. Hildebrandt, W. A. Weber and M. E. Davis (2007). "Impact of tumor-specific targeting on the biodistribution and efficacy of siRNA nanoparticles measured by multimodality in vivo imaging." Proc Natl Acad Sci U S A **104**(39): 15549-54.

Basu, H. S., H. C. Schwietert, B. G. Feuerstein and L. J. Marton (1990). "Effects of variation in the structure of spermine on the association with DNA and the induction of DNA conformational changes." Biochem J **269**(2): 329-34.

Behlke, M. A. (2008). "Chemical modification of siRNAs for in vivo use." Oligonucleotides **18**(4): 305-19.

Belliveau, N. M., J. Huft, P. J. Lin, S. Chen, A. K. Leung, T. J. Leaver, A. W. Wild, J. B. Lee, R. J. Taylor, Y. K. Tam, C. L. Hansen and P. R. Cullis (2012). "Microfluidic Synthesis of Highly Potent Limit-size Lipid Nanoparticles for In Vivo Delivery of siRNA." Mol Ther Nucleic Acids **1**: e37.

Bernstein, E., A. A. Caudy, S. M. Hammond and G. J. Hannon (2001). "Role for a bidentate ribonuclease in the initiation step of RNA interference." Nature **409**(6818): 363-6.

Bevilacqua, P. C. and T. R. Cech (1996). "Minor-groove recognition of double-stranded RNA by the double-stranded RNA-binding domain from the RNA-activated protein kinase PKR." Biochemistry **35**(31): 9983-94.

Boturyn, D., J. L. Coll, E. Garanger, M. C. Favrot and P. Dumy (2004). "Template assembled cyclopeptides as multimeric system for integrin targeting and endocytosis." J Am Chem Soc **126**(18): 5730-9.

Brannon-Peppas, L. and J. O. Blanchette (2004). "Nanoparticle and targeted systems for cancer therapy." Adv Drug Deliv Rev **56**(11): 1649-59.

Brey, E. M., Z. Lalani, C. Johnston, M. Wong, L. V. McIntire, P. J. Duke and C. W. Patrick, Jr. (2003). "Automated selection of DAB-labeled tissue for immunohistochemical quantification." J Histochem Cytochem **51**(5): 575-84.

Brower, V. (2010). "RNA interference advances to early-stage clinical trials." J Natl Cancer Inst **102**(19): 1459-61.

Burckhardt, G., C. Zimmer and G. Luck (1976). "Conformation and reactivity of DNA in the complex with proteins. IV. Circular dichroism of poly-L-histidine model complexes with DNA polymers and specificity of the interaction." Nucleic Acids Res **3**(3): 561-80.

Buyens, K., M. Meyer, E. Wagner, J. Demeester, S. C. De Smedt and N. N. Sanders (2010). "Monitoring the disassembly of siRNA polyplexes in serum is crucial for predicting their biological efficacy." J Control Release **141**(1): 38-41.

Caliceti, P. and F. M. Veronese (2003). "Pharmacokinetic and biodistribution properties of poly(ethylene glycol)-protein conjugates." Advanced drug delivery reviews **55**(10): 1261-77.

Chen, D., K. T. Love, Y. Chen, A. A. Eltoukhy, C. Kastrup, G. Sahay, A. Jeon, Y. Dong, K. A. Whitehead and D. G. Anderson (2012). "Rapid discovery of potent siRNA-containing lipid nanoparticles enabled by controlled microfluidic formulation." J Am Chem Soc **134**(16): 6948-51.

Chen, Q. R., L. Zhang, P. W. Luther and A. J. Mixson (2002). "Optimal transfection with the HK polymer depends on its degree of branching and the pH of endocytic vesicles." Nucleic Acids Res **30**(6): 1338-45.

Chen, Q. R., L. Zhang, S. A. Stass and A. J. Mixson (2001). "Branched co-polymers of histidine and lysine are efficient carriers of plasmids." Nucleic Acids Res **29**(6): 1334-40.

Chen, Y., T. Kortemme, T. Robertson, D. Baker and G. Varani (2004). "A new hydrogen-bonding potential for the design of protein-RNA interactions predicts specific contacts and discriminates decoys." Nucleic Acids Res **32**(17): 5147-62.

Chien, P. Y., J. Wang, D. Carbonaro, S. Lei, B. Miller, S. Sheikh, S. M. Ali, M. U. Ahmad and I. Ahmad (2005). "Novel cationic cardiolipin analogue-based liposome for efficient DNA and small interfering RNA delivery in vitro and in vivo." Cancer Gene Ther **12**(3): 321-8.

Chiu, Y. L., A. Ali, C. Y. Chu, H. Cao and T. M. Rana (2004). "Visualizing a correlation between siRNA localization, cellular uptake, and RNAi in living cells." Chem Biol **11**(8): 1165-75.

Chiu, Y. L. and T. M. Rana (2003). "siRNA function in RNAi: a chemical modification analysis." Rna **9**(9): 1034-48.

Chou, S. T., Q. Leng, P. Scaria, J. D. Kahn, L. J. Tricoli, M. Woodle and A. J. Mixson (2013). "Surface-modified HK:siRNA nanoplexes with enhanced pharmacokinetics and tumor growth inhibition." Biomacromolecules **14**(3): 752-60.

Chou, S. T., Q. Leng, P. Scaria, M. Woodle and A. J. Mixson (2011). "Selective modification of HK peptides enhances siRNA silencing of tumor targets in vivo." Cancer Gene Ther **18**(10): 707-16.

Christie, R. J., Y. Matsumoto, K. Miyata, T. Nomoto, S. Fukushima, K. Osada, J. Halnaut, F. Pittella, H. J. Kim, N. Nishiyama and K. Kataoka (2012). "Targeted polymeric micelles for siRNA treatment of experimental cancer by intravenous injection." ACS nano **6**(6): 5174-89.

Clarke, S. J. and L. P. Rivory (1999). "Clinical pharmacokinetics of docetaxel." Clin Pharmacokinet **36**(2): 99-114.

Dassie, J. P., X. Y. Liu, G. S. Thomas, R. M. Whitaker, K. W. Thiel, K. R. Stockdale, D. K. Meyerholz, A. P. McCaffrey, J. O. McNamara, 2nd and P. H. Giangrande (2009). "Systemic administration of optimized aptamer-siRNA chimeras promotes regression of PSMA-expressing tumors." Nat Biotechnol **27**(9): 839-49.

Davidson, T. J., S. Harel, V. A. Arboleda, G. F. Prunell, M. L. Shelanski, L. A. Greene and C. M. Troy (2004). "Highly efficient small interfering RNA delivery to primary mammalian neurons induces MicroRNA-like effects before mRNA degradation." J Neurosci **24**(45): 10040-6.

Davis, M. E., J. E. Zuckerman, C. H. Choi, D. Seligson, A. Tolcher, C. A. Alabi, Y. Yen, J. D. Heidel and A. Ribas (2010). "Evidence of RNAi in humans from systemically administered siRNA via targeted nanoparticles." Nature **464**(7291): 1067-70.

Delaglio, F., S. Grzesiek, G. W. Vuister, G. Zhu, J. Pfeifer and A. Bax (1995). "NMRPipe: a multidimensional spectral processing system based on UNIX pipes." J Biomol NMR **6**(3): 277-93.

El-Sayed, A., I. A. Khalil, K. Kogure, S. Futaki and H. Harashima (2008). "Octaarginine- and octalysine-modified nanoparticles have different modes of endosomal escape." J Biol Chem **283**(34): 23450-61.

Elmen, J., H. Thonberg, K. Ljungberg, M. Frieden, M. Westergaard, Y. Xu, B. Wahren, Z. Liang, H. Orum, T. Koch and C. Wahlestedt (2005). "Locked nucleic acid (LNA) mediated improvements in siRNA stability and functionality." Nucleic Acids Res **33**(1): 439-47.

Esbjorner, E. K., P. Lincoln and B. Norden (2007). "Counterion-mediated membrane penetration: cationic cell-penetrating peptides overcome Born energy barrier by ion-pairing with phospholipids." Biochim Biophys Acta **1768**(6): 1550-8.

Farr-Jones, S., W. Y. L. Wong, W. G. Gutheil and W. W. Bachovchin (1993). "Direct observation of the tautomeric forms of histidine in nitrogen-15 NMR spectra

at low temperatures. Comments on intramolecular hydrogen bonding and on tautomeric equilibrium constants." J Am Chem Soc **115**(15): 6813-9.

Felding-Habermann, B., T. E. O'Toole, J. W. Smith, E. Fransvea, Z. M. Ruggeri, M. H. Ginsberg, P. E. Hughes, N. Pampori, S. J. Shattil, A. Saven and B. M. Mueller (2001). "Integrin activation controls metastasis in human breast cancer." Proc Natl Acad Sci U S A **98**(4): 1853-8.

Fire, A., S. Xu, M. K. Montgomery, S. A. Kostas, S. E. Driver and C. C. Mello (1998). "Potent and specific genetic interference by double-stranded RNA in Caenorhabditis elegans." Nature **391**(6669): 806-11.

Fischer, D., Y. Li, B. Ahlemeyer, J. Krieglstein and T. Kissel (2003). "In vitro cytotoxicity testing of polycations: influence of polymer structure on cell viability and hemolysis." Biomaterials **24**(7): 1121-31.

Frankel, A. D. and C. O. Pabo (1988). "Cellular uptake of the tat protein from human immunodeficiency virus." Cell **55**(6): 1189-93.

Fu, I. W., C. B. Markegard, B. K. Chu and H. D. Nguyen (2013). "The role of electrostatics and temperature on morphological transitions of hydrogel nanostructures self-assembled by peptide amphiphiles via molecular dynamics simulations." Adv Healthc Mater **2**(10): 1388-400.

Furumoto, K., S. Nagayama, K. Ogawara, Y. Takakura, M. Hashida, K. Higaki and T. Kimura (2004). "Hepatic uptake of negatively charged particles in rats: possible involvement of serum proteins in recognition by scavenger receptor." J Control Release **97**(1): 133-41.

Geisbert, T. W., L. E. Hensley, E. Kagan, E. Z. Yu, J. B. Geisbert, K. Daddario-DiCaprio, E. A. Fritz, P. B. Jahrling, K. McClintock, J. R. Phelps, A. C. Lee, A. Judge, L. B. Jeffs and I. MacLachlan (2006). "Postexposure protection of guinea pigs against a lethal ebola virus challenge is conferred by RNA interference." J Infect Dis **193**(12): 1650-7.

Giljohann, D. A., D. S. Seferos, A. E. Prigodich, P. C. Patel and C. A. Mirkin (2009). "Gene regulation with polyvalent siRNA-nanoparticle conjugates." J Am Chem Soc **131**(6): 2072-3.

Grimm, D., K. L. Streetz, C. L. Jopling, T. A. Storm, K. Pandey, C. R. Davis, P. Marion, F. Salazar and M. A. Kay (2006). "Fatality in mice due to oversaturation of cellular microRNA/short hairpin RNA pathways." Nature **441**(7092): 537-41.

Halder, J., A. A. Kamat, C. N. Landen, Jr., L. Y. Han, S. K. Lutgendorf, Y. G. Lin, W. M. Merritt, N. B. Jennings, A. Chavez-Reyes, R. L. Coleman, D. M. Gershenson, R. Schmandt, S. W. Cole, G. Lopez-Berestein and A. K. Sood (2006). "Focal adhesion kinase targeting using in vivo short interfering RNA delivery in neutral liposomes for ovarian carcinoma therapy." Clin Cancer Res **12**(16): 4916-24.

Hammond, S. M., E. Bernstein, D. Beach and G. J. Hannon (2000). "An RNA-directed nuclease mediates post-transcriptional gene silencing in Drosophila cells." Nature **404**(6775): 293-6.

Hammond, S. M., S. Boettcher, A. A. Caudy, R. Kobayashi and G. J. Hannon (2001). "Argonaute2, a link between genetic and biochemical analyses of RNAi." Science **293**(5532): 1146-50.

Hatefi, A., Z. Megeed and H. Ghandehari (2006). "Recombinant polymer-protein fusion: a promising approach towards efficient and targeted gene delivery." J Gene Med **8**(4): 468-76.

Heidel, J. D., Z. Yu, J. Y. Liu, S. M. Rele, Y. Liang, R. K. Zeidan, D. J. Kornbrust and M. E. Davis (2007). "Administration in non-human primates of escalating intravenous doses of targeted nanoparticles containing ribonucleotide reductase subunit M2 siRNA." Proc Natl Acad Sci U S A **104**(14): 5715-21.

Heneweer, C., J. P. Holland, V. Divilov, S. Carlin and J. S. Lewis (2011). "Magnitude of enhanced permeability and retention effect in tumors with different phenotypes: 89Zr-albumin as a model system." J Nucl Med **52**(4): 625-33.

Hoeflich, K. P., C. O'Brien, Z. Boyd, G. Cavet, S. Guerrero, K. Jung, T. Januario, H. Savage, E. Punnoose, T. Truong, W. Zhou, L. Berry, L. Murray, L. Amler, M. Belvin, L. S. Friedman and M. R. Lackner (2009). "In vivo antitumor activity of MEK and phosphatidylinositol 3-kinase inhibitors in basal-like breast cancer models." Clin Cancer Res **15**(14): 4649-64.

Hood, J. D., M. Bednarski, R. Frausto, S. Guccione, R. A. Reisfeld, R. Xiang and D. A. Cheresh (2002). "Tumor regression by targeted gene delivery to the neovasculature." Science **296**(5577): 2404-7.

Hornung, V., M. Guenthner-Biller, C. Bourquin, A. Ablasser, M. Schlee, S. Uematsu, A. Noronha, M. Manoharan, S. Akira, A. de Fougerolles, S. Endres and G. Hartmann (2005). "Sequence-specific potent induction of IFN-alpha by short interfering RNA in plasmacytoid dendritic cells through TLR7." Nat Med **11**(3): 263-70.

Huh, M. S., S. Y. Lee, S. Park, S. Lee, H. Chung, Y. Choi, Y. K. Oh, J. H. Park, S. Y. Jeong, K. Choi, K. Kim and I. C. Kwon (2010). "Tumor-homing glycol chitosan/polyethylenimine nanoparticles for the systemic delivery of siRNA in tumor-bearing mice." J Control Release **144**(2): 134-43.

Ishimoto, T., Y. Takei, Y. Yuzawa, K. Hanai, S. Nagahara, Y. Tarumi, S. Matsuo and K. Kadomatsu (2008). "Downregulation of monocyte chemoattractant protein-1 involving short interfering RNA attenuates hapten-induced contact hypersensitivity." Mol Ther **16**(2): 387-95.

Jackson, A. L., J. Burchard, D. Leake, A. Reynolds, J. Schelter, J. Guo, J. M. Johnson, L. Lim, J. Karpilow, K. Nichols, W. Marshall, A. Khvorova and P. S. Linsley (2006). "Position-specific chemical modification of siRNAs reduces "off-target" transcript silencing." Rna **12**(7): 1197-205.

Jensen, L. B., K. Mortensen, G. M. Pavan, M. R. Kasimova, D. K. Jensen, V. Gadzhyeva, H. M. Nielsen and C. Foged (2010). "Molecular characterization of the interaction between siRNA and PAMAM G7 dendrimers by SAXS, ITC, and molecular dynamics simulations." Biomacromolecules **11**(12): 3571-7.

Jiang, G., K. Park, J. Kim, K. S. Kim, E. J. Oh, H. Kang, S. E. Han, Y. K. Oh, T. G. Park and S. Kwang Hahn (2008). "Hyaluronic acid-polyethyleneimine conjugate for target specific intracellular delivery of siRNA." Biopolymers **89**(7): 635-42.

Jiang, T., E. S. Olson, Q. T. Nguyen, M. Roy, P. A. Jennings and R. Y. Tsien (2004). "Tumor imaging by means of proteolytic activation of cell-penetrating peptides." Proc Natl Acad Sci U S A **101**(51): 17867-72.

Judge, A. D., M. Robbins, I. Tavakoli, J. Levi, L. Hu, A. Fronda, E. Ambegia, K. McClintock and I. MacLachlan (2009). "Confirming the RNAi-mediated mechanism of action of siRNA-based cancer therapeutics in mice." J Clin Invest **119**(3): 661-73.

Judge, A. D., V. Sood, J. R. Shaw, D. Fang, K. McClintock and I. MacLachlan (2005). "Sequence-dependent stimulation of the mammalian innate immune response by synthetic siRNA." Nat Biotechnol **23**(4): 457-62.

Kamimura, K., G. Zhang and D. Liu (2010). "Image-guided, intravascular hydrodynamic gene delivery to skeletal muscle in pigs." Mol Ther **18**(1): 93-100.

Karatasos, K., P. Posocco, E. Laurini and S. Pricl (2012). "Poly(amidoamine)-based dendrimer/siRNA complexation studied by computer simulations: effects of pH and generation on dendrimer structure and siRNA binding." Macromol Biosci **12**(2): 225-40.

Kichler, A., A. J. Mason and B. Bechinger (2006). "Cationic amphipathic histidine-rich peptides for gene delivery." Biochim Biophys Acta **1758**(3): 301-7.

Kim, E., Y. Jung, H. Choi, J. Yang, J. S. Suh, Y. M. Huh, K. Kim and S. Haam (2010). "Prostate cancer cell death produced by the co-delivery of Bcl-xL shRNA and doxorubicin using an aptamer-conjugated polyplex." Biomaterials **31**(16): 4592-9.

Kim, J. Y., S. Choung, E. J. Lee, Y. J. Kim and Y. C. Choi (2007). "Immune activation by siRNA/liposome complexes in mice is sequence- independent: lack of a role for Toll-like receptor 3 signaling." Mol Cells **24**(2): 247-54.

Kim, S. H., J. H. Jeong, S. H. Lee, S. W. Kim and T. G. Park (2006). "PEG conjugated VEGF siRNA for anti-angiogenic gene therapy." J Control Release **116**(2): 123-9.

Kim, S. H., J. H. Jeong, S. H. Lee, S. W. Kim and T. G. Park (2008). "LHRH receptor-mediated delivery of siRNA using polyelectrolyte complex micelles self-assembled from siRNA-PEG-LHRH conjugate and PEI." Bioconjug Chem **19**(11): 2156-62.

Kim, S. H., J. H. Jeong, S. H. Lee, S. W. Kim and T. G. Park (2008). "Local and systemic delivery of VEGF siRNA using polyelectrolyte complex micelles for effective treatment of cancer." J Control Release **129**(2): 107-16.

Kim, S. H., H. Mok, J. H. Jeong, S. W. Kim and T. G. Park (2006). "Comparative evaluation of target-specific GFP gene silencing efficiencies for antisense ODN, synthetic siRNA, and siRNA plasmid complexed with PEI-PEG-FOL conjugate." Bioconjug Chem **17**(1): 241-4.

Kim, S. W., N. Y. Kim, Y. B. Choi, S. H. Park, J. M. Yang and S. Shin (2010). "RNA interference in vitro and in vivo using an arginine peptide/siRNA complex system." J Control Release **143**(3): 335-43.

Kim, T., K. A. Afonin, M. Viard, A. Y. Koyfman, S. Sparks, E. Heldman, S. Grinberg, C. Linder, R. P. Blumenthal and B. A. Shapiro (2013). "In Silico, In

Vitro, and In Vivo Studies Indicate the Potential Use of Bolaamphiphiles for Therapeutic siRNAs Delivery." Mol Ther Nucleic Acids **2**: e80.

Kim, W. J., L. V. Christensen, S. Jo, J. W. Yockman, J. H. Jeong, Y. H. Kim and S. W. Kim (2006). "Cholesteryl oligoarginine delivering vascular endothelial growth factor siRNA effectively inhibits tumor growth in colon adenocarcinoma." Mol Ther **14**(3): 343-50.

Kim, W. J., J. W. Yockman, J. H. Jeong, L. V. Christensen, M. Lee, Y. H. Kim and S. W. Kim (2006). "Anti-angiogenic inhibition of tumor growth by systemic delivery of PEI-g-PEG-RGD/pCMV-sFlt-1 complexes in tumor-bearing mice." J Control Release **114**(3): 381-8.

Kim, W. J., J. W. Yockman, M. Lee, J. H. Jeong, Y. H. Kim and S. W. Kim (2005). "Soluble Flt-1 gene delivery using PEI-g-PEG-RGD conjugate for anti-angiogenesis." J Control Release **106**(1-2): 224-34.

Kircheis, R., L. Wightman, A. Schreiber, B. Robitza, V. Rossler, M. Kursa and E. Wagner (2001). "Polyethylenimine/DNA complexes shielded by transferrin target gene expression to tumors after systemic application." Gene Ther **8**(1): 28-40.

Korolev, N., N. V. Berezhnoy, K. D. Eom, J. P. Tam and L. Nordenskiold (2012). "A universal description for the experimental behavior of salt-(in)dependent oligocation-induced DNA condensation." Nucleic Acids Res **40**(6): 2808-21.

Kumar, P., H. Wu, J. L. McBride, K. E. Jung, M. H. Kim, B. L. Davidson, S. K. Lee, P. Shankar and N. Manjunath (2007). "Transvascular delivery of small interfering RNA to the central nervous system." Nature **448**(7149): 39-43.

Lakhal, S. and M. J. Wood (2011). "Exosome nanotechnology: an emerging paradigm shift in drug delivery: exploitation of exosome nanovesicles for systemic in vivo delivery of RNAi heralds new horizons for drug delivery across biological barriers." Bioessays **33**(10): 737-41.

Landen, C. N., Jr., A. Chavez-Reyes, C. Bucana, R. Schmandt, M. T. Deavers, G. Lopez-Berestein and A. K. Sood (2005). "Therapeutic EphA2 gene targeting in vivo using neutral liposomal small interfering RNA delivery." Cancer Res **65**(15): 6910-8.

Landen, C. N., W. M. Merritt, L. S. Mangala, A. M. Sanguino, C. Bucana, C. Lu, Y. G. Lin, L. Y. Han, A. A. Kamat, R. Schmandt, R. L. Coleman, D. M. Gershenson, G. Lopez-Berestein and A. K. Sood (2006). "Intraperitoneal delivery of liposomal siRNA for therapy of advanced ovarian cancer." Cancer Biol Ther **5**(12): 1708-13.

Lee, E. R., J. Marshall, C. S. Siegel, C. Jiang, N. S. Yew, M. R. Nichols, J. B. Nietupski, R. J. Ziegler, M. B. Lane, K. X. Wang, N. C. Wan, R. K. Scheule, D. J. Harris, A. E. Smith and S. H. Cheng (1996). "Detailed analysis of structures and formulations of cationic lipids for efficient gene transfer to the lung." Hum Gene Ther **7**(14): 1701-17.

Lee, J. H., K. Lee, S. H. Moon, Y. Lee, T. G. Park and J. Cheon (2009). "All-in-one target-cell-specific magnetic nanoparticles for simultaneous molecular imaging and siRNA delivery." Angew Chem Int Ed Engl **48**(23): 4174-9.

Lee, J. S., J. J. Green, K. T. Love, J. Sunshine, R. Langer and D. G. Anderson (2009). "Gold, poly(beta-amino ester) nanoparticles for small interfering RNA delivery." Nano Lett **9**(6): 2402-6.

Lee, M. J., O. Veiseh, N. Bhattarai, C. Sun, S. J. Hansen, S. Ditzler, S. Knoblaugh, D. Lee, R. Ellenbogen, M. Zhang and J. M. Olson (2010). "Rapid pharmacokinetic and biodistribution studies using cholorotoxin-conjugated iron oxide nanoparticles: a novel non-radioactive method." PLoS One **5**(3): e9536.

Leng, Q. and A. J. Mixson (2005). "Modified branched peptides with a histidine-rich tail enhance in vitro gene transfection." Nucleic Acids Res **33**(4): e40.

Leng, Q. and A. J. Mixson (2005). "Small interfering RNA targeting Raf-1 inhibits tumor growth in vitro and in vivo." Cancer Gene Ther **12**(8): 682-90.

Leng, Q., P. Scaria, O. B. Ioffe, M. Woodle and A. J. Mixson (2006). "A branched histidine/lysine peptide, H2K4b, in complex with plasmids encoding antitumor proteins inhibits tumor xenografts." J Gene Med **8**(12): 1407-15.

Leng, Q., P. Scaria, P. Lu, M. C. Woodle and A. J. Mixson (2008). "Systemic delivery of HK Raf-1 siRNA polyplexes inhibits MDA-MB-435 xenografts." Cancer Gene Ther **15**(8): 485-95.

Leng, Q., P. Scaria, J. Zhu, N. Ambulos, P. Campbell and A. J. Mixson (2005). "Highly branched HK peptides are effective carriers of siRNA." J Gene Med **7**(7): 977-86.

Leng, Q., M. C. Woodle, P. Y. Lu and A. J. Mixson (2009). "Advances in Systemic siRNA Delivery." Drugs Future **34**(9): 721.

Levchenko, T. S., R. Rammohan, A. N. Lukyanov, K. R. Whiteman and V. P. Torchilin (2002). "Liposome clearance in mice: the effect of a separate and combined presence of surface charge and polymer coating." Int J Pharm **240**(1-2): 95-102.

Li, J., Y. C. Chen, Y. C. Tseng, S. Mozumdar and L. Huang (2010). "Biodegradable calcium phosphate nanoparticle with lipid coating for systemic siRNA delivery." J Control Release **142**(3): 416-21.

Li, S. D., Y. C. Chen, M. J. Hackett and L. Huang (2008). "Tumor-targeted delivery of siRNA by self-assembled nanoparticles." Mol Ther **16**(1): 163-9.

Li, S. D., S. Chono and L. Huang (2008). "Efficient gene silencing in metastatic tumor by siRNA formulated in surface-modified nanoparticles." J Control Release **126**(1): 77-84.

Li, S. D. and L. Huang (2006). "Targeted delivery of antisense oligodeoxynucleotide and small interference RNA into lung cancer cells." Mol Pharm **3**(5): 579-88.

Li, S. D. and L. Huang (2008). "Pharmacokinetics and biodistribution of nanoparticles." Mol Pharm **5**(4): 496-504.

Liu, F., Y. Song and D. Liu (1999). "Hydrodynamics-based transfection in animals by systemic administration of plasmid DNA." Gene Ther **6**(7): 1258-66.

Lodi, P. J. and J. R. Knowles (1991). "Neutral imidazole is the electrophile in the reaction catalyzed by triosephosphate isomerase: structural origins and catalytic implications." Biochemistry **30**(28): 6948-56.

Lohman, T. M., P. L. deHaseth and M. T. Record, Jr. (1980). "Pentalysine-deoxyribonucleic acid interactions: a model for the general effects of ion

concentrations on the interactions of proteins with nucleic acids." Biochemistry **19**(15): 3522-30.
Lohman, T. M. and L. B. Overman (1985). "Two binding modes in Escherichia coli single strand binding protein-single stranded DNA complexes. Modulation by NaCl concentration." J Biol Chem **260**(6): 3594-603.
Love, K. T., K. P. Mahon, C. G. Levins, K. A. Whitehead, W. Querbes, J. R. Dorkin, J. Qin, W. Cantley, L. L. Qin, T. Racie, M. Frank-Kamenetsky, K. N. Yip, R. Alvarez, D. W. Sah, A. de Fougerolles, K. Fitzgerald, V. Koteliansky, A. Akinc, R. Langer and D. G. Anderson (2010). "Lipid-like materials for low-dose, in vivo gene silencing." Proc Natl Acad Sci U S A **107**(5): 1864-9.
Lowe, D. M., A. R. Fersht, A. J. Wilkinson, P. Carter and G. Winter (1985). "Probing histidine-substrate interactions in tyrosyl-tRNA synthetase using asparagine and glutamine replacements." Biochemistry **24**(19): 5106-9.
Lundberg, M., S. Wikstrom and M. Johansson (2003). "Cell surface adherence and endocytosis of protein transduction domains." Mol Ther **8**(1): 143-50.
Lyseng-Williamson, K. A. and C. Fenton (2005). "Docetaxel: a review of its use in metastatic breast cancer." Drugs **65**(17): 2513-31.
Ma, P. L., M. Lavertu, F. M. Winnik and M. D. Buschmann (2009). "New insights into chitosan-DNA interactions using isothermal titration microcalorimetry." Biomacromolecules **10**(6): 1490-9.
Manning, G. S. (1969). "Limiting Laws and Counterion Condensation in Polyelectrolyte Solutions I. Colligative Properties." The Journal of Chemical Physics **51**: 9.
Manning, G. S. (1978). "The molecular theory of polyelectrolyte solutions with applications to the electrostatic properties of polynucleotides." Q Rev Biophys **11**(2): 179-246.
Markley, J. L. (1975). "Observation of histidine residues in proteins by nuclear magnetic resonance spectroscopy." Accounts of Chemical Research **8**(2): 11.
Mascotti, D. P. and T. M. Lohman (1992). "Thermodynamics of single-stranded RNA binding to oligolysines containing tryptophan." Biochemistry **31**(37): 8932-46.
Mascotti, D. P. and T. M. Lohman (1997). "Thermodynamics of oligoarginines binding to RNA and DNA." Biochemistry **36**(23): 7272-9.
Matsuda, T. and C. L. Cepko (2004). "Electroporation and RNA interference in the rodent retina in vivo and in vitro." Proc Natl Acad Sci U S A **101**(1): 16-22.
Matulis, D., I. Rouzina and V. A. Bloomfield (2000). "Thermodynamics of DNA binding and condensation: isothermal titration calorimetry and electrostatic mechanism." J Mol Biol **296**(4): 1053-63.
Mears, R., R. A. Craven, S. Hanrahan, N. Totty, C. Upton, S. L. Young, P. Patel, P. J. Selby and R. E. Banks (2004). "Proteomic analysis of melanoma-derived exosomes by two-dimensional polyacrylamide gel electrophoresis and mass spectrometry." Proteomics **4**(12): 4019-31.
Meckes, D. G., Jr., K. H. Shair, A. R. Marquitz, C. P. Kung, R. H. Edwards and N. Raab-Traub (2010). "Human tumor virus utilizes exosomes for intercellular communication." Proc Natl Acad Sci U S A **107**(47): 20370-5.

Medina-Kauwe, L. K., J. Xie and S. Hamm-Alvarez (2005). "Intracellular trafficking of nonviral vectors." Gene Ther **12**(24): 1734-51.

Melnikova, V. O., G. J. Villares and M. Bar-Eli (2008). "Emerging roles of PAR-1 and PAFR in melanoma metastasis." Cancer Microenviron **1**(1): 103-11.

Merkel, O. M., D. Librizzi, A. Pfestroff, T. Schurrat, K. Buyens, N. N. Sanders, S. C. De Smedt, M. Behe and T. Kissel (2009). "Stability of siRNA polyplexes from poly(ethylenimine) and poly(ethylenimine)-g-poly(ethylene glycol) under in vivo conditions: effects on pharmacokinetics and biodistribution measured by Fluorescence Fluctuation Spectroscopy and Single Photon Emission Computed Tomography (SPECT) imaging." J Control Release **138**(2): 148-59.

Merritt, W. M., Y. G. Lin, W. A. Spannuth, M. S. Fletcher, A. A. Kamat, L. Y. Han, C. N. Landen, N. Jennings, K. De Geest, R. R. Langley, G. Villares, A. Sanguino, S. K. Lutgendorf, G. Lopez-Berestein, M. M. Bar-Eli and A. K. Sood (2008). "Effect of interleukin-8 gene silencing with liposome-encapsulated small interfering RNA on ovarian cancer cell growth." J Natl Cancer Inst **100**(5): 359-72.

Michael, A., K. Syrigos and H. Pandha (2009). "Prostate cancer chemotherapy in the era of targeted therapy." Prostate Cancer Prostatic Dis **12**(1): 13-6.

Midoux, P. and M. Monsigny (1999). "Efficient gene transfer by histidylated polylysine/pDNA complexes." Bioconjug Chem **10**(3): 406-11.

Minko, T., M. L. Patil, M. Zhang, J. J. Khandare, M. Saad, P. Chandna and O. Taratula (2010). "LHRH-targeted nanoparticles for cancer therapeutics." Methods Mol Biol **624**: 281-94.

Mislick, K. A. and J. D. Baldeschwieler (1996). "Evidence for the role of proteoglycans in cation-mediated gene transfer." Proc Natl Acad Sci U S A **93**(22): 12349-54.

Molineux, I. J., A. Pauli and M. L. Gefter (1975). "Physical studies of the interaction between the Escherichia coli DNA binding protein and nucleic acids." Nucleic Acids Res **2**(10): 1821-37.

Morrissey, D. V., K. Blanchard, L. Shaw, K. Jensen, J. A. Lockridge, B. Dickinson, J. A. McSwiggen, C. Vargeese, K. Bowman, C. S. Shaffer, B. A. Polisky and S. Zinnen (2005). "Activity of stabilized short interfering RNA in a mouse model of hepatitis B virus replication." Hepatology **41**(6): 1349-56.

Morrissey, D. V., J. A. Lockridge, L. Shaw, K. Blanchard, K. Jensen, W. Breen, K. Hartsough, L. Machemer, S. Radka, V. Jadhav, N. Vaish, S. Zinnen, C. Vargeese, K. Bowman, C. S. Shaffer, L. B. Jeffs, A. Judge, I. MacLachlan and B. Polisky (2005). "Potent and persistent in vivo anti-HBV activity of chemically modified siRNAs." Nat Biotechnol **23**(8): 1002-7.

Mozafari, M. R., C. J. Reed and C. Rostron (2007). "Cytotoxicity evaluation of anionic nanoliposomes and nanolipoplexes prepared by the heating method without employing volatile solvents and detergents." Pharmazie **62**(3): 205-9.

Mu, P., S. Nagahara, N. Makita, Y. Tarumi, K. Kadomatsu and Y. Takei (2009). "Systemic delivery of siRNA specific to tumor mediated by atelocollagen: combined therapy using siRNA targeting Bcl-xL and cisplatin against prostate cancer." Int J Cancer **125**(12): 2978-90.

Nakase, I., M. Niwa, T. Takeuchi, K. Sonomura, N. Kawabata, Y. Koike, M. Takehashi, S. Tanaka, K. Ueda, J. C. Simpson, A. T. Jones, Y. Sugiura and S. Futaki (2004). "Cellular uptake of arginine-rich peptides: roles for macropinocytosis and actin rearrangement." Mol Ther **10**(6): 1011-22.

Narayan, K., C. L. Chou, A. Kim, I. Z. Hartman, S. Dalai, S. Khoruzhenko and S. Sadegh-Nasseri (2007). "HLA-DM targets the hydrogen bond between the histidine at position beta81 and peptide to dissociate HLA-DR-peptide complexes." Nat Immunol **8**(1): 92-100.

Nishina, K., T. Unno, Y. Uno, T. Kubodera, T. Kanouchi, H. Mizusawa and T. Yokota (2008). "Efficient in vivo delivery of siRNA to the liver by conjugation of alpha-tocopherol." Mol Ther **16**(4): 734-40.

Noguchi, Y., J. Wu, R. Duncan, J. Strohalm, K. Ulbrich, T. Akaike and H. Maeda (1998). "Early phase tumor accumulation of macromolecules: a great difference in clearance rate between tumor and normal tissues." Jpn J Cancer Res **89**(3): 307-14.

Nomoto, T., Y. Matsumoto, K. Miyata, M. Oba, S. Fukushima, N. Nishiyama, T. Yamasoba and K. Kataoka (2011). "In situ quantitative monitoring of polyplexes and polyplex micelles in the blood circulation using intravital real-time confocal laser scanning microscopy." J Control Release **151**(2): 104-9.

Ofek, P., W. Fischer, M. Calderon, R. Haag and R. Satchi-Fainaro (2010). "In vivo delivery of small interfering RNA to tumors and their vasculature by novel dendritic nanocarriers." FASEB J **24**(9): 3122-34.

Pantarotto, D., J. P. Briand, M. Prato and A. Bianco (2004). "Translocation of bioactive peptides across cell membranes by carbon nanotubes." Chem Commun (Camb)(1): 16-7.

Peer, D., E. J. Park, Y. Morishita, C. V. Carman and M. Shimaoka (2008). "Systemic leukocyte-directed siRNA delivery revealing cyclin D1 as an anti-inflammatory target." Science **319**(5863): 627-30.

Pelton, J. G., D. A. Torchia, N. D. Meadow and S. Roseman (1993). "Tautomeric states of the active-site histidines of phosphorylated and unphosphorylated IIIGlc, a signal-transducing protein from Escherichia coli, using two-dimensional heteronuclear NMR techniques." Protein Sci **2**(4): 543-58.

Perales, J. C., T. Ferkol, H. Beegen, O. D. Ratnoff and R. W. Hanson (1994). "Gene transfer in vivo: sustained expression and regulation of genes introduced into the liver by receptor-targeted uptake." Proc Natl Acad Sci U S A **91**(9): 4086-90.

Prevette, L. E., T. E. Kodger, T. M. Reineke and M. L. Lynch (2007). "Deciphering the role of hydrogen bonding in enhancing pDNA-polycation interactions." Langmuir **23**(19): 9773-84.

Putnam, D., C. A. Gentry, D. W. Pack and R. Langer (2001). "Polymer-based gene delivery with low cytotoxicity by a unique balance of side-chain termini." Proc Natl Acad Sci U S A **98**(3): 1200-5.

Rehman, Z. U., D. Hoekstra and I. S. Zuhorn (2013). "Mechanism of Polyplex- and Lipoplex-Mediated Delivery of Nucleic Acids: Real-Time Visualization of Transient Membrane Destabilization without Endosomal Lysis." ACS nano **7**(5): 3767-77.

Reynolds, A., D. Leake, Q. Boese, S. Scaringe, W. S. Marshall and A. Khvorova (2004). "Rational siRNA design for RNA interference." Nat Biotechnol **22**(3): 326-30.

Robbins, M., A. Judge, E. Ambegia, C. Choi, E. Yaworski, L. Palmer, K. McClintock and I. MacLachlan (2008). "Misinterpreting the therapeutic effects of small interfering RNA caused by immune stimulation." Hum Gene Ther **19**(10): 991-9.

Robbins, M., A. Judge, L. Liang, K. McClintock, E. Yaworski and I. MacLachlan (2007). "2'-O-methyl-modified RNAs act as TLR7 antagonists." Mol Ther **15**(9): 1663-9.

Roberts, J. D., Y. Chun, C. Flanagan and T. R. Birdseye (1982). "A nitrogen-15 nuclear magnetic resonance study of the acid-base and tautomeric equilibriums of 4-substituted imidazoles and its relevance to the catalytic mechanism of .alpha.-lytic protease." J Am Chem Soc **115**(14): 3945-9.

Rosi, N. L., D. A. Giljohann, C. S. Thaxton, A. K. Lytton-Jean, M. S. Han and C. A. Mirkin (2006). "Oligonucleotide-modified gold nanoparticles for intracellular gene regulation." Science **312**(5776): 1027-30.

Ross, P. D. and S. Subramanian (1981). "Thermodynamics of protein association reactions: forces contributing to stability." Biochemistry **20**(11): 3096-102.

Rowland, M. and T. N. Tozer (2011). Clinical pharmacokinetics and pharmacodynamics : concepts and applications. Philadelphia, Lippincott Williams & Wilkins.

Rudzinski, W. E. and T. M. Aminabhavi (2010). "Chitosan as a carrier for targeted delivery of small interfering RNA." Int J Pharm **399**(1-2): 1-11.

Sato, A., S. W. Choi, M. Hirai, A. Yamayoshi, R. Moriyama, T. Yamano, M. Takagi, A. Kano, A. Shimamoto and A. Maruyama (2007). "Polymer brush-stabilized polyplex for a siRNA carrier with long circulatory half-life." J Control Release **122**(3): 209-16.

Schiffelers, R. M., A. Ansari, J. Xu, Q. Zhou, Q. Tang, G. Storm, G. Molema, P. Y. Lu, P. V. Scaria and M. C. Woodle (2004). "Cancer siRNA therapy by tumor selective delivery with ligand-targeted sterically stabilized nanoparticle." Nucleic Acids Res **32**(19): e149.

Schmedt, C., S. R. Green, L. Manche, D. R. Taylor, Y. Ma and M. B. Mathews (1995). "Functional characterization of the RNA-binding domain and motif of the double-stranded RNA-dependent protein kinase DAI (PKR)." J Mol Biol **249**(1): 29-44.

Schraa, A. J., R. J. Kok, A. D. Berendsen, H. E. Moorlag, E. J. Bos, D. K. Meijer, L. F. de Leij and G. Molema (2002). "Endothelial cells internalize and degrade RGD-modified proteins developed for tumor vasculature targeting." J Control Release **83**(2): 241-51.

Schuster, I. I. and J. D. Roberts (1979). "Nitrogen-15 nuclear magnetic resonance spectroscopy. Effects of hydrogen bonding and protonation on nitrogen chemical shifts in imidazoles." The journal of organic chemistry **44**(22): 4.

Seferos, D. S., A. E. Prigodich, D. A. Giljohann, P. C. Patel and C. A. Mirkin (2009). "Polyvalent DNA nanoparticle conjugates stabilize nucleic acids." Nano Lett **9**(1): 308-11.

Snove, O., Jr. and J. J. Rossi (2006). "Chemical modifications rescue off-target effects of RNAi." ACS Chem Biol **1**(5): 274-6.

Snove, O., Jr. and J. J. Rossi (2006). "Toxicity in mice expressing short hairpin RNAs gives new insight into RNAi." Genome Biol **7**(8): 231.

Solodin, I., C. S. Brown, M. S. Bruno, C. Y. Chow, E. H. Jang, R. J. Debs and T. D. Heath (1995). "A novel series of amphiphilic imidazolinium compounds for in vitro and in vivo gene delivery." Biochemistry **34**(41): 13537-44.

Song, E., P. Zhu, S. K. Lee, D. Chowdhury, S. Kussman, D. M. Dykxhoorn, Y. Feng, D. Palliser, D. B. Weiner, P. Shankar, W. A. Marasco and J. Lieberman (2005). "Antibody mediated in vivo delivery of small interfering RNAs via cell-surface receptors." Nat Biotechnol **23**(6): 709-17.

Spankuch, B., E. Kurunci-Csacsko, M. Kaufmann and K. Strebhardt (2007). "Rational combinations of siRNAs targeting Plk1 with breast cancer drugs." Oncogene **26**(39): 5793-807.

Steiner, T. (2002). "The hydrogen bond in the solid state." Angew Chem Int Ed Engl **41**(1): 49-76.

Strumberg, D., B. Schultheis, W. Meyer-Sabellek, C. Vank, F. Gebhardt, A. Santel, O. Keil, K. Giese, J. Kaufmann and J. Drevs (2012). Antimetastatic activity of Atu027, a liposomal small interfering RNA formulation, targeting protein kinase N3 (PKN3): Final results of a phase I study in patients with advanced solid tumors. 2012 ASCO Annual Meeting, Chicago, Illinois, Journal of Clinical Oncology.

Strumberg, D., B. Schultheis, U. Traugott, C. Vank, A. Santel, O. Keil, K. Giese, J. Kaufmann and J. Drevs (2012). "Phase I clinical development of Atu027, a siRNA formulation targeting PKN3 in patients with advanced solid tumors." Int J Clin Pharmacol Ther **50**(1): 76-8.

Sugahara, K. N., T. Teesalu, P. P. Karmali, V. R. Kotamraju, L. Agemy, O. M. Girard, D. Hanahan, R. F. Mattrey and E. Ruoslahti (2009). "Tissue-penetrating delivery of compounds and nanoparticles into tumors." Cancer Cell **16**(6): 510-20.

Sun, T. M., J. Z. Du, Y. D. Yao, C. Q. Mao, S. Dou, S. Y. Huang, P. Z. Zhang, K. W. Leong, E. W. Song and J. Wang (2011). "Simultaneous delivery of siRNA and paclitaxel via a "two-in-one" micelleplex promotes synergistic tumor suppression." ACS Nano **5**(2): 1483-94.

Takeshita, F., Y. Minakuchi, S. Nagahara, K. Honma, H. Sasaki, K. Hirai, T. Teratani, N. Namatame, Y. Yamamoto, K. Hanai, T. Kato, A. Sano and T. Ochiya (2005). "Efficient delivery of small interfering RNA to bone-metastatic tumors by using atelocollagen in vivo." Proc Natl Acad Sci U S A **102**(34): 12177-82.

Tanaka, T., S. Shiramoto, M. Miyashita, Y. Fujishima and Y. Kaneo (2004). "Tumor targeting based on the effect of enhanced permeability and retention (EPR) and the mechanism of receptor-mediated endocytosis (RME)." Int J Pharm **277**(1-2): 39-61.

Thiel, K. W., L. I. Hernandez, J. P. Dassie, W. H. Thiel, X. Liu, K. R. Stockdale, A. M. Rothman, F. J. Hernandez, J. O. McNamara, 2nd and P. H. Giangrande

(2012). "Delivery of chemo-sensitizing siRNAs to HER2+-breast cancer cells using RNA aptamers." Nucleic Acids Res **40**(13): 6319-37.

Utsuno, K. and H. Uludag (2010). "Thermodynamics of polyethylenimine-DNA binding and DNA condensation." Biophys J **99**(1): 201-7.

Valadi, H., K. Ekstrom, A. Bossios, M. Sjostrand, J. J. Lee and J. O. Lotvall (2007). "Exosome-mediated transfer of mRNAs and microRNAs is a novel mechanism of genetic exchange between cells." Nat Cell Biol **9**(6): 654-9.

Van Dijk, A. A., R. M. Scheek, K. Dijkstra, G. K. Wolters and G. T. Robillard (1992). "Characterization of the protonation and hydrogen bonding state of the histidine residues in IIAmtl, a domain of the phosphoenolpyruvate-dependent mannitol-specific transport protein." Biochemistry **31**(37): 9063-72.

Villares, G. J., M. Zigler, H. Wang, V. O. Melnikova, H. Wu, R. Friedman, M. C. Leslie, P. E. Vivas-Mejia, G. Lopez-Berestein, A. K. Sood and M. Bar-Eli (2008). "Targeting melanoma growth and metastasis with systemic delivery of liposome-incorporated protease-activated receptor-1 small interfering RNA." Cancer Res **68**(21): 9078-86.

Waite, C. L. and C. M. Roth (2009). "PAMAM-RGD conjugates enhance siRNA delivery through a multicellular spheroid model of malignant glioma." Bioconjug Chem **20**(10): 1908-16.

Wallace, J. A. and J. K. Shen (2012). "Charge-leveling and proper treatment of long-range electrostatics in all-atom molecular dynamics at constant pH." The Journal of Chemical Physics **137**(18): 184105.

Watanabe, K., M. Harada-Shiba, A. Suzuki, R. Gokuden, R. Kurihara, Y. Sugao, T. Mori, Y. Katayama and T. Niidome (2009). "In vivo siRNA delivery with dendritic poly(L-lysine) for the treatment of hypercholesterolemia." Mol Biosyst **5**(11): 1306-10.

Whitehead, K. A., J. Matthews, P. H. Chang, F. Niroui, J. R. Dorkin, M. Severgnini and D. G. Anderson (2012). "In vitro-in vivo translation of lipid nanoparticles for hepatocellular siRNA delivery." ACS Nano **6**(8): 6922-9.

Wolfrum, C., S. Shi, K. N. Jayaprakash, M. Jayaraman, G. Wang, R. K. Pandey, K. G. Rajeev, T. Nakayama, K. Charrise, E. M. Ndungo, T. Zimmermann, V. Koteliansky, M. Manoharan and M. Stoffel (2007). "Mechanisms and optimization of in vivo delivery of lipophilic siRNAs." Nat Biotechnol **25**(10): 1149-57.

Wong, N. C., B. M. Mueller, C. F. Barbas, P. Ruminski, V. Quaranta, E. C. Lin and J. W. Smith (1998). "Alphav integrins mediate adhesion and migration of breast carcinoma cell lines." Clin Exp Metastasis **16**(1): 50-61.

Woodle, M. C., L. R. Collins, E. Sponsler, N. Kossovsky, D. Papahadjopoulos and F. J. Martin (1992). "Sterically stabilized liposomes. Reduction in electrophoretic mobility but not electrostatic surface potential." Biophys J **61**(4): 902-10.

Woodle, M. C. and D. D. Lasic (1992). "Sterically stabilized liposomes." Biochim Biophys Acta **1113**(2): 171-99.

Xiong, X. B. and A. Lavasanifar (2011). "Traceable multifunctional micellar nanocarriers for cancer-targeted co-delivery of MDR-1 siRNA and doxorubicin." ACS Nano **5**(6): 5202-13.

Yagi, N., I. Manabe, T. Tottori, A. Ishihara, F. Ogata, J. H. Kim, S. Nishimura, K. Fujiu, Y. Oishi, K. Itaka, Y. Kato, M. Yamauchi and R. Nagai (2009). "A nanoparticle system specifically designed to deliver short interfering RNA inhibits tumor growth in vivo." Cancer Res **69**(16): 6531-8.

Yang, J. P. and L. Huang (1997). "Overcoming the inhibitory effect of serum on lipofection by increasing the charge ratio of cationic liposome to DNA." Gene Ther **4**(9): 950-60.

Yang, X. Z., S. Dou, T. M. Sun, C. Q. Mao, H. X. Wang and J. Wang (2011). "Systemic delivery of siRNA with cationic lipid assisted PEG-PLA nanoparticles for cancer therapy." J Control Release **156**(2): 203-11.

Yoshimoto, M., K. Ogawa, K. Washiyama, N. Shikano, H. Mori, R. Amano and K. Kawai (2008). "alpha(v)beta(3) Integrin-targeting radionuclide therapy and imaging with monomeric RGD peptide." Int J Cancer **123**(3): 709-15.

Yoshino, H., K. Hashizume and E. Kobayashi (2006). "Naked plasmid DNA transfer to the porcine liver using rapid injection with large volume." Gene Ther **13**(24): 1696-702.

Zamanian-Daryoush, M., J. T. Marques, M. P. Gantier, M. A. Behlke, M. John, P. Rayman, J. Finke and B. R. Williams (2008). "Determinants of cytokine induction by small interfering RNA in human peripheral blood mononuclear cells." J Interferon Cytokine Res **28**(4): 221-33.

Zhang, G., V. Budker, P. Williams, V. Subbotin and J. A. Wolff (2001). "Efficient expression of naked dna delivered intraarterially to limb muscles of nonhuman primates." Hum Gene Ther **12**(4): 427-38.

Zhang, G., V. Budker and J. A. Wolff (1999). "High levels of foreign gene expression in hepatocytes after tail vein injections of naked plasmid DNA." Hum Gene Ther **10**(10): 1735-7.

Zhang, L., N. Ambulos and A. J. Mixson (2004). "DNA delivery to cells in culture using peptides." Methods Mol Biol **245**: 33-52.

Zhang, Z., X. Yang, Y. Zhang, B. Zeng, S. Wang, T. Zhu, R. B. Roden, Y. Chen and R. Yang (2006). "Delivery of telomerase reverse transcriptase small interfering RNA in complex with positively charged single-walled carbon nanotubes suppresses tumor growth." Clin Cancer Res **12**(16): 4933-9.

Zheng, D., D. A. Giljohann, D. L. Chen, M. D. Massich, X. Q. Wang, H. Iordanov, C. A. Mirkin and A. S. Paller (2012). "Topical delivery of siRNA-based spherical nucleic acid nanoparticle conjugates for gene regulation." Proc Natl Acad Sci U S A **109**(30): 11975-80.

Zheng, M., G. M. Pavan, M. Neeb, A. K. Schaper, A. Danani, G. Klebe, O. M. Merkel and T. Kissel (2012). "Targeting the blind spot of polycationic nanocarrier-based siRNA delivery." ACS nano **6**(11): 9447-54.

Zhu, C., S. Jung, S. Luo, F. Meng, X. Zhu, T. G. Park and Z. Zhong (2010). "Co-delivery of siRNA and paclitaxel into cancer cells by biodegradable cationic micelles based on PDMAEMA-PCL-PDMAEMA triblock copolymers." Biomaterials **31**(8): 2408-16.

Ziegler, A. and J. Seelig (2008). "Binding and clustering of glycosaminoglycans: a common property of mono- and multivalent cell-penetrating compounds." Biophys J **94**(6): 2142-9.

Zimmermann, T. S., A. C. Lee, A. Akinc, B. Bramlage, D. Bumcrot, M. N. Fedoruk, J. Harborth, J. A. Heyes, L. B. Jeffs, M. John, A. D. Judge, K. Lam, K. McClintock, L. V. Nechev, L. R. Palmer, T. Racie, I. Rohl, S. Seiffert, S. Shanmugam, V. Sood, J. Soutschek, I. Toudjarska, A. J. Wheat, E. Yaworski, W. Zedalis, V. Koteliansky, M. Manoharan, H. P. Vornlocher and I. MacLachlan (2006). "RNAi-mediated gene silencing in non-human primates." Nature **441**(7089): 111-4.

Zuckerman, J. E., C. H. Choi, H. Han and M. E. Davis (2012). "Polycation-siRNA nanoparticles can disassemble at the kidney glomerular basement membrane." Proc Natl Acad Sci U S A **109**(8): 3137-42.

Zuiderweg, E. R. (2002). "Mapping protein-protein interactions in solution by NMR spectroscopy." Biochemistry **41**(1): 1-7.

List of Publications and Conference Presentations

List of Publications

1. Woodle, M., Scaria, P.V., Liu, Y., Leng, Q., Chou, S.T., Mixson, A.J., (2014) Enhancement of antifungal activity by integrin-targeting of branched histidine rich peptides. *Journal of Drug Targeting*, accepted.

2. Chou, S.T., Hom, K., Zhang, D., Leng, Q., Tricoli, L.J., Hustedt, J.M., Lee, A., Shapiro, M.J., Seog, J., Kahn, J.D. and Mixson, A.J. (2014) Enhanced silencing and stabilization of siRNA polyplexes by histidine-mediated hydrogen bonds. *Biomaterials*, **35**, 846-855.

3. Chou, S.T., Leng, Q., Scaria, P., Kahn, J.D., Tricoli, L.J., Woodle, M. and Mixson, A.J. (2013) Surface-modified HK:siRNA nanoplexes with enhanced pharmacokinetics and tumor growth inhibition. *Biomacromolecules*, **14**, 752-760.

4. Leng, Q., Chou, S.T., Scaria, P.V., Woodle, M.C. and Mixson, A.J. (2012) Buffering capacity and size of siRNA polyplexes influence cytokine levels. *Mol Ther*, **20**, 2282-2290.

5. Chou, S.T., Leng, Q. and Mixson, A.J. (2012) Zinc Finger Nucleases: Tailor-made for Gene Therapy. *Drugs Future*, **37**, 183-196.

6. Chou, S.T., Leng, Q., Scaria, P., Woodle, M. and Mixson, A.J. (2011) Selective modification of HK peptides enhances siRNA silencing of tumor targets in vivo. *Cancer Gene Ther*, **18**, 707-716.

7. Matejuk, A., Leng, Q., Chou, S.T. and Mixson, A.J. (2011) Vaccines targeting the neovasculature of tumors. *Vasc Cell*, **3**, 7.

8. Matejuk, A., Leng, Q., Begum, M.D., Woodle, M.C., Scaria, P., Chou, S.T. and Mixson, A.J. (2010) Peptide-based Antifungal Therapies against Emerging Infections. *Drugs Future*, **35**, 197.

List of Conference Presentations

The following abstracts were presented by first author.

1. Chou, S.T., Hom, K., Daoning, Z., Leng, Q., Tricoli, L., Hustedt, J., Lee, A., Shapiro, M., Seog, J., Kahn, J., Mixson, A.J. "Histidine-Mediated Hydrogen Bonding Enhances Stability and Silencing Activity of Peptide siRNA Polyplexes" 2013 American Institute of Chemical Engineers Annual Meeting, San Francisco, CA, 2013.

2. Chou, S.T., Hom, K., Zhang, D., Lee, A., Tricoli, L., Hustedt, J., Leng, Q., Seog, J., Kahn, J.D., Mixson, A.J. "Structure and silencing activity of imidazole-containing peptide siRNA polyplexes are dependent on hydrogen bonding." American Society of Gene and Cell Therapy 16th Annual Meeting (ASGCT), Salt Lake City, UT, 2013

3. Lee, A., Zheng, T., Sucayan, S., Chou, S.T., Tricoli, L., Hustedt, J., Kahn J., Mixson, A.J., Seog, J. "Optical tweezers reveal a dynamic mechanical response of cationic peptide-DNA complexes." American Physical Society (APS) March Meeting 2013, Baltimore, MD, 2013

4. Chou, S.T., Leng, Q., Seog, J., Kahn, J.D., Mixson, A.J. "Hydrogen bonding between the imidazole-containing peptide and siRNA mediates greater stability and biological activity of the polyplex." 8th Annual Oligonucleotide Therapeutic Annual Meeting, Boston, MA, 2012

5. Chou, S.T., Leng, Q., Scaria, Woodle, P., Mixson, A.J. "Modified HK siRNA Polyplexes with Improved Pharmacokinetics Enhance Tumor Inhibition." American Society of Gene and Cell Therapy 15th Annual Meeting (ASGCT), Philadelphia, PA, 2012.

6. Chou, S.T., Leng, Q., Scaria, Woodle, P., Mixson, A.J. "Modified siRNA Peptide Carriers with Improved Pharmacokinetics Enhance Tumor Inhibition." 2012 Graduation Research Interaction Day, College Park, MD, 2012

7. Chou, S.T., Leng, Q., Scaria, Woodle P., Mixson, A.J. "A Modified HK Carrier of siRNA Enhances Silencing of Tumor Targets *in vivo*." American Society of Gene and Cell Therapy 14th Annual Meeting (ASGCT), Seattle, WA, 2011.

8. Chou, S.T., Leng, Q., Scaria, Mixson, A.J. "Selective Pegylation Patterns of HK siRNA Nanoparticles Influence Ability to Silence Tumor Targets *in vivo*." 1st Annual Cancer Biology Research Retreat, Baltimore, MD, 2010.

9. Achinivu, E., Chou, S.T., Plata, H., Allen, D., Pickering, K., Ehrman, S., "Towards improve emissions inventories of soil NOx via model/satellite measurement intercomparisons," CMAS 2009 Conference, Chapel Hill, NC, October, 2009.